Title
Essays on Environmental and Urban Economics

Author
Guo, Wei

Publication Date
2023

Essays on Environmental and Urban Economics

By

Wei Guo

A dissertation submitted in partial satisfaction of the

requirements for the degree of

Doctor of Philosophy

in

Agricultural and Resource Economics

in the

Graduate Division

of the

University of California, Berkeley

Committee in charge:

Professor Maximilian Auffhammer, Chair
Professor Joseph Shapiro
Professor William Reed Walker

Spring 2023

Essays on Environmental and Urban Economics

Abstract

Essays on Environmental and Urban Economics

by

Wei Guo

Doctor of Philosophy in Agricultural and Resource Economics

University of California, Berkeley

Professor Maximilian Auffhammer, Chair

This dissertation examines the interplay between environmental disasters, renewable energy development, and housing markets through three interconnected chapters. Using quantitative methods and geospatial databases, I present empirical evidence on the economic and social consequences of environmental challenges and the transition to renewable energy. The findings contribute to a better understanding of the challenges and opportunities in developing effective, equitable, and sustainable disaster mitigation efforts and environmental policies.

Chapter 1 is motivated by the reality that environmental disasters increasingly displace people worldwide with little warning. The rapid expansion of the sharing economy has created a new source of short-term housing for those affected. This chapter investigates the welfare impacts of home sharing for short-term displacement caused wildfires in the Los Angeles area. I develop a structural model of the home-sharing market that accounts for information asymmetry between customer types (disaster evacuees versus regular travelers),

identifying two welfare channels: the increased choice of housing options and altruistic sharing by hosts. The results suggest that home sharing can mitigate 52% of welfare loss due to displacement, with host generosity contributing one-quarter of this reduction. My analysis highlights the equity benefits unlocked by home sharing, as altruistic behavior is primarily carried out by better-off hosts as indicated by demographic and home characteristics. The study also proposes a platform targeting displaced individuals to improve the efficiency and equity of mitigation efforts. The findings speak to the fundamental question of economics on the role of market economy and technology innovation in enhancing emergency response and recovery.

Chapter 2, co-authored with Yanjun (Penny) Liao and Qing Miao, addresses the challenges coastal communities face in limiting population and property exposure to increasing disaster risks while maintaining a strong local economy. This dilemma is often apparent in government buyout and acquisition programs, which offer financial incentives for households to voluntarily relocate from at-risk properties. This chapter examines a major post-disaster buyout and acquisition initiative implemented by New York state after Hurricane Sandy, and its effects on a wide range of property-level and community-level changes. Our results indicate that acquisitions and buyouts can increase property values in the immediate area and enhance business outcomes in the broader neighborhood. Consequently, these neighborhood improvements attract different types of property buyers. By offering the first estimates on general equilibrium effects spilling over to a larger portion of the neighborhoods, our findings contribute to ongoing debates on managed retreat and provide a more comprehensive perspective.

Chapter 3, in collaboration with Maximilian Auffhammer and Leonie Wenz, addresses the contentious issue that renewable power, while increasingly important for its environmental benefits, may impose externalities on local residents. This chapter assesses the social costs of wind power generation in the US, focusing on its impact on property values due to visual

disamenity. We construct a geospatial database on wind turbine visibility nationwide and use a spatial difference-in-difference approach to estimate the impact of wind turbine visibility on housing prices. Results indicate that wind farm developments reduce property values by up to 8% in visible areas of close proximity, primarily in urban neighborhoods. We also explore the adaptation efforts taken by local residents and discuss their implications for future wind farm location decisions. By providing the first nationwide evaluation of the social costs of wind power generation, this study offers essential insights for ongoing debates on the equity implications of renewable energy development.

To visionary pioneers;

To life's enriching odyssey;

To my parents' boundless love;

To steadfast family and friends;

This thesis, dedicated to you. Gratitude abounds.

Contents

List of Figures

List of Tables

Acknowledgments

First and foremost, I extend my deepest gratitude to my advisor, Maximilian Auffhammer, whose unwavering support has been indispensable in the completion of this dissertation. From our first meeting after my initial year of study, Max's invaluable guidance, encouragement, and counsel have illuminated my PhD journey. Through every challenge, his profound wisdom and reassurance have broadened my horizons and allayed my concerns. Max's humor and open-minded nature have rendered the past five years a cherished and delightful life experience. Should I have the opportunity to mentor students in the future, I aspire to emulate Max as an exceptional advisor, shining a light that opens closed doors and windows for those under my guidance.

I would also like to convey my heartfelt appreciation to the professors who have steadfastly supported my studies, including Professors Meredith Fowlie, Sofia Villas-Boas, Brian Wright, Marco Gonzalez-Navarro, and Beia Spiller. Their guidance has been instrumental in my PhD journey. Furthermore, I express my gratitude to my dissertation committee, Professors Joseph Shapiro and Reed Walker, for their invaluable comments, suggestions, and support throughout the process.

My sincere appreciation goes to our department secretaries, Carmen Karahalios and Diana Lazo, for offering continuous advice and support during my study. Carmen's assistance has made my experience as an international student significantly smoother, and Diana's tireless efforts have alleviated the challenges of the job market I encountered.

I am deeply grateful for my fellow classmates at UC Berkeley, with whom I have shared many delightful moments over the years, as well as my former teachers, colleagues, and friends at Peking University. In particular, I wish to acknowledge my co-authors, Penny Liao and Qing Miao, for expanding and enriching my research horizons. Additionally, I am grateful to those who offered challenging questions and critiques during numerous seminars and interviews, as their contributions have shaped me into the person I am today.

Last but certainly not least, I extend my warmest thanks to my parents, who have selflessly sacrificed their own aspirations to bring me into this world and for their unwavering spiritual support throughout my life. Though I do not subscribe to any particular faith, I am deeply thankful to the unknown force that placed my soul within their family. Finally, I extend my wholehearted appreciation to my spouse, who has shared innumerable joyful and trying moments with me. While I may be inherently reserved, I harbor no regrets for any life decisions made with my cherished loved ones in mind.

Chapter 1

The Sharing Economy as Disaster Remedy: The Case of Airbnb

1.1 Introduction

There have been significant increases in short-term displacement over the past decade (The United Nations High Commissioner for Refugees 2022). We often think of most displacement being induced by civil conflict and outbreak of pandemics, yet forced displacement by extreme weather and natural disasters has been on the rise worldwide, some of which can be attributed directly to the acceleration of climate change (Missirian and Schlenker 2017). The onset of these disasters is impossible for individuals to predict; hence the ability to plan ahead is limited. In the immediate aftermath of a disaster, considerable stress is placed on transportation infrastructure and sheltering. There is generally a lack of public resources available from traditional sectors to adequately accommodate all displaced populations. For instance, the Southern California wildfires in 2017 displaced 300,000 people through evacuation, while there were only 100,000 hotel rooms in nearby cities (Ronchi et al. 2021).

Facilitated by the development of cost-reducing technologies, online marketplaces have popularized peer-to-peer housing transactions, which enable individual homeowners and tenants to offer their underutilized housing units to strangers in exchange for compensation. Home-sharing platforms, such as Airbnb, VRBO, and HomeAway in particular, have greatly improved the capacity and supply flexibility of the market for short-term accommodations (Barron et al. 2021). Anecdotal evidence suggests that this channel sometimes unleashes human generosity during moments of emergency. For instance, Airbnb has initiated a so-called "Open Homes Program" to motivate the offering of discounted or free homes to victims after disasters

In this paper, I quantify the welfare loss of temporary displacement by a type of natural disaster (wildfire), and explore how the peer-to-peer production of short-term accommodations mitigates losses for the displaced. The analysis is focused on the response of the prominent home-sharing platform, Airbnb, to the evacuation incidents prompted by wildfires in one of the world's largest home-sharing markets – the Los Angeles area. I highlight two welfare channels operating through Airbnb. First, the effect from an increased set of accommodation choices due to Airbnb can benefit all customers, particularly through the variety of housing options and the lower price relative to hotels. Second, some peer hosts display altruistic behavior, by increasing supply and setting price to be lower than usual, to further assist displaced households.

In order to test the hypothesis on the existence of altruistic sharing, I first present a set of stylized facts on the response of Airbnb market outcomes during wildfire incidents. Based on an event study framework using the issuance of evacuation orders as treatment, I find a supply expansion immediately following wildfire in both extensive margin (new rooms/homes) and intensive margin (rooms previously listed being made available), which add the offerings by 4% of the number of customers on Airbnb. There is systematic heterogeneity in the pricing between the entries of both margins and the incumbents, which cannot be predicted by housing characteristics alone. Relative to the incumbents, the new openings are superior in property size and quality, are expected to operate for a shorter period, and are priced significantly lower on days immediately after the wildfire. Together with a host of anecdotal evidence on altruistic behaviors, these facts provide evidence in support of a mechanism of altruistic sharing at play when a wildfire evacuation is in place.

To rationalize these facts and to quantify the welfare impacts of Airbnb, I then construct and estimate a structural model of the home-sharing market, where housing services are provided by heterogeneous hosts, and are demanded differentially by regular travelers and evacuees. The model incorporates three key innovations. First, because the customer type is not observed in the data, I develop a mixed Poisson model to microfound the arrival processes for different agents, which is identified by the nature of evacuation. Second, due to the fact that the Airbnb market is mostly uncleared with excess supply, it is unable to trace out the supply coefficients using the market equilibrium condition. Instead, I take advantage of observations in the supply-side data, namely the price offered and the opening status for each listing. Finally, by incorporating a rich set of interacted parameters, the model captures the heterogeneity in the home-sharing cost and the altruism across residents in different demographic groups.

The construction of the Airbnb demand model is shouldered on the literature of differentiated products with constrained capacity (Huang 2022) and residential sorting models (McFadden 1978; Bayer et al. 2007). I model the demand as a discrete choice problem over accommodation decisions defined by neighborhood and housing type. In addition to differential price elasticities and housing tastes between disaster evacuees and travelers, the model allows for heterogeneity in the horizontal preference over wildfire and smoke exposure. To address the price endogeneity, I propose two novel instruments. The first relies on the fact that manually adjusting price night by night is costly for resident hosts; as a result, the lack of temporal variation in price may reflect the cost of price adjustment. The second follows the standard BLP instrument on the characteristic space of competitors (Berry and Haile 2014). By averaging the individual-level time-invariant features to each neighborhood, the panel variations over time provide identifying variations on the change of market composition driven by the entry and exit.

I model the Airbnb supply of local residents as a discrete choice problem based on Calder-Wang (2021), where each resident makes a choice on whether and how to share her home at the prevailing price. The decision involves a trade-off between the price offered and the cost of providing such housing service. Motivated by the evidence of altruistic sharing, I incorporate a component on the additional benefit from home-sharing for disaster incidents. To estimate the coefficients in the presence of excessive supply, I leverage the high-frequency observations on the supply side of each listing, which contain the offered price and opening status for both occupied and unoccupied units. I employ an innovative adaptation of BLP methods (Berry et al. 1995; 2004) in the estimation of a heterogeneous supply system, where agents are local residents and products are home-sharing choices. I also exploit the individual-level data from the American Community Survey to obtain a full vector of demographic characteristics at the neighborhood level. The location of each Airbnb listing, together with the cross-sectional variations in neighborhood demographics, allow me to estimate the distribution of home-sharing cost and altruism by demographic features including income, education, family structure and home ownership. To address the price endogeneity, I exploit the correlation in demand shocks among different cities of California, and the lagged effect of disaster exposure on customer arrival through its impact on reservations.

To recover the model primitives, I use the transaction data spanning September 2014 to October 2016 for the Los Angeles Airbnb market, which has experienced numerous significant incidents of wildfire evacuation. The model estimates allow me to evaluate the welfare losses from short-term displacements, as well as the aggregate and distributional impacts of Airbnb on the mitigation. I conduct a counterfactual analysis to measure how the welfare consequences would change in the absence of altruistic sharing, in the absence of a home-sharing market, or if the customer type is fully observable to altruistic hosts. There are four primary findings.

First, there are large welfare losses of short-term displacement from disaster evacuation. In the absence of home-sharing accommodations, an average displaced household would lose a minimum of \$232 per day from not having the option of staying in their home, which equates to \$89 per capita. A small set of displaced families suffers a much heavier loss, at a magnitude of \$1000 per day. Aggregating over all affected households, I find the displacement losses are equivalent to at least 31% of the property damages directly related to wildfire in California.

Second, I find the option of Airbnb accommodations reduces the displacement losses by more than half, and the altruistic sharing contributes roughly 25% of the mitigation effect. Because of a failure to distinguish displaced households, there exists widespread free riding by regular travelers taking advantage of altruistic hosts. I find the welfare gains from altruistic sharing are of similar scale between evacuees and travelers, implying a substantial loss of efficiency due to free riders.

Third, the altruistic behavior comes exclusively from a subset of residents who are at a relatively high socioeconomic status, featuring high-income, well-educated, families with children, and homeowners. The altruistic hosts suffer a loss of $28 per day on average due to their generosity, as otherwise they would increase price by 5% and reduce supply by 2%. Due to free riders, non-altruistic hosts also lose from spillovers of generosity, at a magnitude comparable to the direct loss for altruistic hosts. This implies a failure in not only efficiency but also equity of the mitigation consequences.

Finally, I suggest that the free riding and the induced spillovers result from a failure to target displaced households. If one introduced a matching mechanism between altruistic hosts and displaced families, for example by home ZIP code, regular travelers would face a price increase of 4% and a supply expansion of 10% over the status quo. As a direct consequence, the generosity losses for non-altruistic hosts would be cancelled out, as would the gains from altruistic sharing for regular travelers. I find this would also slightly reduce the losses for altruistic hosts, and further increase the displacement mitigation gains.

For policy-making, this paper highlights three fundamental reasons why the peer production facilitated by digital innovation has a particular role to play in displacement mitigation. First, peer-to-peer marketplaces can make the previously underutilized resources held by local residents available online. These products, despite not being a perfect substitute for commercial facilities offered by companies, are valued by some customers because of increased variety and relatively lower price. The home-sharing products are particularly valuable to displaced households, who typically have a higher price elasticity and demand places that feature a more homey style for their entire family. Second, the traditional hospitality industry, primarily constituted by hotels, is technically constrained by a fixed inventory over a short term. This can result in a price increase and a failure to handle all arrivals during periods of peak demands, such as in the immediate aftermath of large-scale evacuation. Home-sharing production, instead, is rather flexible and can expand at exactly these emergencies, thus improving the consumer surplus for all and in particular displaced people. Finally, the sharing economy enables production by a wide distribution of peers, which also includes those who are keen on altruistic engagement. This demonstrates a market tool for emergency relief through human generosity. Contrary to typical policy prescriptions for disaster relief, the welfare implications through generous sharing neither involve price compression nor anticipate financial assistance. With a policy correction based on information disclosure, the generosity through peer-to-peer production can further demonstrate efficiency improvement and equity gain without intervention of policy makers.

Related Literature

This paper seeks to contribute to existing literature in three main ways. To the best of my knowledge, this paper is the first to construct a model of peer production in the presence of *supplier altruism*, while evaluating the economic impacts of a digital platform marketplace during *emergency incidents*. In carrying out the study, I contribute to the growing empirical literature on the sharing economy, such as Einav et al. (2016) for peer-to-peer production in general, Cohen et al. (2016) for Uber, Kroft and Pope (2014) and Seamans and Zhu (2014) for Craigslist, and Aguiar and Waldfogel (2018) for Spotify. The structural modeling in this paper enriches the growing body of reduced-form studies on the economic impacts of home-sharing platforms from various angles, including Zervas et al. (2017) on the hotel industry, Barron et al. (2021) and Horn and Merante (2017) on the rental market, and Koster et al. (2018), Valentin (2021), and Garcia-López et al. (2020) on the housing market. This paper in particular complements the few existing studies that adopt structural modelling to explore the impact of Airbnb. Farronato and Fradkin (2022) examine the welfare consequences of peer entry through Airbnb on the accommodation industry, highlighting the differential supply elasticities of resident hosts as opposed to incumbent hotels. Calder-Wang (2021) examines the impacts of Airbnb on the rental market through housing reallocation to quantify the welfare consequences on renters over the long term. Almagro and Domınguez-Iino (2019) estimate the externality of home-sharing on the endogenous neighborhood amenities, leveraging the substantial growth of Airbnb in Amsterdam. While they carry out a welfare analysis of Airbnb from different aspects, this paper is the first to examine the role of peer production on emergency incidents in the presence of supplier altruism.

The second main contribution of the paper is providing the first empirical estimate on the welfare loss of short-term displacement due to natural disaster and a discussion of the role of policy in its mitigation. An idealized disaster management cycle consists of three stages, namely preparedness, response, and recovery (Council et al. 2007; Dari-Mattiacci and Faure 2015). Existing literature on disaster mitigation is extensively focused on the first and the third stages. On the one hand, there is a rich body of study on disaster precaution to improve risk management and build resilience ex ante, such as Wagner (2022) and Bradt et al. (2021) for increasing the take-up of disaster insurance, Boustan et al. (2012), Bakkensen and Ma (2020), and Bernstein et al. (2020) for relocating residents away from disaster-prone areas, and Kocornik-Mina et al. (2020) and Mulder (2021) for improving the information on disaster predictions and recurring damages. On the other hand, there has been huge interest in policy solutions for disaster recovery over a period of months or years after disaster, such as Deryugina (2017), Baylis and Boomhower (2019), and Liao and Kousky (2022) for the utilization of government aid to assist the affected populations, McCaughey et al. (2018) and Mach et al. (2019) for the reconstruction of physical property damaged by disaster, and Taylor and Druckenmiller (2022) and Karwowski (2022) for the enhancement of land use and zoning regulations. This paper departs from existing literature by emphasizing the character of relief actions in the immediate aftermath of a disaster, and examining the role of peer-to-peer production in accommodation of the displaced over the short term. In doing so, I examine the peer production and generosity enabled by platform marketplaces as a market-based prescription for disaster mitigation.

Finally, I contribute to the nascent stream of literature on policy design for peer-to-peer marketplaces. Pan and Wang (2021) and Huang (2022) document the lack of price variation on Airbnb and attribute the frictions to menu costs and platform interface design. Brown and MacKay (2021) discuss the adaption of pricing algorithms of online retailers. In addition to the pricing rules, Belleflamme and Peitz (2020) explore theoretically a set of non-pricing decisions, including the setup of consumer ratings, recommendation systems, search rankings, price transparency, information accuracy, and certification systems. Empirically, Jia et al. (2021) highlight the role of cancellation policy in the presence of platform competition within the home-sharing industry, Hui et al. (2022) demonstrate the effect of a quality standard using replacement of the "Power Seller" badge with a more stringent "Top Rated Seller" badge on Ebay, and Lee et al. (2015) point out the effect of host reputation on the pricing decisions of Airbnb. My work complements the above by shedding some light on price discrimination and information asymmetry on platform marketplaces. In doing so, I also examine the efficiency and equity gains from the introduction of matching between altruistic suppliers and suffering customers. The findings suggest that some sort of third-degree discrimination, such as information disclosure based on home address, can improve the social welfare of platform companies for emergency responses.

The remainder of the paper is organized as follows. Section 1.2 discusses the background, introduces the data, and documents stylized facts. Section 1.3 presents the structural model. Section 1.4 discusses the estimation results. Section 1.5 presents counterfactual simulations and implications. Section 1.6 concludes the paper.

1.2 Background, Data, and Stylized Facts

In this section, I provide background on Airbnb and wildfire evacuation, discuss primary data sources, and document stylized facts to motivate the structured model in the next section.

Background

There have been an increasing number of devastating wildfires in the U.S., which have pushed many residents into challenging evacuation or displacement situations. California, in particular, experienced more than 11 catastrophic wildfires that prompted an evacuation of 10,000 or more households in 2017-2019 (Wong et al. 2020). Wildfire evacuation is designed to safeguard all households possibly in danger. In practice, a mandatory order is sent to all homes immediately threatened by the flames, and a warning is sent to all homes possibly threatened or under high-risk circumstances. Because utilities usually turn off power in places with possible ignition to reduce further risks of flames, even more homes are affected by a power outage and might choose to flee temporarily for power access.

In the immediate aftermath of a wildfire, considerable stress is placed on transportation infrastructure and sheltering. People who have the means to do so generally seek shelter at the homes of friends or relatives, followed by hotels and other commercial facilities, making public shelters a refuge of last resort (Lindell et al. 2018). A survey on wildfire evacuation suggests that more than half of evacuees do not have the option to stay with families or friends (Wong et al. 2020). Due to limited space in public shelters, the majority of evacuees have to pay to shelter at short-term rental facilities, such as hotels (Wong et al. 2022). Meanwhile, evacuation-induced costs remain largely under-insured and under-reimbursed. Federal assistance for evacuation reimbursement only applies to presidential declared disasters, and evacuees can seldom seek assistance from local agencies. [1] As a last resort, while many home insurance policies include some sort of coverage for “additional living expenses”

[1] Of the 81 wildfires in California that have received a governor’s declaration since 2015, only 16 have received a presidential declaration. Local emergency agencies generally lack public resources to adequately evacuate all populations in danger.

induced by natural disasters, policyholders are generally advised to avoid filing claims for evacuation-related expenses only, as the reimbursements are usually not large enough to justify the permanent increase in the insurance premium.

Home-sharing platforms have created a novel market for a previously rare transaction – the short-term rental of housing units supplied by residents directly to strangers. Among various platform companies, Airbnb, founded in 2008 and having experienced rapid growth over a decade, has become one of the dominant marketplaces in the U.S., accounting for approximately 75% of the total market revenue of the home-sharing industry nationwide (Schultz 2022). Los Angeles is the largest Airbnb market in California. More than 70,000 Airbnb listings experienced an active transaction during 2014-2016, representing 1.6% of all housing units. As Figure 1.1 shows, the average level of Airbnb activity masks an extensive geographic heterogeneity across neighborhoods.

Implied by its name, the sharing economy is built on the idea of collaborative consumption, breeding trust, generosity, and compassion among people. In 2012, inspired by altruistic hosts who requested permission to welcome people free of charge during Hurricane Sandy, Airbnb launched the "Open Homes Program" to facilitate offering free and discounted accommodations in times of emergency. This platform-wide initiative was formalized with the creation of the foundation Airbnb.org in 2020. [2] Starting with the outbreak of COVID-19, Airbnb has proposed a global initiative, the "Frontline Stays Program," to provide free and subsidized stays for health care professionals and relief workers. Instead of helping hosts defray all costs, the platform stimulates generosity by waiving service fees and partnering people in need with willing hosts during emergency incidents. [3] The recurring generosity of hosts has facilitated a reputation system among hosts, as Airbnb.org grants a supporter badge to hosts who have offered free or discounted stays to people during an emergency. [4]

[2] In 2020, Airbnb's Open Homes program turned into Airbnb.org, a 501(c)(3) nonprofit.
[3] Airbnb hosts don't have to offer their properties for free, but will still have all fees waived by Airbnb.
[4] Though Airbnb shares community members with Airbnb.org, Airbnb.org is an independent organization with a different board of directors.

Data

Airbnb Transaction

Data on the full sample of Airbnb transactions are obtained from a third-party data vendor, AirDNA, which has scraped Airbnb.com comprehensively on a daily basis since 2014. For each listing, the data consist of key characteristics, including listing type (entire home, private room, or shared room), the number of bedrooms, and the number of bathrooms, along with information related to Airbnb policies. The data allow for mapping each property to its corresponding neighborhood based on longitude and latitude information. [5] Figure A.2 displays the geographic distribution of Airbnb listings based on the property type.

An important feature of the data is the high-frequency panel at a daily level. The data contain the date on which a listing is first available and the date of its last appearance, which provides insight on the operation status. For each listing and every day of operation, the data allow for an observation on whether it is opened for booking, the offered price, whether a reservation has occurred, and, if so, when the booking has been made. I eliminate listings requiring a minimum stay of above 7 days, to limit the study to listings designed for short-term stays. I also reclassify the listing type to combine "private room" and "shared room" into a single category: "shared place." As hosts may set their rates prohibitively high in lieu of blocking off the calendar, I redefine an opening with a daily price above $1000 as unavailable.

Dynamic patterns exist in the Airbnb market, as Figure A.3 suggests. The Airbnb demand depicts a strong seasonality within a year, with peak demand in July and August and a trough season between September and New Year's Eve. In contrast, the price remains rather stable without seasonal trends. The capacity of Airbnb has more than quadrupled over the research period. In comparison, the growth of hotel room capacity has been less than 1% over the same period. [6] Interestingly, the market-clearing condition does not

[5] Airbnb adds a small perturbation to ensure privacy. The perturbation, up to 500 feet in distance, is unlikely to cause any measurement error in the neighborhood mapping.
[6] The hotel metrics come from Smith Travel Research (STR) Trend Reports and Farronato and Fradkin

hold for the Airbnb market, as the occupied units are far fewer than the units available for reservation. Table A.1 summarizes the statistics for the Airbnb transactions and property features over the research period. An average Airbnb listing charges \$155 per night, is open 71% of the time, and experiences an occupancy rate of 26%, very different from hotel rooms that are on average priced at \$220 per night, open throughout the entire year, and occupied 67% of the time. The standard deviations suggest great variation in listings on Airbnb. The distribution of price is highly skewed to the left with a long right tail (top panel of Figure A.4), indicating the broad availability of low-priced properties. Additionally, although an average listing expects customers to book 30 days ahead of arrival, "short booking" within 10 days is generally available for a significant share of listings (bottom panel of Figure A.4). These patterns indicate that Airbnb not only differs from hotels in terms of average price and housing quality, but also in market composition and the extent to which market conditions evolve over time.

Wildfire, Smoke and Evacuation Orders

The wildfire data come from the U.S. Geological Survey (USGS). As one of the most precise and comprehensive sets of wildfire observations, the data are created by merging and dissolving fire information from 12 different original fire observation sources. [7] The data include all fires in the US and consist of timelines of each fire, including ignition date, date controlled, and containment date. I limit the data to fires that were sourced within driving distance (300 km) from Los Angeles.

The smoke data come from the National Oceanic and Atmospheric Administration's Hazard Mapping System (HMS). HMS collects imaging information from seven NOAA and NASA satellites on an hourly basis, to perform automation and digitization of smoke plumes.

(2022).

[7] The data sources involve a variety of sources, such as satellite images, GPS points, and state and federal wildfire registries. The merged data are further corrected by an internal check based on topographic maps to eliminate duplicate boundaries.

[8] The data consist of geo-referenced shapes of all smoke plumes on a daily basis, with an estimate on the smoke-plume concentration categorized into three levels: $5\mu g/m^3$, $16\mu g/m^3$, and $27\mu g/m^3$. I limit the data to plumes of $27\mu g/m^3$ density, to remove the anthropogenic haze plumes mistakenly assigned as low-density smoke plumes and to better locate the source of fire. [9]

Smoke plumes data enable me to measure the smoke exposure for each property without predicting a smoke transport model. As a downside, technically, the smoke plumes are not paired with their fire sources. I connect each fire with its induced smoke, by constructing a spatial overlay of the fire's polygons with smoke plumes that happened between the ignition date and the containment date of the fire. [10] As Figure A.5 displays, while some fires are geographically small in scale, they have nevertheless generated significant smoke plumes that travel long distances.

When officials of the fire agency have determined the locations to be evacuated in response to a wildfire, formal documents are published to guide law enforcement agencies in executing the evacuation order. As an example, Figure A.6 shows an evacuation warning for the Soberanes Fire, issued on July 31, 2016. The document clearly states the fire name, the time of issuance, affected jurisdictions or locations, and the level of enforcement (evacuation order or warning). [11] I manually collect and digitize all wildfire evacuation documents to

[8] Smoke detection is done with visible-band imagery and is occasionally assisted by infrared to distinguish between clouds and smoke when possible (Ruminski et al. 2006; Rolph et al. 2009). Geostationary GOES acronym imagery, with its frequent refresh rate (typically every 15 minutes for each spacecraft), is used almost exclusively for smoke detection, although on rare occasions polar orbiting satellite imagery is used.

[9] Smoke can sometimes be transported to areas with anthropogenic haze pollution and then mix with and become indistinguishable from the anthropogenic haze pollution. Smoke and anthropogenic haze cannot be distinguished or directed because no information about the vertical location or extent of smoke plumes is provided. Smoke plumes of varying concentrations are often nested as higher-density plumes occurring within a lower-density plume, implying smoke transportation.

[10] I limit the data to high-density plumes to eliminate smoke that transported over a long distance with a faded density and coincidentally overlays smoke from the fire of interest. A potential concern with the pairing is that it does not allow separation of smoke from fires that happened within a small geographical range. This is unlikely to be an issue here, as a treatment event is defined as a *day* of fire instead of a *fire*, as discussed later in Section 11.

[11] When an evacuation order is relaxed, a similar document is published for the law enforcement agency and on social media platforms (e.g. Twitter).

construct the full history of wildfire evacuation over the research period. Furthermore, the geo-referenced locations of evacuation zones allow me to obtain the demographic information of evacuated populations, using the Population Density Grid data from NASA's Socioeconomic Data and Applications Center (SEDAC). Hereafter, I do not distinguish between evacuation order and evacuation warning, and incorporate both in the analysis.

Figure 1.2 plots the location of fires that happened within driving distance (300km) from Los Angeles and prompted an evacuation over the research period. Ninety wildfire events occurring in 22 days led to evacuation, and none of them occurred within the Los Angeles metropolitan area. Because the question of interest is the response in the Airbnb market *when* an evacuation becomes active, I combine evacuation orders that were issued on the same day or within three days. Figure 1.3 summarizes the timing and magnitude of the 15 evacuation events over the research period. On average, the number of people forced to evacuate is more than 10 times the population directly affected by the flames. More summary statistics of these evacuations are provided in Table A.2.

Stylized Facts

I begin by presenting evidence on the supply expansion of Airbnb in response to wildfire evacuation, then compare the characteristics of the new listings relative to the incumbents. I show that these facts are consistent with altruistic sharing. Technically, Airbnb hosts make decisions about supply in two stages: whether to become a host and have their housing service appear online, and whether to have their listing open for reservation on a given day. I define these decisions respectively as the extensive margin and intensive margin of supply, and document them separately.

Extensive Margin of Supply

I develop an event study framework to compare the number of Airbnb hosts across neighborhoods, defined by Public Use Microdata Areas (PUMA), with different evacuation timing and fire intensity:

$$\ln(\#\ \text{Host}_{nt}) = \sum_{\tau=-7}^{7} \beta_\tau \text{Post}_{t\tau} + \alpha' \mathbf{X}_{nt} + \alpha_t + \alpha_n + \epsilon_{nt}$$

The dependent variable is the log transformation of the number of Airbnb hosts in PUMA n for day t. The main regressor is a set of dummy variables together capturing an event time frame starting from 7 days before the evacuation issuance and extending to 7 days after. The variable $\text{Post}_{t\tau}$ is an indicator of the τ-th day after the evacuation issuance. The model includes a vector of controls, $\mathbf{X}_{nt}$, which contains the acreage of the evacuation zone and the number of people evacuated. The model also includes PUMA fixed effects α_n to control for time-invariant features at the neighborhood level, and a set of time controls α_t, including year-month, day-of-week and holiday fixed effects, to control for the general trends in the market composition of Airbnb.

In Panel A of Figure 1.4, each coefficient corresponds to a day relative to the evacuation issuance and estimates the response in the extensive margin of supply. These coefficients trace out an immediate response in the number of Airbnb hosts equivalent to 0.5% of the number of incumbents, a peak of an 0.8% increase at 5 days after the evacuation, and a subsequent decline back to the pre-disaster level after 7 days. The responses are more pronounced for the shared places, slightly less intense but still significant for the entire units. This suggests that wildfire evacuation leads to an expansion of Airbnb supply by favoring the entry of all types of listings. To see that the increasing entry is not caused by a demand surge or market power, I re-estimate the event study framework using public holiday events. If market power were a decisive determinant, we would see a similar supply expansion following the demand shocks of holidays. As Panel A of Figure A.7 shows, in contrast, the number of Airbnb hosts shows an imprecise drop after a public holiday. This suggests that the expansion in the extensive supply after wildfire evacuation is not driven by market power or demand surge.

Intensive Margin of Supply

Next, I document the response in the *intensive* margin of Airbnb supply, measured by the probability of opening for reservation. Similarly, I exploit an event study framework with a logistic linkage, to capture the response to a wildfire evacuation:

$$\Pr(\text{Open})_{it} = \sum_{\tau=-7}^{7} \beta_\tau \text{Post}_{t\tau} + \alpha' \mathbf{X}_{it} + \alpha_t + \alpha_i + \epsilon_{nt}$$

where, similarly, the main regressor is a set of dummy variables together capturing an event time frame starting from 7 days before and extending to 7 days after a wildfire evacuation. The main dependent variable is the indicator for opening of listing i on day t, transformed by a logistic model. The vector of controls, $\mathbf{X}_{it}$, is on the listing-by-day level. Aside from controlling for the acreage and the number of households in the evacuation zone, it further contains the property characteristics, including the number of bedrooms, the number of bathrooms, the rating score, and the cancellation policy. In addition to the full set of time fixed effects α_t, I also include the zip-code-by-listing-type fixed effects, denoted by α_i, to control for time-invariant features based on property type.

In Panel B of Figure 1.4, coefficients report the marginal effect at the mean (MEM) on the intensive margin of supply. I find the average opening probability increases immediately after the issuance of the evacuation order, peaking at 0.3% at 4 days after, and staying high relative to the pre-evacuation level over the following week. Both entire and sharing units experience a higher probability of opening; the responses for the sharing units are slightly larger in percentage magnitude. Similarly, as a placebo test, I find the demand shocks of public holidays instead cause a pre-trend reduction in the opening probability of 0.8% of the pre-holiday level, and a slightly recovering post-trend that is not large enough to make up for the pre-trend reduction. These contradictions suggest that the expansion in the intensive supply following a wildfire evacuation is not a result of the demand surge caused by evacuees' arrival.

Comparison of New and Incumbent Listings

Knowing that an evacuation can lead to supply expansions in both extensive and intensive margins, I then explore the differences between the new openings that became available only after a wildfire evacuation order, relative to the incumbents. I utilize a event study framework to compare the characteristics with different evacuation timing between the new and incumbent listings:

$$Y_{it} = \sum_{\tau=-7}^{7} \beta_{1,\tau} \text{Post}_{t\tau} \cdot I(\text{Old})_i + \sum_{\tau=0}^{7} \beta_{2,\tau} \text{Post}_{t\tau} (\text{New})_i + \alpha' \mathbf{X}_{it} + \alpha_t + \alpha_i + \epsilon_{nt}$$

where the main regressor is a set of dummies together capturing an event time frame starting from 7 days before the evacuation was announced to 7 days after for the incumbents, and from the day the evacuation was announced to 7 days afterwards for the new openings. I define the incumbent properties as those that have ever been available in the month before the evacuation. The vector of controls, $\mathbf{X}_{it}$, includes the same set of property characteristics as the previous model. Again, the model includes a full set of time fixed effects α_t and zip code by listing type fixed effects α_i.

The set of dependent variables captures four property patterns of interest: the property size measured by the number of bedrooms, the property quality measured by the rating score, the time length of operation, and the price. The first three patterns are rather stable at the property level. The results are shown in Figure 1.5. For the incumbent listings, I find that the three time-invariant patterns do not respond to an evacuation, indicating a stable composition of the incumbents during disasters. In comparison, the new openings have a higher number of bedrooms, have a slightly higher rating score, and are expected to operate for a significantly shorter period. In the bottom-right panel, I find the prices of the new openings are significantly lower than the incumbents, after controlling for all relevant property features and location fixed effects. Combining all the facts suggests that the new openings are of larger size and better quality, but are priced substantially lower than the incumbents, and they are likely intended only for disaster accommodation instead of long-term operation. These observations provide motivating facts for the existence of altruistic sharing, which appears more pronounced among the new entries.

Anecdotal Evidence of Altruistic Sharing

Airbnb has self-reported that it has made more than 100,000 free or discounted stays available to people in crises, including asylum seekers, essential workers on the front lines of the global pandemic, and evacuees fleeing catastrophic disasters around the world (Lyons 2020). Since the facilitation of generous offering and formalization of disaster response was initiated on the platform level, there has been a good deal of anecdotal evidence of benevolent offerings made by warmhearted hosts on Airbnb during moments of emergency.

For instance, in the aftermath of Superstorm Sandy, Shell, an Airbnb host in Brooklyn, contacted Airbnb and asked if she could offer her place for free to people who had to evacuate, and was approved by the platform. Soon afterwards, over 1,400 hosts had opened their homes to those hit by the storm (Airbnb 2018). To date, generous offerings have been made in hundreds of disasters and provided temporary housing for the displaced around the world (Gibson 2019). For instance, in response to the 2018 wildfire season in California, over 2,500 people found temporary housing free of charge on Airbnb. After Hurricane Harvey hit Houston in 2016, over 1,000 hosts opened their homes and housed over 1,400 people impacted by the disaster. Other activations include Puerto Rico after Hurricane Maria, the 2017 Puebla earthquake in Mexico, Hurricane Florence in 2018, and currently for Ukrainian refugees.

These lessons suggest that effective empathy and compassion are the root of the generous offering and benevolent sharing. This is conveyed by many families who have made their homes available to those in need. For example, after Hurricane Matthew, a host said, “the fact that you get to meet great people that you would never have met if it wasn’t for the terrible circumstances is the good side of any tragedy.” (Airbnb 2020) A family in Portland has hosted five frontline workers for a total of 59 free nights, and described their appreciation of these offerings as, "I feel really grateful that we had an opportunity to feel like we were part of trying to make things better... It was such a hard time, you felt like you wanted to do something, and you just didn't know what to do." Many displaced people would have no place to stay otherwise. A nurse in British Columbia, for example, "was feeling increasingly desperate and was considering living in her car... [she] can't thank [her] host enough for inviting [her] to use their fantastic house that is well-stocked, safe, and quiet."

1.3 Structural Model

This section introduces the structural model, which consists of three parts: (1) arrival of customers of different types, (2) customer demand for Airbnb housing, and (3) the supply decision on home sharing by resident hosts. The purpose of structural modeling is to estimate the arrival parameters, demand primitives, and residents' opportunity costs for home sharing, which form the basis for market simulation under counterfactual circumstances.

The model features a random utility framework on the demand and supply sides of the Airbnb market based on Calder-Wang (2021) and Huang (2022), with two key innovations. First, I take advantage of the nature of evacuation to identify the customer arrivals of different types. This allows me to separate out regular visitors and evacuees from the aggregate data observed. Second, I incorporate "altruistic sharing" by allowing the opportunity costs for home sharing to vary by evacuation status, which enables easy transformation of the primitives for altruism to monetary value.

Arrival of Customers by Type

I begin by developing a mixture of a Poisson arrival model to separate out the arrival of customers by type, namely regular travelers and evacuees. The necessity for modelling the arrival process stems from the *Nondiscrimination* policy on Airbnb, which results in a failure to distinguish between travelers and evacuees from the aggregate data observed. [12]

Two types of customers, denoted $k = 1$ for regular travelers and $k = 2$ for evacuees, arrive at the Los Angeles Airbnb market. Customer i of type k looks for Airbnb housing for day t. Her possibility for booking on day $\tau \leq t$ follows a Poisson process at parameter $\lambda_{t\tau}^k$. [13] Thanks to the additivity of the Poisson process, the number of customers of type k for day t, denoted as M_t^k, follows a Poisson process of parameter $\lambda_t^k = \sum_{\tau \leq t} \lambda_{t\tau}^k$. The aggregate number of customers for day t, denoted as M_t, also follows a Poisson process with the parameter as the sum of parameters for travelers and evacuees, $\lambda_t^1 + \lambda_t^2$.

I assume the arrival parameter of regular travelers depends on the wildfire exposure (the share of residents exposed to fire), smoke exposure (the share of residents exposed to smoke), the indicator for public holiday, the day-of-week and month fixed effects, and a quadratic time trend, under an exponential linkage:

$$\lambda_t^1 = \exp(\gamma_1 \mathbf{X}_t^1 + u_t^1) \text{ , where } \mathbf{X}_t^1 = [\text{Fire}_t, \text{Smoke}_t, \text{Holiday}_t, \text{DOW}_t, \text{Month}_t, t, t^2]$$

I assume evacuees would only arrive if there is an evacuation in place. In other words, on days without an active evacuation, all customers on Airbnb are regular travelers. Given a day under evacuation, I assume the arrival rate of evacuees depends on the number of evacuated households, the demographics of evacuees, including the share of white, black, Hispanic, Asian, female-headed, young, and elderly evacuees, as well as the wildfire exposure, the smoke exposure, the indicator for public holiday, and the day-of-week fixed effects. Specifically:

$$\lambda_t^2 = E_t \exp(\gamma_2 \mathbf{X}_t^2 + u_t^2) \text{ , where } \mathbf{X}_t^2 = [\#\text{HH}_t, \text{Demog}_t, \text{Fire}_t, \text{Smoke}_t, \text{Holiday}_t, \text{DOW}_t]$$

and E_t is the indicator for active evacuation order on day t.

[12] Nondiscrimination policy of Airbnb: https://www.airbnb.com/help/article/2867/nondiscrimination-policy

[13] In practice, how far in advance a customer can book depends on how far the host sets in the calendar. Airbnb allows hosts to set up the calendar up to two years in advance, so $\tau \geq t - 730$.

Customer Demand for Airbnb

I model the demand system as a random utility framework based on McFadden (1978), Bayer et al. (2007), and Huang (2022). The two types of customers, regular travelers and evacuees, have heterogeneous preferences over short-term accommodations. Each custumer faces a discrete choice problem over Airbnb housing defined by neighborhood and property type, which is generated from a re-categorization: *Upscale* (entire place with more than 2 bedrooms), *Midscale* (entire place with 1 bedroom), and *Shared*. In total, this results in 261 housing choices in the Los Angeles Airbnb market.

Customer i of type k looks for housing on Airbnb and chooses among neighborhoods $n \in N$ and property type $h \in \{\text{Upscale, Midscale, Shared}\}$, with the choice variable denoted as $j = (n, h)$. Her utility for housing choice j is

$$u_{ijt}^D = \beta_i^D \mathbf{X}_{jt} + \xi_{jt}^D + \epsilon_{ijt}^D$$

where the superscript D indicates parameters pertaining to customer demand. $\mathbf{X}_{jt}$ controls for property features and neighborhood attributes, including the housing price, property type, fire exposure, smoke exposure, and time-invariant features captured by the neighborhood fixed effects. I also control for a set of time variables, including the indicator for public holiday, the day-of-week and month fixed effects, and a quadratic time trend. ξ_{jt}^D captures unobserved demand shocks such as temporary local events, which could be correlated with price. ϵ_{ijt}^D is assumed to be a Type-1 extreme value error term.

The taste parameters β_i^D are determined in a flexible way based on customer type, reflecting the differences in preferences between travelers and evacuees. I parameterize β_i^D as the sum of three components: a linear coefficient common to all customers, a heterogeneous component that is specific to evacuees, and a random component capturing unobserved preference shocks:

$$\beta_i^D = \underbrace{\beta_0^D}_{\text{linear coefficient}} + \underbrace{\mathcal{B}^{\mathcal{D}} \cdot I_{\{k=2\}}}_{\text{evacuee specific}} + \underbrace{\Omega^D \cdot \omega_i^D}_{\text{random part}}$$

where Ω^D is the variance covariance matrix of the random component, and ω_i^D is the vector of error terms, which is assumed to follow an i.i.d. normal distribution.

The outside choice of not staying in an Airbnb place is normalized as $u_{i0t}^D = 0$. With this structure, the demand for housing j on day t is obtained by integrating the individual choice over all customers

$$D_{jt} = \int_i I_{\{u_{it,j}^D > u_{it,-j}^D\}} dP(\epsilon_{ijt}^D) dP(k)$$

where $P(k)$ is the empirical composition of customers of type k, between evacuees and travelers. [14]

Airbnb Supply from Resident Host

An important difference between home-sharing platforms and traditional commercial facilities is the option for residents to host strangers at their homes. With this difference in mind, I model the supply of Airbnb as a discrete choice problem on home sharing, where each resident decides whether and how to share her home at the prevailing market price. Her trade-off is based on the payment received from hosting and the perceived opportunity cost from offering her home. The model features a novel extension of the canonical BLP methods for demand estimation (Berry et al. 1995) to estimating a heterogeneous supply system.

Residents are differentiated into types $k \in K$ by their demographic features, including income, education, family structure, and homeownership. Resident i of type k living in neighborhood n makes a decision on whether and how to share her home on a given day t, between *entire* sharing or *partial* sharing, denoted as $j \in \{\text{Entire, Partial}\}$. Her utility for home-sharing choice j is

$$u_{intj}^S = \beta_i^S \mathbf{X}_{njt}^S + \xi_{njt}^S + \epsilon_{injt}^S$$

where the superscript S indicates parameters pertaining to the supply side. $\mathbf{X}_{njt}^S$ captures the benefits and costs related to home sharing, including three components. First, the monetary

[14] Unlike most literature on demand system estimation, the customer proportions are not observed from data. Hence, I will need to simulate the customer fractions M_t^k from the previous subsection.

benefit of home-sharing is the income she makes from sharing her home, measured by the market prevailing price p_{ntj}. Second, providing housing service is accompanied with a cost, such as the opportunity costs from not being able to stay by herself, the noise made by guests, and other hassles related to home sharing. Such cost depends on whether her home is entirely or partially shared, so it is measured by an indicator for the home-sharing choice j. Finally, to incorporate the altruistic incentive, I augment the model by a component on the *perceived benefit* of home sharing in the presence of wildfire evacuation. Specifically,

$$\mathbf{X}_{njt}^{S} = (\underbrace{p_{njt}}_{\text{Monetary Benefit}} , \underbrace{j}_{\text{Home-sharing Cost}} , \underbrace{j \cdot I_{\{E_t=1\}}}_{\text{Perceived Benefit from Altruism}})$$

where E_t is a dummy for whether there is an evacuation in place on day t. X_{njt}^{S} also includes a set of neighborhood attributes and time variables, such as fire exposure, smoke exposure, neighborhood fixed effects defined by PUMA, an indicator for public holidays, the day-of-week and month fixed effects, and a quadratic time trend.

The model allows for unobserved home-sharing costs, ξ_{njt}^{S}, which could be correlated with the prevailing price. ϵ_{injt}^{S} captures household-specific idiosyncratic taste shocks for home-sharing and is assumed to be a Type-1 extreme value error term. The outside option of not sharing is normalized as $u_{int0}^{S} = 0$. [15]

The home-sharing decision depends on how the monetary and altruism benefits are valued relative to the costs. To capture heterogeneity, I parameterize the taste coefficients β_i^S as the sum of three components: a common component, a heterogeneous component that depends on observed demographic characteristics, and a random component capturing unobserved heterogeneity:

$$\beta_i^S = \underbrace{\beta^S}_{\text{common coefficient}} + \underbrace{\mathcal{B}^S \cdot \mathbf{D}_i}_{\text{by demographics}} + \underbrace{\Omega^S \cdot \omega_i^S}_{\text{random part}}$$

where $\mathbf{D}_i$ captures demographic features including income, education, family structure, and home ownership. Ω^S is the variance-covariance matrix of the random component, and ω_i^S is the error term drawn from an i.i.d. normal distribution.

[15] Under this assumption, the model incorporates entry and exit as switching between the sharing options and the outside option.

1.4 Estimation

The estimation of the structural model is composed of three steps. First, I estimate the model of customer arrival using the aggregate data across all neighborhoods. Second, I estimate demand using the customer size estimated from the first step. Finally, I estimate supply using high-frequency observations on the opening status of Airbnb listings.

Estimating Customer Arrival by Type

Recall that the observation is the aggregate arrival for each day, which needs to be separated into arrivals of travelers and of evacuees. The basis of identification is to restrict the evacuees' arrival only to days with an active evacuation order. This assumption enables particular use of the days in the absence of evacuation, where the aggregate arrivals observed are exclusively from regular travelers. Additionally, because I allow wildfire and smoke exposure to affect the arrival of both travelers and evacuees, identifying them separately would fail if the evacuation timing coincides with the occurrence of wildfire or smoke. Therefore, the identification also relies on misalignment in the evacuation timing with the occurrence of wildfire and smoke. This is justified by the data, as Figure 1.6 shows. Because not every flame leads to an evacuation, the occurrence of wildfire and smoke is more dispersed over time.

To recover the arrival parameters, I implement the estimation strategy using the mixture of Poisson regression model from the statistics literature (Land et al. 1996; Wang et al. 2007; Papastamoulis et al. 2016). [16] The log-likelihood function for the best linear unbiased prediction (BLUP) is given by the sum of two components: the log-likelihood function when the random effects are conditionally fixed, and the penalty of random errors for the conditional log-likelihood. I implement the Expected Maximum (EM) algorithm to maximize the observed log-likelihood. More details on the algorithm and the model fit are discussed in Appendix A.1.

[16] The mixture of Poisson regression modeling usually applies to the circumstance where the count data are overdispersed, which is naturally satisfied here as the variance of the aggregate arrival far exceeds its mean in the data.

Table 1.1 presents the arrival parameters. For regular travelers, I find the wildfire exposure in a destination has a pronounced yet imprecisely estimated negative effect on the arrivals, while smoke exposure can significantly discourage the arrivals at a magnitude of roughly a quarter of the additional arrival attracted on a public holiday. This is because wildfire is usually concentrated in the northern hills of Los Angeles, which are far from tourism attractions and business centers, while smoke is more dispersed over space. For every 1000 households forced to evacuate, approximately 120 of them turned to the Airbnb market for shelter. The arrival rate also varies by demographics. White and female-headed households are more inclined to evacuate and stay at Airbnb, while elderly people are less likely to choose Airbnb for shelter. The fire exposure of the destination place also strongly discourages the arrival of evacuees.

Estimating Demand for Airbnb

Under the assumption of logit error, the probability for customer i of type k on housing choice j is

$$\Pr(j; i \in k, \delta^D, \mathcal{B}^D, \Omega^D, t) = \frac{\exp(\delta_{jt}^D + \mu_{ijt}^D)}{1 + \sum_{j'} \exp(\delta_{j't}^D + \mu_{ij't}^D)}$$

where δ_{jt}^D is the mean utility from housing choice j, and μ_{ijt}^D is the heterogeneous utility specific to customer i. Because the customer type is not observed from the data, I use the estimates from Section 1.4. Then, the market share for housing choice j on day t can be estimated as the probability that travelers and evacuees choose that housing type, weighted by the model fits on their respective arrival size. I construct a moment condition to match the market shares:

$$\forall j: \; E\left[\Pr(j; \delta^D, \mathcal{B}^D, \Omega^D, t)\right] = s_{jt}^D$$

where the left-hand side is the model prediction based on the fitted value of customer arrivals, and the right-hand side is the empirical market share implied from the occupancy status from the data.

The model has an endogeneity issue, as the demand shifters ξ_{jt} capture shocks by unobserved local events that might correlate with price. I instrument the price using two sets of measures that can shift the supply exogenously. The first instrument leverages the extent of pricing frictions on Airbnb. Because most hosts have to set price manually for each day of opening, there are widespread intentions for uniform pricing across unrelated nights (Huang 2022). [17] The behavioral costs for manual pricing cause the prices of consecutive days, or days of the same day-of-the-week, either to be persistent or to adjust at the same time. For instance, Figure A.8 shows the clustering pattern of pricing for 20 randomly drawn listings; roughly 80% of all listings show no more than two unique price levels every month. Based on this observation, I construct a set of price instruments using the average price of the same day-of-the-week in the previous month, the one-month lagged price of the same day, and the average price in the lagged month. The second instrument takes advantage of the rich scope of housing characteristics, and exploits the panel variations driven by the entry and exit of listings of similar characteristics (Berry et al. 1995; Bayer et al. 2007). Some characteristics tend to be time-invariant, including the rating score, the cancellation policy, the cleaning fee, and the security deposit. After averaging them out to the neighborhood level, what remains to drive the panel variation can only be the evolution of market composition driven by entry and exit. Therefore, I construct the instrument by averaging the time-invariant characteristics to the neighborhood level. I find these instruments strongly predict the prices, with an excluded-variable F-statistic on the order of 100 with the same control of time and neighborhood fixed effects.

To estimate a demand system with 155,744 moment conditions on market share, I cast the problem as a minimization routine over the GMM objective, applying a nested fixed point algorithm. Table 1.2 summarizes the demand coefficients of travelers and evacuees. In columns (1) and (2), I find the price coefficient is more negative for evacuees, implying

[17] Starting November 2015, Airbnb introduced a smart pricing tool to assist its users in setting prices automatically. Over the research period up to October 2016, the majority of hosts had not yet chosen to opt into the pricing tool.

that evacuees are more price elastic to short-term housing than regular travelers. Columns (3) and (4) report the derived willingness to pay (WTP) for Airbnb accommodations. An average traveler is willing to pay $138, $202, and $97 for a day in Midscale, Upscale and Shared listings respectively. The WTP of evacuees are generally lower, at $116, $192, and $77 respectively. Evacuees hold lower WTP for two reasons: there remains an outside choice of public shelter free of charge, and they are more price elastic due to the stringency of the budget constraint resulting from other logistical needs associated with evacuation. I also find a pronounced disutility from fire exposure for both travelers and evacuees; smoke exposure reduces the WTP for Airbnb by a moderate magnitude.

Figure 1.7 shows the destination of evacuees to the Los Angeles Airbnb market. Evacuees are disproportionately concentrated over a handful of neighborhoods, featuring low prices and smaller distances from their origins (Figure A.9). The majority of neighborhoods are generally not popular for sheltering, attracting less than 1% of evacuees in aggregate. Moreover, I find evacuees are more inclined toward housing units with larger size. 53.9% of evacuees choose to shelter at an Upscale house, 34.5% of evacuees choose to stay in a Midscale house, and only 11.6% of evacuees choose a shared place for sheltering. The allocation of housing choice reflects the need for spatial and private accommodations during evacuation to care for the entire family and material possessions. The destination is also disproportionately distributed over space for each type of housing, as illustrated in Figure A.10.

Estimating Home-sharing Supply from Resident Hosts

Although the BLP framework is typically used in demand system estimation, the data on Airbnb supply make it possible to adapt it for estimating a random-coefficient supply system. The key insight is to match the market share of home-sharing decisions implied from the observations on opening status. Under the assumption of logit error, the probability of resident i in neighborhood n making home-sharing choice j is

$$\Pr(j; i, \delta^S, \mathcal{B}^S, \Omega^S, t, n) = \frac{\exp(\delta^S_{jnt} + \mu^S_{ijnt})}{1 + \sum_{j'} \exp(\delta^S_{j'nt} + \mu^S_{ij'nt})}$$

where δ^S_{jnt} is the mean utility of choice j in neighborhood n, and μ^S_{ijnt} is the heterogeneous part of the utility specific to resident i. Then, the moment condition is to match the aggregate supply of home sharing implied from the model estimates with the empirical supply observed in the data.

The cost shifters ξ^S_{jnt} capture the unobserved opportunity cost of home-sharing, which could be correlated with price. For instance, ξ^S_{jnt} includes the increased hassle of hosting visitors during an overnight shared housing event, which remains observable to hosts and may affect the hosting price. To tackle the endogeneity concern, I construct two sets of instruments based on the demand shifters for Airbnb. First, I leverage the extent of demand shocks that are common to all Californian cities and utilize their correlation. Specifically, I construct the average occupancy rates and the average market prices for the same days of the Airbnb market in San Diego and San Francisco. [18] Second, I take advantage of the fact that Airbnb reservations happen 30 days ahead of arrival on average. Then, the wildfire and smoke exposure of 30 days ago may reduce customer arrival today by discouraging reservations. Meanwhile, the 30-day lagged exposure to wildfire and smoke is unlikely to have an effect on home-sharing decisions today. [19] Based on this fact, I use the one-month-lagged wildfire and smoke exposure for each property as a price instrument. [20] I find these

[18] After controlling for a set of calendar-related effects, these instruments then exploit the variations in the Airbnb demand of Los Angeles and San Diego that are idiosyncratic by time, for instance, an extreme weather event in Southern California that affects the desirability of visiting both Los Angeles and San Diego. There is unlikely to be any correlation remaining in the home-sharing cost between San Diego and Los Angeles after controlling a host of calendar-related effects, including month, day-of-the-week, and holiday fixed effects.

[19] After limiting the sample to listings that remained open over the research period, the wildfire and smoke events a month ago are unlikely to affect the cost of home-sharing at the time of study. Because all evacuation orders of interest are in place for no more than three weeks, there is little concern for a wildfire evacuation to continue affecting home-sharing behaviors one month after the fire.

[20] Wildfire and smoke exposure can also have a persistent effect on customer demand, as customers can update their expectations of the disaster risk based on historical information. Therefore, customers may change their travel plans for the near future based on disaster exposure information.

instruments can strongly predict the prevailing price of Airbnb, with an excluded-variable F statistic on the order of 100.

Similar to the demand analysis in the previous section, to estimate the supply system with 132,302 aggregate supply conditions, I cast the problem as a minimization routine over the GMM objective, applying a nested fixed point algorithm. Table 1.3 summarizes willingness to accept (WTA) for home sharing in monetary value as transformed from the raw coefficients (Table A.3). I find the home-sharing cost for an average resident is high, \$220 per night for entire sharing and \$79 for partial sharing. The home-sharing cost varies with the demographic features of the host; it is higher for those with high income, the well-educated, families with children, and homeowners. In terms of altruism, as column (1) shows, an average host does not obtain additional utility from home-sharing in the presence of evacuation, so she chooses to not provide altruistic sharing. The additional WTA for home-sharing during evacuation is negative only for households with high income, with a college degree, and with children. This suggests that altruistic sharing is provided only by hosts with relatively good socioeconomic status. In contrast, households of low income, without a college degree, and without children have a higher WTA for home-sharing when there is an active wildfire evacuation.

1.5 Counterfactuals

Given the estimates, I perform three counterfactual analyses to measure the welfare impacts of Airbnb. The first removes the welfare gains from altruism. The second terminates the Airbnb option to estimate its net impact. Finally, I discuss the welfare consequences if there were a perfect pairing for altruistic sharing. Table 1.4 summarizes the changes in market outcomes under the three counterfactuals relative to the baseline (the status quo).

Analysis Strategy

No Altruistic Sharing

The first scenario looks at what would happen if the generosity were fully removed. In this world, Airbnb hosts would not obtain additional gains or losses from home-sharing in disaster times. Appendix A.2 describes how the counterfactual equilibrium is computed.

I find that Airbnb price and supply would change in a significant manner if there were no generosity. The average price would increase by 4.8%, with the prices of entire sharing and partial sharing increasing by 3.2% and 9.1% respectively. The counterfactual supply would drop by 1.8%, which consists of an 18.4% reduction in entire sharing and a 19.5% increase in partial sharing. In terms of heterogeneity over geography, Figure 1.8 suggests that neighborhoods that have attracted more evacuees would see a higher counterfactual price if the altruistic sharing became unavailable. [21] This is primarily driven by entire sharing rather than partial sharing (Figure A.12), which is consistent with the dominance of evacuees' choice on Upscale and Midscale listings.

No Airbnb

To estimate the overall welfare impacts of Airbnb, I perform a counterfactual analysis where Airbnb is removed. Airbnb accommodation is no long available for customers, and the option for residents to host on Airbnb is terminated. This would result in all agents losing, and the welfare loss measures the gains that Airbnb brings in the baseline. Appendix A.2 describes how the counterfactual equilibrium is computed.

No Free-Riding

Due to an inability to limit offerings to evacuees, regular travelers can free ride on the altruistic sharing offered at a lower price, and non-altruistic hosts are expected to suffer a

[21] These places would also experience more reduction in supply if altruistic sharing were unavailable, as Figure A.11 sshows.

loss from having fewer customers. As a result, both altruistic and non-altruistic hosts are exposed to the welfare consequences from altruism. I next explore what would happen if such free-riding were prohibited. This could be realized by some sort of platform intervention, such as a matching between evacuees and altruistic hosts, or a disclosure of information on customer home ZIP code.

In this scenario, regular travelers are hosted only by non-altruistic families, and altruistic hosts can target evacuees. Therefore, there exist separate pricing levels for evacuees and travelers, where the price for evacuees is determined by altruistic hosts, and the price for travelers by non-altruistic hosts. Nor surprisingly, I find the price for travelers would increase by 6.3%, with the supply from non-altruistic hosts rising by 11.9%. Meanwhile, the pricing level for evacuees would drop by 7.8%, with the supply of altruistic sharing slightly lower, by 0.6%. There are two drivers for the change in supply made by altruistic hosts. First, the WTP for Airbnb is generally lower among evacuees, resulting in a reduction of the pricing for altruistic sharing. Second, as altruistic hosts are less price elastic, their supply would not drop as much as the price. [22]

Displacement Costs

I first calculate the welfare losses from displacement in the absence of Airbnb, which can illustrate the extent to which home-sharing accommodation mitigates losses for displaced people. Intuitively, households who are forced to flee from their homes lose from displacement, measured by the welfare difference between displaced status and staying home. Based on the fact that many evacuated families choose a home-style accommodation for sheltering, I assume that households are indifferent between staying home and staying at the Airbnb free of charge. [23] Appendix A.2 provides more details on the welfare calculation.

[22] The model ignores any behavioral response, as the intention for altruistic sharing might become stronger if free-riding is removed.

[23] This assumption likely produces a lower bound on the displacement cost, because displaced people may actually choose a sheltering place inferior to their homes due to tightened budget constraints and a high price elasticity. Moreover, the estimation ignores other logistical costs related to displacement, such as

Not surprisingly, displaced people suffer a loss from not having the option of staying home. An average household loses \$231.99 per day from being displaced. In terms of heterogeneity, I find the distribution of displacement loss features a heavy right tail, suggesting the bulk of losses accrue to a concentrated few people (Figure A.13). The median loss is \$119.8 per day, while a household at the 95th percentile loses \$849.2 per day from displacement.

In 2019, the four major wildfire incidents in California forced more than 375,000 households to evacuate (Wong et al. 2020). Integrating over all displaced households produces a total welfare loss of \$870 million. As the property damage induced by the same wildfire season is approximately \$2.8 billion (Ahrens and Evarts 2021), I find the displacement cost amounts to at least 31% of the direct damage to physical property.

Correction of Free Riding

The Status Quo

Although altruistic sharing is intended for disaster refugees, regular travelers can also enjoy the discounted price and expanded supply offered by generous hosts due to information asymmetry. I find the welfare gains from altruistic sharing are of a comparable magnitude for evacuees and regular travelers. An average evacuee gains \$29.57 per day from altruistic sharing, while an average traveler can obtain a surplus of \$23.14 per day from free-riding. The distributions of the gains are also similar between evacuees and travelers, as Figure A.14 and A.15 show.

Moreover, the non-altruistic hosts, who are likely to be in a lower socioeconomic status, lose from altruistic sharing due to the free riding of travelers. Figure 1.9 plots the welfare consequences from altruistic sharing by demographic groups. Considering income distribution, recall that only hosts in the top income quartile conduct altruistic sharing, while hosts in the bottom income quartile charge a higher price for disaster incidents. By contrast,

transportation to the sheltering place and losses from missed working days. Thus, the estimated cost likely provides a lower bound, meaning disaster refugees may have shouldered an even larger welfare loss from displacement.

although those who conduct altruistic sharing lose slightly more, almost all hosts suffer from altruistic sharing at a comparable magnitude regardless of their generosity. Such spillovers exist with other demographic categories, including education, family structure, and homeownership. This implies a failure in efficiency and equity, as the welfare consequences from generosity spill over to regular travelers at a cost to non-altruistic hosts.

Evacuee Targeting

A direct correction of this failure is to allow for evacuee targeting, that is, enabling altruistic hosts to distinguish evacuees from other travelers based on some sort of information disclosure, for example by billing ZIP code. Under this scenario, regular travelers are no longer able to free ride on altruistic hosts. I find evacuees would gain more from altruistic sharing, with the average gain rising from $29.57 to $31.06 per day. There are two drivers of the increase in evacuees' gains. First, the counterfactual price is determined by the supply of altruistic hosts and the demand of disaster evacuees, which would equilibrate at a level lower than the status quo. Second, without the peer effect of regular travelers, displaced households now have more housing options offered by altruistic hosts. [24]

Moreover, the removal of free-riding can provide equity improvements by reducing the spillovers to non-altruistic hosts. Figure 1.10 plots the welfare consequences from altruistic sharing by demographic groups with evacuee targeting. If non-altruistic hosts were no longer exposed to the spillovers, a substantial share of hosts would no longer bear a welfare loss from generosity. As the top left panel shows, high-income households suffer significantly more losses than low-income households, consistent with their generosity. Such equity corrections also exist for other demographic characteristics.

[24] It is worth noting that there can also exist a behavioral channel of altruistic sharing, which is not captured by the model estimates. If regular travelers were not allowed to free ride, altruistic hosts would likely become more motivated to perform in a generous manner. Thus, the estimated gains for evacuees likely provide a lower bound, meaning the removal of free-riding could bring even larger mitigation benefits.

Summary of Welfare Implications

Table 1.5 summarizes the welfare consequences of wildfire displacement and Airbnb accommodation, for evacuees, travelers, and resident hosts, under the baseline (Column (1)) and a counterfactual world where free riding is eliminated (Column (2)). There are four primary findings.

First, I find large welfare losses from displacement in the absence of Airbnb, \$231.99 per day for an average household (Panel A). This equates to a loss of \$89.23 per day per capita. As discussed, the welfare losses are equivalent to at least 31% of the direct property damages caused by wildfire. Moreover, the displacement losses are not equally distributed among households. As the confidence interval suggests, a small set of families suffers a much heavier loss from being displaced, at a magnitude of \$1000 per day.

Second, the Airbnb accommodations can substantially mitigate the welfare losses for the displaced (Panel B), reducing 51.8% of the displacement losses on average in the baseline. The channel of altruistic sharing contributes approximately 25% of the mitigation. If free-riding of regular visitors is prohibited, the mitigation effect increases slightly, by 1%, and the contribution of altruistic sharing remains roughly constant. As discussed, the model only captures the response in price and induced supply, but not the behavioral response in supply as altruistic hosts become more self-motivated. Therefore, the estimates likely underestimate the contribution of altruistic sharing under perfect targeting.

Third, I find large spillovers of altruistic sharing as a result of free riding (Panel C). The loss of efficiency can be observed from two perspectives. On the one hand, the spillovers to regular travelers are comparable to the gains of evacuees (\$23.14 relative to \$29.57), while eliminating free-riding can entirely remove such spillovers. On the other hand, the average generosity loss in the supplier surplus is \$23.96 per day, which is not significantly different between altruistic hosts (\$27.67) and non-altruistic hosts (\$23.41). Meanwhile, correcting free riding can fully eliminate the generosity losses for non-altruistic hosts, and slightly reduces the losses for altruistic hosts to \$24.99 per day.

Finally, the existence of Airbnb brings about substantial welfare benefits to all agents involved in disaster incidents. As Panel D suggests, an average evacuee can gain \$120.24 per day from Airbnb accommodations, and an average traveler enjoys a surplus of \$146.17 per day from Airbnb. Despite the losses from generosity and their spillovers, resident hosts can still gain from the option of Airbnb supply, on average \$62.76 per day of hosting. Under the scenario with a correction of free riding, the welfare benefits would become even more pronounced for evacuees (\$122.91) and resident hosts (\$67.22), and less significant for regular travelers (\$128.05). This suggests an equity gain from the removal of free riding over altruism.

1.6 Conclusion

The spread of digital technology has facilitated peer production in various industries. Despite heated social disputes and debates among policy makers, the implications of the sharing economy during emergency incidents remain largely unknown. This paper explores the role of home sharing in the accommodation of families suffering short-term displacement, an essential aspect for disaster relief that has been rarely discussed. For quantification, I construct a structural model of the home-sharing market, where disaster evacuees and travelers consume housing services offered by local residents. The model highlights two channels of welfare impacts, the increased choice set and altruistic sharing, as the main drivers for the beneficial implications for the displaced.

I first show evidence that wildfire evacuation has led to a supply expansion on Airbnb, where the new entries are superior in various characteristics, but are priced lower than the incumbents. This provides intuition for the mechanism of altruistic sharing at play when a disaster occurs. To rationalize the facts, I build a structural model of the Airbnb market with customers of unobserved types and heterogeneous resident hosts. The estimation draws on advanced tools from the statistical and empirical industrial organization literature. Unlike studies on demand system estimation with well-observed customer composition, I micro-found the data generation processes of travelers' and evacuees' arrival using a mixed Poisson model, which is identified using the nature of evacuation. As the Airbnb market differs from most marketplaces analyzed in equilibrium estimation by featuring excess supply, I leverage the high-frequency observations on the supply side and endogenize the heterogeneous cost of home-sharing across residents. I further incorporate altruistic sharing as an additional perceived component of the utility from home-sharing, and estimate how it varies among residents of different socio-economic status.

Armed with the estimated model, I explore the welfare impacts of Airbnb on the displaced people. First, I find substantial losses from being displaced in the absence of Airbnb, at a cost of 31% of the direct damage to physical property. Enabling home-sharing accommodations can alleviate the losses by more than half. The primary contributor is the peer effect, as Airbnb provides an increased consumer choice set, which gets strengthened by the variety of housing options that are usually priced lower than hotels. The contribution from altruistic sharing is material but smaller in size, amounting to 25% of the total mitigation. The heterogeneity allowed in supply estimation suggests that altruistic sharing is provided more by residents with high income, high education, children, and home ownership. However, the inability of altruistic hosts to target displaced families leads to spillover effects, allowing travelers to free ride on altruistic sharing. This results in widespread losses for all resident hosts regardless of their altruism.

The analysis informs a message on the platform design of home-sharing marketplaces, particularly on the rules for price discrimination. I find that enabling matching between altruistic hosts and displaced disaster evacuees by home ZIP code can correct the free-riding problem and thus provide an improvement in welfare. Besides cancelling out the spillovers, this would generate additional surpluses for both altruistic hosts and displaced households. This also has important equity implications by forming a market-based transfer, from unaffected households who possess better social economic status, to displaced people who suffer more from the disaster.

This paper highlights three fundamental reasons why a home-sharing platform has a role to play in displacement relief. First, home-sharing marketplaces allow for better utilizing the housing resources of local residents. Such housing, despite not being a perfect substitute for hotel rooms, is valuable to some customers because of increased variety and lower price. Home sharing is particularly valuable to displaced households, who typically hold a higher price elasticity and want places that feature a more homey style for their family. Second, the hotel sector has a fixed capacity, which cannot be easily expanded in a short time. This can result in a failure to be able to accommodate all customers, as well as high prices during periods of peak demand, such as in the immediate aftermath of large-scale displacement. Home-sharing production can expand at exactly these times of emergencies, thus improving consumer surplus for all, and in particular for displaced people. Finally, the home-sharing platforms enable production from a wide distribution of peers, which includes those who are keen on altruistic engagement. This demonstrates a market tool for emergency relief through human generosity. Similar altruistic behaviors have not been observed in the hotel sector.

The findings also add to our understanding of policy-making for displacement mitigation. In contrast to most studies that focus on disaster destruction over the long term, this paper sheds light on the immediate aftermath of a disaster, which involves temporary displacement of substantial populations. This poses a critical challenge for policy-makers, as it aggregates to substantial welfare losses for all displaced populations, yet the loss for each individual is usually too small to justify compensation. Furthermore, this paper expands the scope of policy prescriptions for disaster relief to the novel industry of the sharing economy. Different from traditional tools such as government aid, the sharing economy can mitigate damages in a market-based, spontaneous, and equitable manner. With policy adjustments for customer targeting and sharing incentives, it can further improve equity gains for displacement mitigation.

Although this paper concerns wildfire evacuation and the home-sharing industry of the U.S., the key findings can be applied more generally to a global context and to other peer-to-peer industries, such as the ride-sharing sector. It also has policy implications beyond the natural disaster I study — wildfires — including conflict- and climate-driven displacement. Displaced households can benefit from peer production of scarce resources and services because the entry of peer providers can improve the flexibility of inventory, enrich the choice set of consumers, increase the competition of incumbent industries, and potentially induce altruistic behaviors. These effects are particularly strong when existing providers have binding capacity constraints, which are likely to be the case, for example, in developing countries or in the transportation industry. The altruistic channel may also be pronounced in countries with particular religious beliefs.

This paper has explored the welfare implications of home sharing on wildfire incidents, with a focus on the agents directly involved, including evacuees, travelers, and resident hosts. There are other parties involved in the short-term accommodation market, who also may be affected by natural disasters, such as hotels (Farronato and Fradkin 2022). Over the long run, the dynamics and composition of home-sharing platforms are likely to evolve in response to disaster risks. These issues provide an engaging avenue for future work.

Figure 1.1: Percentage of Housing Units on Airbnb

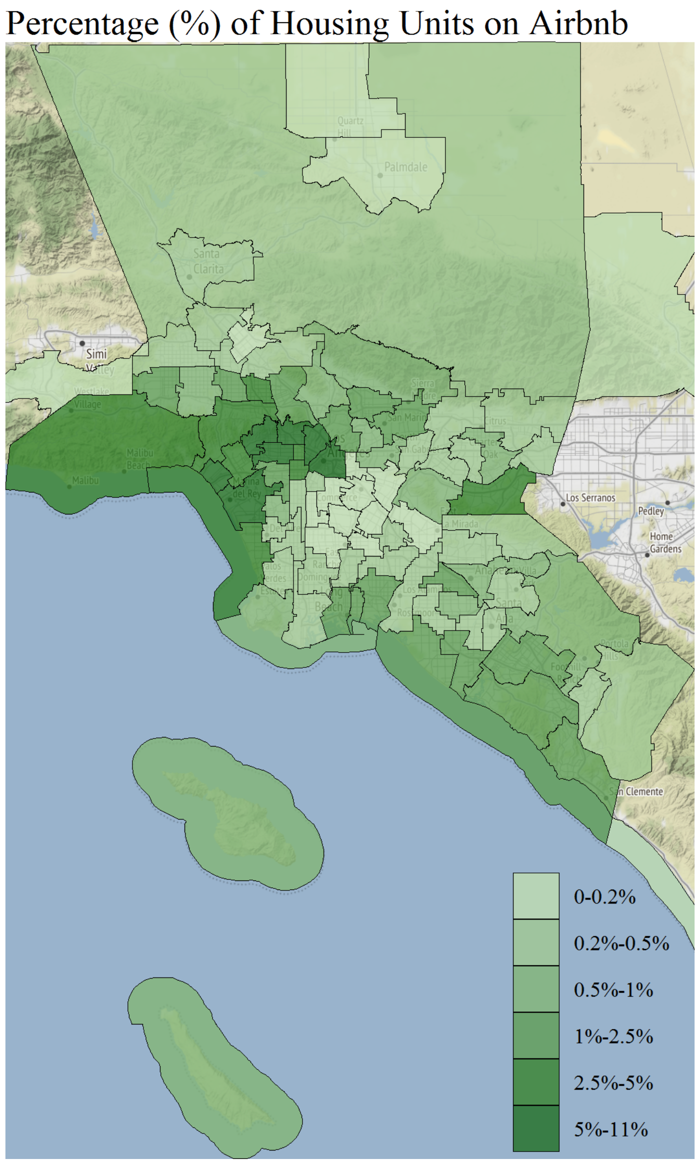

Notes: The color displays the share of housing units on Airbnb relative to the total number of housing units, at the level of Public Use Microdata Area. The number of housing units in total is approximated from the U.S. Census Grids of 2010 at a resolution of 30 arc-seconds.
Source: AirDNA, SEDAC.

Figure 1.2: Wildfire with Evacuation Order/Warning

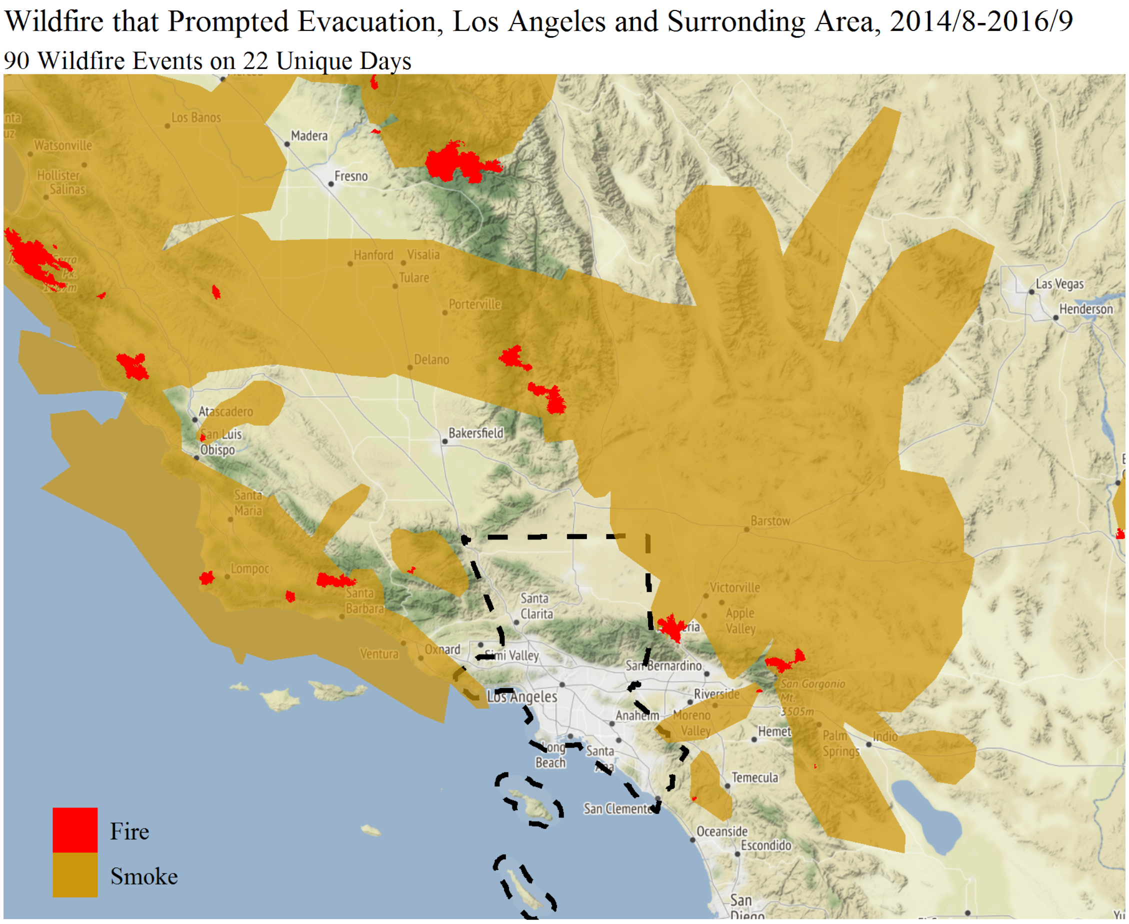

Notes: The graph shows all fires that have prompted an evacuation and their associated smoke plumes, within 300km from Los Angeles over the research period. Red polygons represent fire extent, brown polygons represent smoke plumes.

Figure 1.3: Summary of Evacuation and Associated Fire

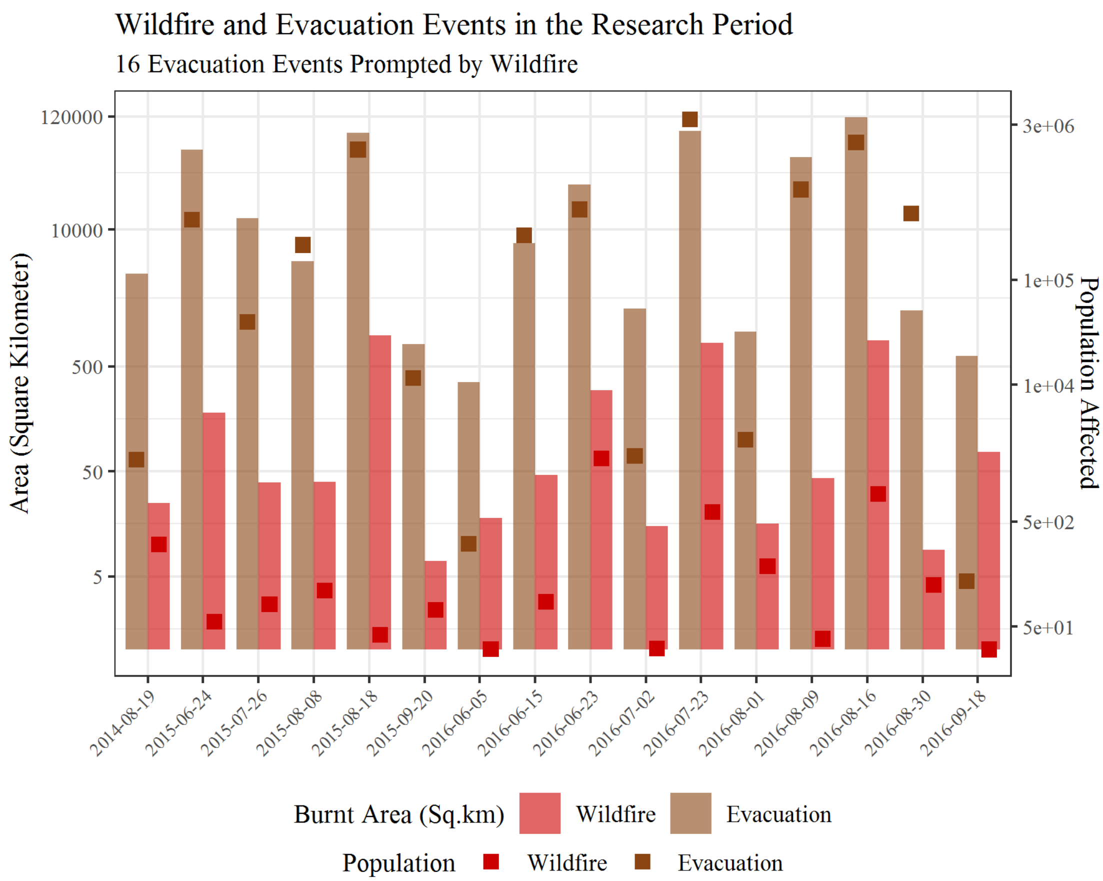

Notes: The graph plots the date of the wildfire evacuation order and warning, and the magnitude of the effect in terms of geographical area and population affected. Red represents fire, brown represents evacuation, bars represent geographical area measured in km^2, square points represent affected population. The vertical axes are transformed by a log function.

Figure 1.4: Event Study Based on Evacuation Issuance

Panel A: Extensive Margin of Supply - Log of the Number of Hosts

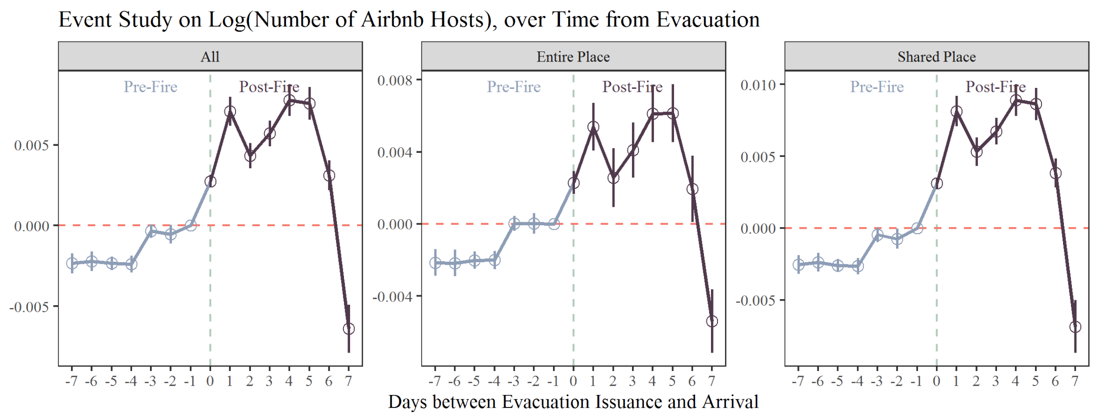

Panel B: Intensive Margin of Supply - Probability for Opening

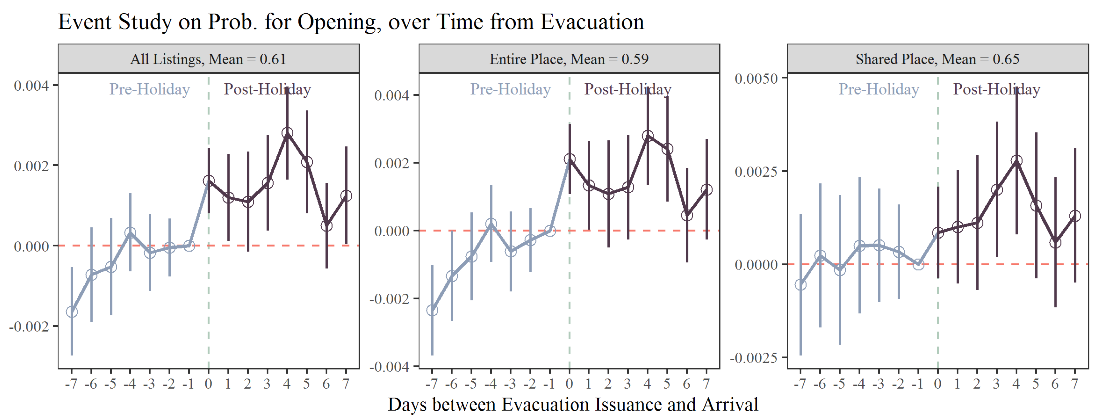

Notes: Top panels show event study regression coefficient on the log of the number of hosts at the PUMA level, controlling for evacuation acreage, evacuation population, PUMA fixed effects, year-month fixed effects, day-of-week fixed effects and holiday fixed effects. Bottom panels run a event study logit regression on the opening dummy at the property level, controlling for the evacuation acreage, the evacuation population, the full set of property characteristics including the number of bedrooms, the number of bedrooms, the number of bathrooms, the rating score, and the cancellation policy, as well as the zip code by listing type fixed effects, year-month fixed effects, day-of-week fixed effects and holiday fixed effects, and the coefficients reported are the marginal effects at the mean (MEM). Both panels use a 14-days window around the evacuation issuance day (day 0), and controls for the acreage and the number of households affected by the evacuation zone. Bars show 95% confidence intervals constructed using standard errors clustered at the PUMA level for Panel A, and at the zip code level for Panel B.

Figure 1.5: Property Features of New and Incumbent Listings

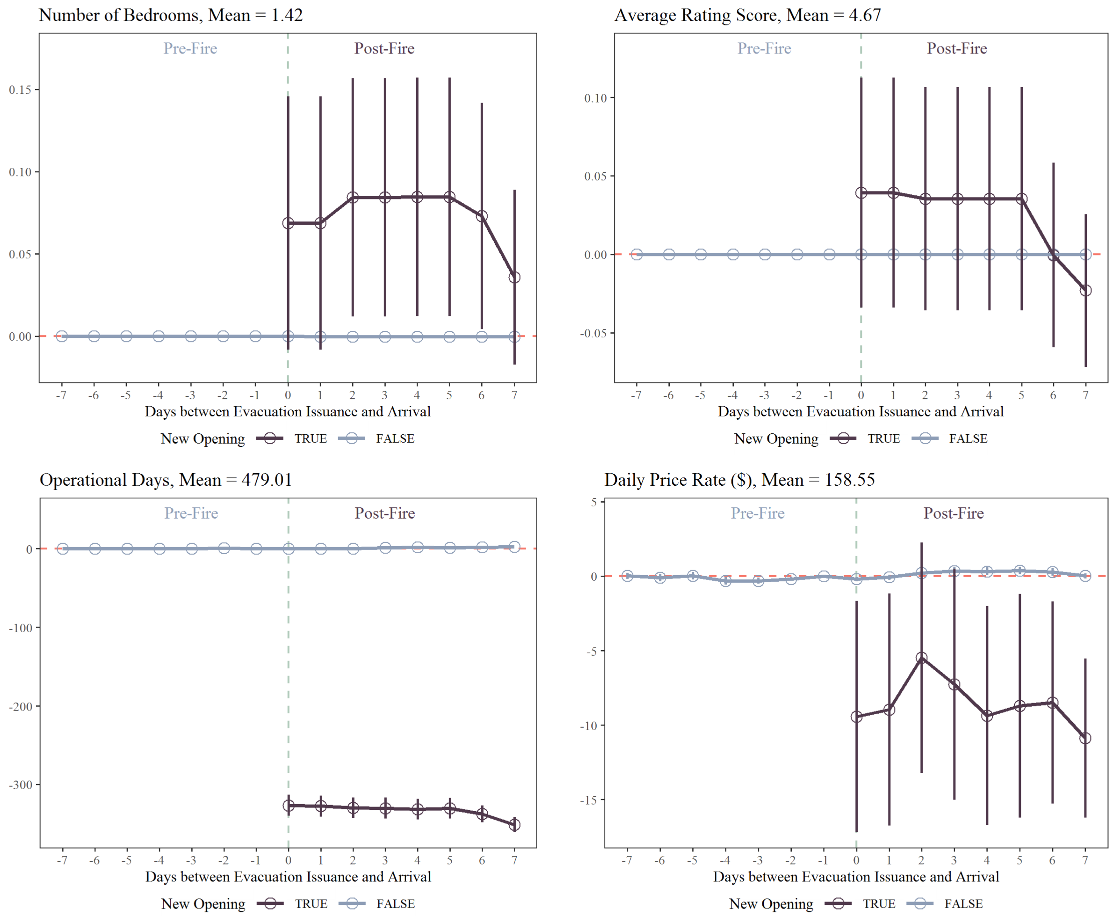

Notes: All four panels plot the average outcomes of the Airbnb market within a 14-day window around the evacuation issuance (day 0), controlling for the evacuation acreage, the evacuation population, the full set of property characteristics (the number of bedrooms, the number of bathrooms, the rating score, and the cancellation policy) other than the dependent variable of each panel, as well as the day-of-week fixed effects and the zip code by listing type fixed effects. Dark color reflects new openings after the evacuation, light color reflects incumbent openings. Top left panel shows the number of bedrooms, top right panel shows the average rating score, bottom left panel shows the number of operational days, bottom right panel shows the daily price rate. Bars show the 95% confidence intervals constructed using standard errors clustered at the zip code level.

Figure 1.6: Incidence of Wildfire, Smoke, and Evacuation Order

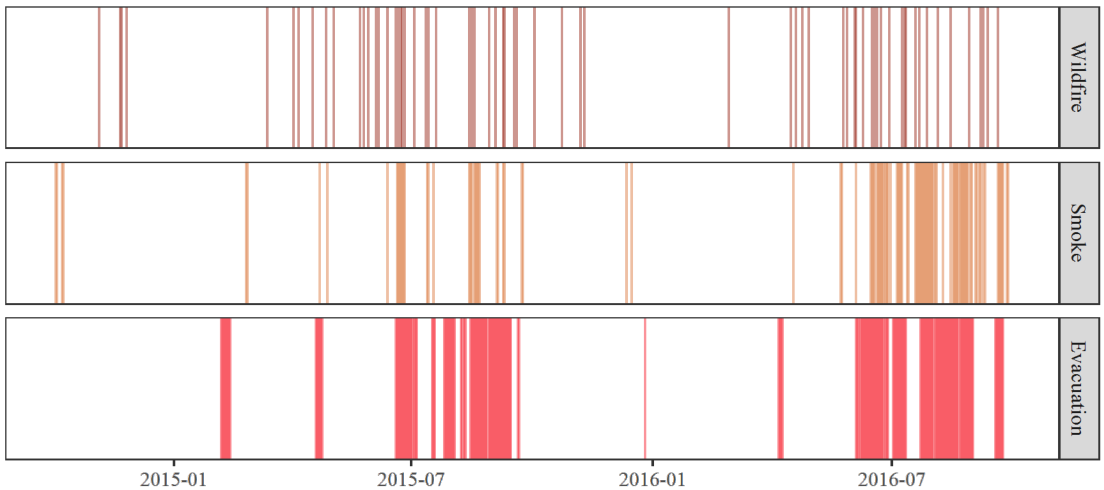

Notes: The colored bar shows the day with wildfire exposure, with smoke exposure, and with active evacuation order, in the three panels respectively. Data ranges from 2014-09-01 to 2016-10-01

Source: Evacuation documents.

Figure 1.7: Percentage of Evacuees' Destination on Airbnb

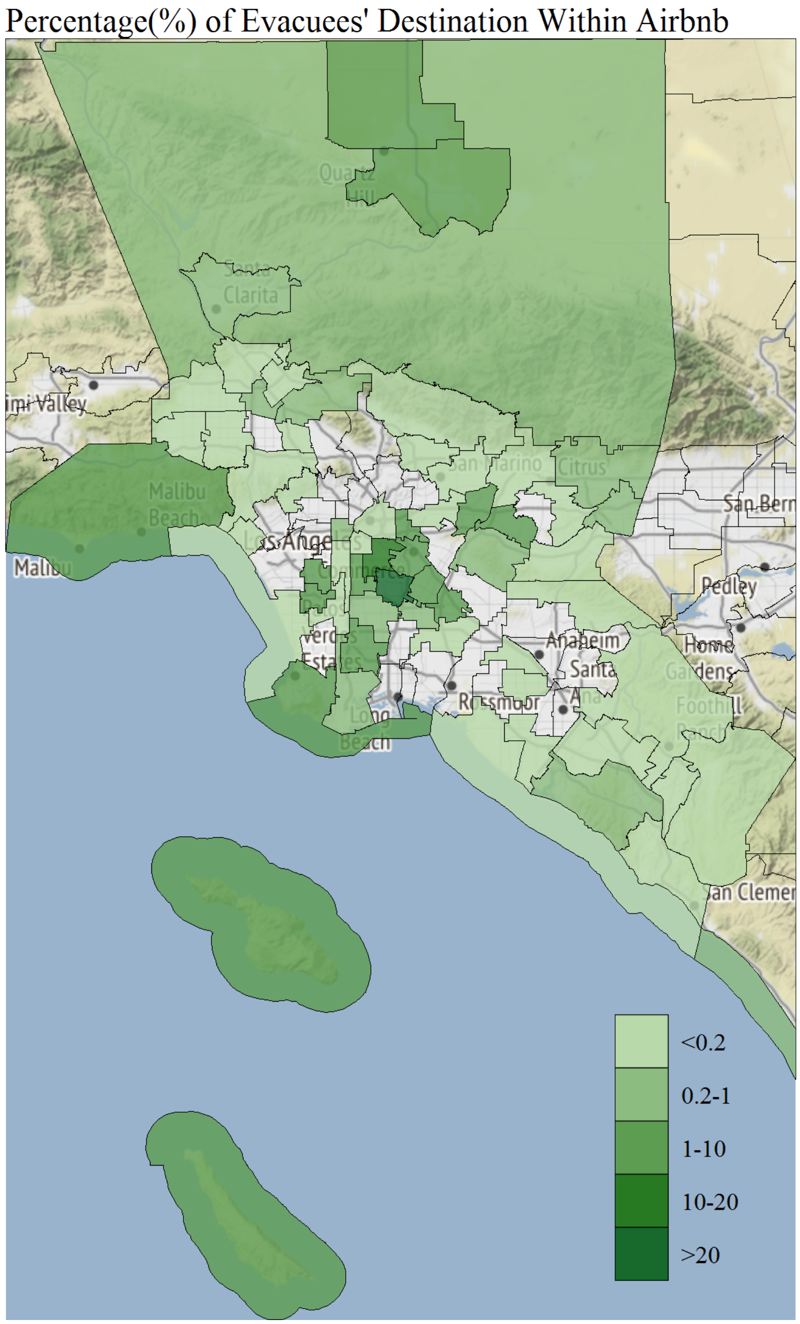

Notes: The share of evacuees' destination defined as the number of housing units taken by evacuees relative to the total number of evacuees, at the level of Public Use Microdata Area. The number of evacuee arrivals is estimated from the mixed Poisson regression model in section 1.4.
Source: model predictions.

Figure 1.8: Percentage Change in Airbnb Price if No Altruistic Sharing

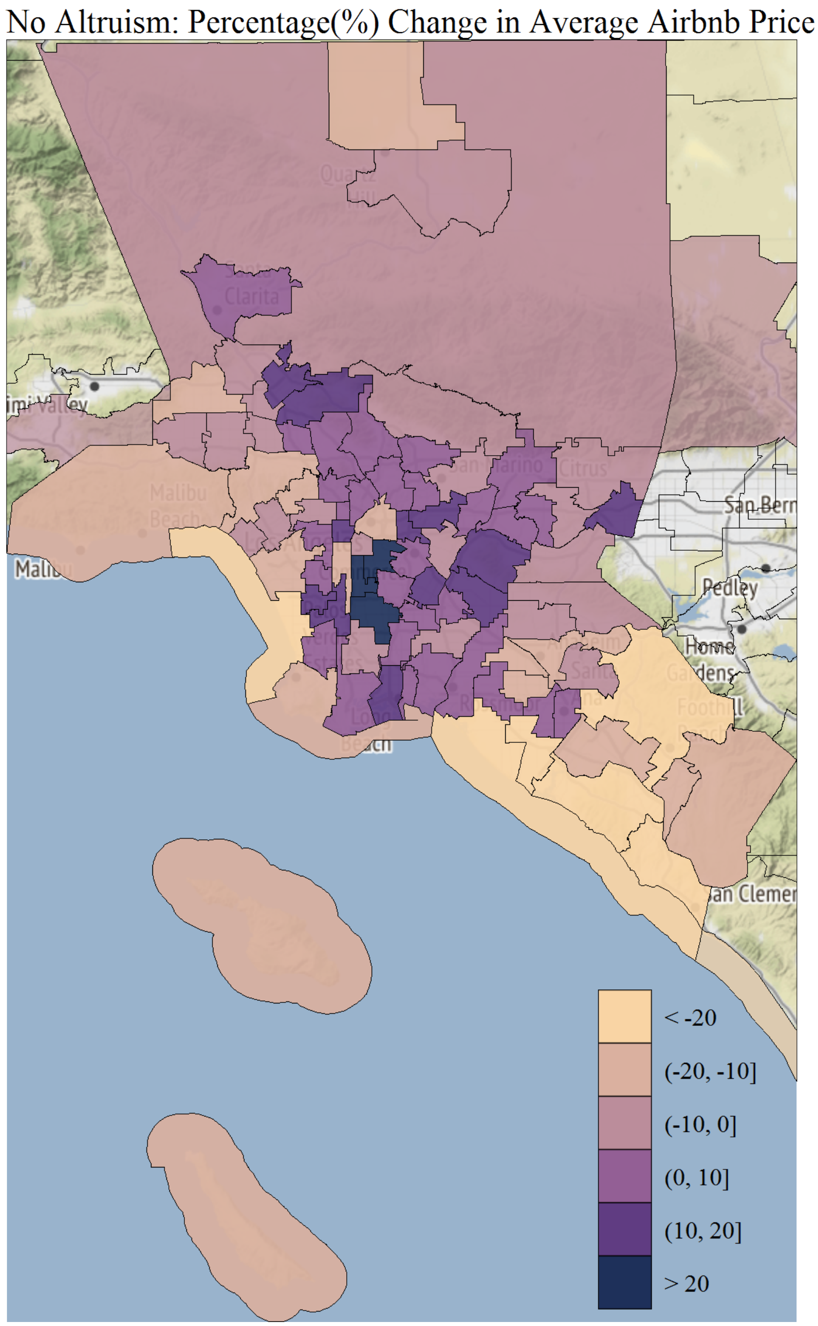

Notes: The percentage change in the average market price of Airbnb if the utility gains from altruistic sharing are removed, at the level of Public Use Microdata Area. Samples are limited to the days with an evacuation order in place.
Source: model estimate.

Figure 1.9: Welfare Loss from Altruistic Sharing, by Demographics

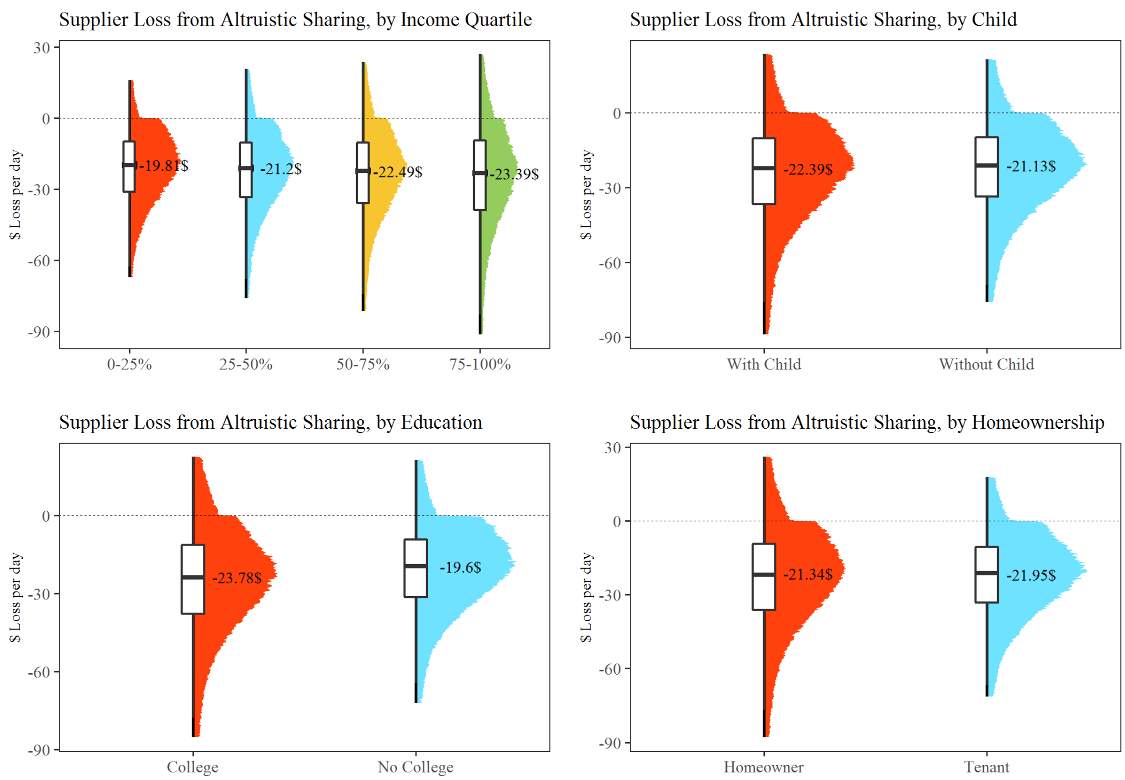

Notes: The panels plot the distribution in welfare consequences from altruistic sharing, by different demographic groups. The top left panel is by income quartiles, the top right panel is by college degree, the bottom left panel is by having children or not, the bottom right panel is by home ownership. The labeled numbers indicate the category median. The box in the center indicates roughly the 95% confidence intervals of the distribution.
Source: model estimates.

Figure 1.10: Welfare Loss from Altruistic Sharing if No Free Riding, by Demographics

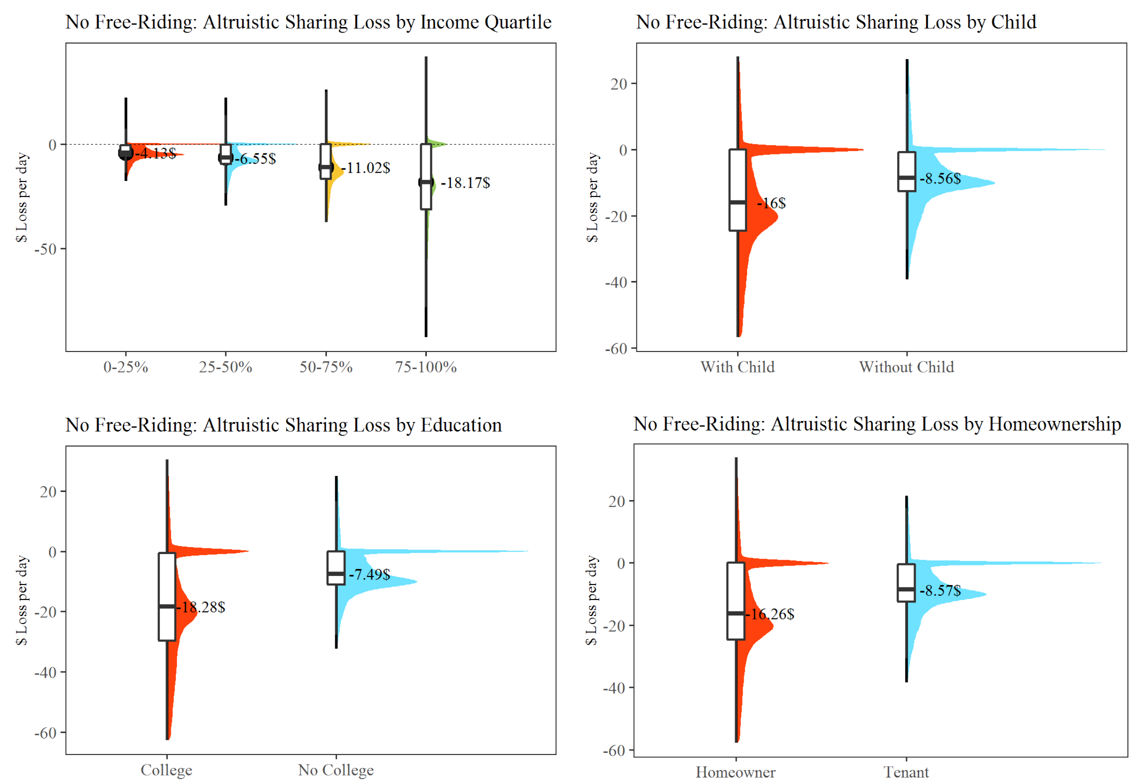

Notes: The panels plot the distribution in the welfare consequences from altruistic sharing if free riding is eliminated, by demographic groups. The top left panel is by income quartiles, the top right panel is by college degree, the bottom left panel is by having children or not, and the bottom right panel is by home ownership. The labeled numbers indicate the category median. The box in the center indicates roughly the 95% confidence interval of the distribution.
Source: model estimates.

Table 1.1.
Parameter Estimates for Customer Arrival

Dependent Variable	(1) λ		(2) # Arrival	
	Coef.	Stn. Err.	Coef.	Stn. Err.
Panel A. Regular Travelers (Mean = 6479)				
Destination Fire Exposure	−0.333	(0.645)	−2410.918	(4673.921)
Destination Smoke Exposure	−0.042***	(0.013)	−288.077***	(95.795)
Holiday = 1	0.179***	(0.010)	1002.361***	(75.404)
DOW FE	Y		Y	
Year-Month FE	Y		Y	
Quadratic Time	Y		Y	
N	731		731	
Log Likelihood	887.966		887.966	
Adj. R^2	0.958		0.947	
Panel B. Evacuees (Mean = 1339)				
# Evacuee HHs ($\times 1,000$)	0.075***	(0.015)	120.836***	(22.156)
White Share (Mean = 0.708)	0.012***	(0.003)	126.137***	(42.227)
Hispanic Share (Mean = 0.155)	0.032	(0.041)	38.681	(63.444)
Black Share (Mean = 0.018)	−0.117	(0.119)	−168.136	(182.859)
Asian Share (Mean = 0.044)	−0.088	(0.081)	−99.435	(124.189)
Female-Headed Share (Mean = 0.012)	1.643***	(0.483)	2315.894***	(740.229)
Age < 18 Share (Mean = 0.168)	−0.075	(0.089)	−107.139	(135.747)
Age > 60 Share (Mean = 0.162)	−0.222***	(0.060)	−264.318***	(91.455)
Destination Fire Exposure	−3.068***	(0.714)	−3247.659***	(1093.556)
Destination Smoke Exposure	0.008	(0.009)	6.816	(14.540)
Holiday = 1	0.087***	(0.016)	94.595***	(24.676)
DOW FE	Y		Y	
Year-Month FE	Y		Y	
N	170		170	
Log Likelihood	887.966		887.966	
Adj R^2	0.987		0.977	

Notes: * p<0.1, ** p<0.05, *** p<0.01.

Table 1.2.
Parameter Estimates for the Airbnb Demand

	Utility (Instrumented, F-Stat= 128)		Willingness To Pay ($)	
	Common Part	Evacuee-specific	Travelers	Evacuees
	(1)	(2)	(3)	(4)
Daily Rate ($)	-0.077^{***}	-0.010^{***}		
	(0.000)	(0.001)		
Compact House	10.586^{***}	-0.605^{***}	138.241^{***}	115.691^{***}
	(0.062)	(0.097)	(1.177)	(1.663)
Luxury House	15.450^{***}	1.101^{***}	201.758^{***}	191.843^{***}
	(0.117)	(0.044)	(1.968)	(2.186)
Shared House	7.406^{***}	-0.803^{***}	96.712^{***}	76.538^{***}
	(0.042)	(0.053)	(0.814)	(1.022)
Fire = 1	-20.254^{***}	-0.813^{***}	-264.488^{***}	-244.181^{***}
	(0.115)	(0.001)	(2.219)	(2.487)
Smoke = 1	-3.894^{***}	0.500^{***}	-50.845^{***}	-39.335^{***}
	(0.052)	(0.074)	(0.741)	(1.098)
Neighborhood FE	Y	Y	Y	Y
DOW FE	Y	Y	Y	Y
Holiday FE	Y	Y	Y	Y
Month FE	Y	Y	Y	Y
Quadratic Time	Y	Y	Y	Y
N	$155,744$	$155,744$	$155,744$	$155,744$
GMM objective	24580.569	24580.569	24580.569	24580.569

Notes: Column (1) and (2) report the estimation results for demand coefficients on the utility of Airbnb accommodation. Column (3) and (4) further transform them into monetary value by dividing all by the corresponding price coefficient. Standard errors are clustered at the PUMA level. * p<0.1, ** p<0.05, *** p<0.01.

Table 1.3.
Estimated Willingness to Accept for Home-sharing

	(1) Average	(2) Income> 75%	(3) Income< 25%	(4) College= 1	(5) College= 0	(6) Child≥ 1	(7) Child= 0	(8) Tenant	(9) Homeowner
Entire Sharing	219.97***	292.82***	178.28***	259.82***	183.86***	255.98***	193.21***	178.11***	266.04***
	(14.94)	(23.44)	(11.05)	(19.96)	(11.13)	(17.80)	(12.78)	(11.36)	(19.45)
Partial Sharing	79.11***	107.35***	62.97***	92.73***	66.65***	97.00***	67.12***	61.34***	99.53***
	(8.14)	(11.79)	(6.35)	(10.33)	(6.37)	(9.41)	(7.17)	(6.50)	(10.13)
Entire × Evac	1.15	−9.53***	7.28***	−10.58***	10.48***	−8.96***	7.27***	1.46	2.37
	(2.81)	(3.79)	(2.29)	(3.48)	(2.30)	(3.12)	(2.57)	(2.34)	(3.30)
Partial × Evac	0.22	−15.81***	8.78***	−21.23***	16.21***	−1.33	1.97	2.29	−1.33
	(5.23)	(7.04)	(4.26)	(6.50)	(4.27)	(5.75)	(4.75)	(4.37)	(6.14)

Notes: Estimation results for the average WTA for entire sharing in normal moments (first row), the average WTA for the partial sharing in normal moments (second row), the additional WTA for entire sharing under evacuation (third row), and the additional WTA for partial sharing under evacuation (last row), by various demographic groups, including the average (column (1)), the highest income quartile (column (2)), the lowest income quartile (column (3)), with college degree (column (4)), without college degree (column (5)), with kids (column (6)), without kids (column (7)), tenants (column (8)), and homeowners (column (9)). Standard errors are clustered at the PUMA level. * $p<0.1$, ** $p<0.05$, *** $p<0.01$.

Table 1.4.
Change of Counterfactual Outcomes Relative to the Status Quo

	Change in Supply (%)			Change in Price (%)		
	Average	Entire	Shared	Average	Entire	Shared
No Altruism	−1.77	−18.43	19.52	4.81	3.22	9.06
No Airbnb	−100.00	−100.00	−100.00	Not Applicable		
No Free Riding	10.02	3.58	28.38	4.14	3.69	5.39
Altruistic Host	−0.60	−26.17	20.23	−7.80	−7.22	−9.30
Non-Altruistic Host	11.93	6.61	32.27	6.29	5.11	9.47

Notes: This table displays the percentage change of market outcomes (Airbnb supply and price) on average, of entire places, and of shared places, under the three counterfactual scenarios relative to the status quo.

Table 1.5.
Welfare Consequences of Airbnb ($ per household per day)

	(1) Actual World	(2) No Free-Riding
Panel A: Welfare Losses of Displacement		
Displacement Loss	-231.99	-231.99
	$[-1287.93, -6.01]$	$[-1287.93, -6.01]$
Panel B: Disaster Mitigation Effect		
Overall Evacuee Gains	120.24	122.91
	$[2.72, 788.42]$	$[2.72, 789.76]$
From Altruistic Sharing	29.57	31.06
	$[1.08, 76.84]$	$[1.99, 76.84]$
Panel C: Spillover of Altruism		
Regular Traveler Gains	23.14	0
	$[-16.71, 76.12]$	$[0, 0]$
Average Host Loss from Generosity	-23.96	-2.92
	$[-109.15, 48.88]$	$[-49.76, 0.00]$
Altruistic Host	-27.67	-24.99
	$[-110.12, 44.01]$	$[-80.05, 74.29]$
Non-Altruistic Host	-23.41	0
	$[-106.38, 47.33]$	$[0, 0]$
Panel D: Overall Gains from Airbnb		
Evacuee	120.24	122.91
	$[2.72, 788.42]$	$[2.72, 789.76]$
Regular Traveler	146.17	128.05
	$[2.72, 1068.04]$	$[0.65, 665.15]$
Resident Host	62.76	67.22
	$[1.70, 261.45]$	$[1.93, 268.59]$

Notes: This table displays the welfare consequences ($ per household per day) for all agents (evacuees, regular travelers, and hosts) under the status quo and the no-free-riding scenario. The coefficients displayed are the average value, with the 95% confidence intervals in parentheses.

Chapter 2

Managed Retreat and Flood Recovery: Evidence from Property Buyout and Acquisition Program

2.1 Introduction

Many coastal communities are struggling to balance the need to protect their population and properties from the increasing risk of disasters while maintaining a thriving local economy and tax base. This tension is often addressed through buyout and acquisition programs, which offer households financial incentives to move out of risky areas voluntarily.

However, these federally-funded programs have stirred controversy. Local governments tend to view them unfavorably because of their potential negative impacts on the local economy and tax base. Residents are often skeptical about how such programs might alter the fabric of their community, as well as their implications for social justice and equity.

Despite these concerns, there are several reasons to expect the actual economic impacts of buyout and acquisition programs to be less negative than often projected. For one, such programs may enhance the community's overall resilience by treating the most vulnerable properties and providing more amenities to the neighborhood. Furthermore, large-scale buyouts and acquisitions often occur after a disaster, presenting a unique opportunity for a community to upgrade and reorganize its housing stock during the recovery process, which might create positive general equilibrium effects at the community level. However, there is little empirical evidence on the extent of these effects.

In this paper, we examine the impact of a major post-disaster buyout and acquisition program, the NY Rising Program which was administered by the state of New York following Hurricane Sandy. We aim to evaluate a comprehensive set of outcomes to capture not only property-level but also community-level changes. Specifically, we investigate three key aspects: (i) the effect of a buyout or acquisition on nearby property values, (ii) whether these neighborhood changes attract a different set of property buyers in terms of key demographics, and (iii) how a buyout or acquisition affects the nearby business and commercial environment using a unique database of business establishments.

To investigate the causal effect of acquisition and buyout programs, we employ a spatial difference-in-difference design that utilizes both temporal and spatial variations in the programs' occurrence and locations relative to Hurricane Sandy's actual damage. Specifically, we estimate response in areas in proximity or including participating properties after they occurred, relative to changes in areas not proximate or containing the same participating property. We also examine how the selection of acquisition and buyout programs might depend on factors other than the damage level to Hurricane Sandy and find that the demographic factors of all populations play a crucial role in program selection across neighborhoods. This highlights the necessity to account for neighborhood-specific time trend parameters throughout our analysis. Additionally, we carefully account for Hurricane Sandy's destructive effects as an important confounder. As such, our estimates capture how the post-disaster buyout and acquisition program functions in the market dynamics in the recovery process. Moreover, we distinguish between the effect of buyout and acquisition in our estimation, as well as how the effects vary with the intensity of program treatment..

Our primary findings include three components. First, we find that acquisition and buyout programs are effective in aiding the recovery of disaster-stricken properties, as they help properties recover to their pre-disaster levels. The recovery effects differ between programs. Acquisition programs have a significantly positive effect on property values, with the most substantial effects observed in close neighborhoods that decay as the distance from the program site increases. Furthermore, these effects persist over time and even strengthen. In contrast, the effects of buyout programs are much smaller in size, quickly decaying over space and attenuating over time. We also test the robustness of our findings by varying the model settings, including the distance range of control groups, using only repeated sales, and assigning pseudo-treatment to control groups.

Second, we find that acquisition and buyout programs significantly affect the intentions and patterns of internal migration flows across neighborhoods. Specifically, they attract new families to settle down in disaster-stricken areas, with the migration intentions skewed towards high-income households, and play a role in correcting pre-existing racial inequalities within community. The magnitude of these effects is more pronounced in communities with more than five participating properties and remain relatively small and statistically insignificant in places with low program intensity. Evidence from comparisons between programs suggests that while both acquisition and buyout programs help attract wealthy families to move in, the effect of acquisitions is more significant. Furthermore, while both acquisitions and buyouts can help attract more racial minority migrations, their effects operate through different channels. The effect of acquisitions is more focused on attracting families from minority groups, while the effect of buyout programs is more centered on reducing the desirability of families from the dominant group to move in.

Lastly, our analysis of the impact on economic performance of local businesses indicates effectiveness in the business recovery effect of acquisition and buyout programs, in terms of increased business growth rate primarily driven by a reduced death rate after the programs' occurrence. Our results also indicate an effective recovery effect on employment, as these programs have helped the disaster-stricken areas to partially recover from Sandy's damage with increased job creation and larger employment size per enterprise. Moving on to the differential effects between programs, we find that both acquisitions and buyouts have a positive impact on the growth of local businesses but through different channels, with acquisition programs more on an increased birth rate of new businesses and buyout programs more on a reduced death rate of survived firms. The job creation effects are more salient within communities near buyout properties, while acquisitions did not play a significant role in affecting the employment of local businesses. We further identify significant differences across industries, which can be attributed to three factors: the nature of the acquisition and buyout programs, the effect of land and property values, and the demographic distribution of migration flows. Our analysis reveals that the most pronounced recovery effects occur in the Service, Retail Trade, and Construction industries.

Our study provides significant policy implications for managed retreat strategies in disaster-prone areas. First, our findings suggest that acquisition and buyout programs can be effective tools for aiding in the recovery of disaster-stricken properties and correcting migration patterns by income and race. These programs also have positive effects on business growth, job creation, and employment in affected areas. Policymakers can use this information to support high-risk communities after disasters and to boost local businesses and employment in disaster-stricken areas. Second, our study suggests that the effectiveness of acquisition and buyout programs as components of managed retreat strategies is associated with various factors, such as program intensity within neighborhoods, distance from the program site, and demographic distribution and industrial structure of local businesses. These factors must be considered when designing and implementing such programs as part of managed retreat strategies. Moreover, our study highlights the importance of taking a holistic perspective when designing and implementing policies to address the interconnected challenges faced by communities affected by natural disasters. This underscores the need for interdisciplinary approaches that consider the complex interactions between economic, social, and environmental factors in managed retreat strategies.

The rest of the paper is organized as follows. We first review the related literature to this paper. Section 2.2 introduces the policy background of the acquisition and buyout programs after Hurricane Sandy, followed by the description of data used in the analysis in Section 2.3, Section 2.4 discusses the identification challenges and our empirical framework, followed by Section 2.5, which presents our primary results. Finally, we conclude in Section 2.6,

Literature Review

This paper is related to several bodies of literature. First, we contribute by providing some of the first empirical evidence on economic impacts of managed retreat actions. While there have been studies on households' decisions to rebuild or relocate (Binder et al. 2015; Swapan and Sadeque 2021), development of a conceptual model of managed retreat (Hino et al. 2017; Mach and Siders 2021), and commentary on policy options that reduce inequities in buyout outcomes (Kraan et al. 2021; Shi et al. 2022), empirical economic analyses on managed retreat are very limited. There are only a few recent analyses that look at the determinants and consequences of acquisitions and buyouts, primarily relying on statistics and machine learning strategies. For example, Mach et al. (2019) determine common variables across counties that receive buyouts, using a random forest model to show prior flood damage, population size, and population density are likely influential determinants of a county having a federal buyout. Elliott et al. (2020) studies the impact of racial inequality in the implementation of the program, estimating the probability of participation in the federal program at the county and census tract levels.

A few studies have examined household participation decisions in the voluntary buyout programs to identify the primary factors that influence relocation decisions. For example, Bukvic et al. (2015) conclude that a relocation decision is primarily influenced by household characteristics, including the residents' age, disaster exposure, stress related to recovery, and personal financial concerns, using a survey. In another survey-based study, Frimpong et al. (2019) find that the offer price plays an important role in homeowners' decision to accept government acquisition contracts, and the price responsiveness varies based on non-price characteristics such as the timing of the offer.

Only a few studies have examined the economic and demographic consequences of acquisition and buyout programs following a disaster, most of which have emerged very recently. For example, Jowers et al. (2022) examines the equity implications of managed retreat by analyzing the role of race and ethnicity in buyout bargaining and how those outcomes affect long-run neighborhood change. The only paper of similar topic and as a complementary component to our analysis is Hashida and Dundas (2022), which estimates the effects of managed retreat activities on surrounding housing values in parts of New York City and Long Island. However, using the same research context but not considering the confounding effect of Hurricane Sandy, they find a negative effect of buyout and acquisition programs on nearby property values. As we argue later, we believe that our strategy performs a more empirically valid and robust analysis of the hedonic valuation of managed retreat efforts. Moreover, to the best of our knowledge, no economic studies have empirically inferred the causality between a managed retreat program and a potential change in migration patterns and business performance.

As a final note, our analysis is related to the vast literature documenting flood-related damage in coastal areas. Many studies have documented large negative price effects following hurricanes and other catastrophic events (Hallstrom and Smith 2005; Atreya et al. 2013; Bin and Landry 2013; Zhang 2016). Our paper is also related to studies on the general economic effects of climate change and recovery policies. For instance, McIntosh (2008) and Deryugina et al. (2018) examine the long-term effects of Katrina-related relocations on the urban labor market and individual economic performance, suggesting strong evidence of persistent geographical displacement. Some other papers, such as Deryugina (2017), shed light on the relief effect of recovery policies following climate disasters. In a similar context to our analysis, McCoy and Zhao (2018) use data on building permits to analyze the effects of Hurricane Sandy on house improvements in New York City. Ortega and Taşpınar (2018) analyze the effects of Hurricane Sandy on the New York City housing market and find a persistent negative impact on flood zone housing values. Our analysis complements these studies by showing the differential damage of Hurricane Sandy in the policy design of managed retreats.

2.2 Background

Hurricane Sandy was a catastrophic storm that struck the northeastern United States in late October 2012. The storm caused significant damage to coastal areas in New York, New Jersey, and other states, with storm surge and high winds leading to widespread flooding, power outage, and property damage. In addition to the immediate impacts of the storm, Hurricane Sandy also highlighted the vulnerability of coastal communities to the effects of climate change, including sea level rise and increased frequency and severity of storms.

The storm led to significant changes in disaster preparedness and response efforts, including the implementation of new programs. In the aftermath of the storm, New York State launched a comprehensive recovery program called "New York Rising." The program aimed to help communities impacted by the storm rebuild and become more resilient to future natural disasters.

The acquisition and buyout programs were implemented as a key component of the recovery effort. These programs aimed to provide homeowners in affected areas with options for dealing with substantial damage to their properties or high-risk locations. Both acquisition and buyout programs were designed to provide a voluntary and equitable solution for homeowners who were facing substantial damage to their properties due to the storm.

The acquisition programs offered homeowners the opportunity to sell their properties to the state. After acquiring properties through the programs, the state government typically auctions off these properties to interested buyers. In some cases, the properties acquired through the buyout and acquisition programs are converted into open space or other community uses directly by the state. However, in many instances, the properties are sold at auction to private buyers, who may use the land for a variety of purposes such as housing or commercial development. The auction process involves setting a minimum bid price for the property based on its fair market value, with additional incentives for buyers who plan to use the land for community or open space purposes. For commercial and residential usage, the state government typically requires that any new construction or renovations on the property meet certain elevation requirements to reduce the risk of future damage from natural disasters. In sum, the acquisition and auction processes are designed to ensure that the properties are sold to individuals or organizations that can make the best use of the land while also promoting community resilience and sustainability.

The buyout programs also offered homeowners in areas that were severely impacted by the storm to sell their properties to the state at a price that reflected the pre-storm value of the property. These programs are also voluntary, but unlike acquisition programs, the properties acquired through buyout programs are typically demolished to reduce the risk of future damage from natural disasters. The demolition process involves removing all structures from the property and restoring the land to its natural state. Once the demolition process is complete, the land is typically restored to its natural state or converted into open space or other community uses. By strategically relocating people and property away from high-risk areas, the buyout programs can help reduce the risk of future damage from natural disasters and promote community resilience.

The acquisition and buyout program of "New York Rising" were one of the largest and most successful disaster recovery programs of their kind. Through these programs, the state was able to acquire more than 1200 properties across the state, primarily in areas that were severely affected by the storm, as well as those at high risk of flooding or other natural disasters. The programs were widely praised for the innovative approach to disaster recovery and the emphasis on community-driven solutions.

2.3 Data

Housing Acquisition and Buyout Programs post Storm Sandy

Data on the full sample of the acquisition and buyout programs were obtained through a FOIL request to the New York State Governor's Office of Storm Recovery. This provides us with information for all properties that participated in the New York Rising programs after Hurricane Sandy. For each of the 1289 participating properties, the data include key characteristics, including the program type (acquisition or buyout), the related municipal agency, the street address, the purchase price, along with date information related to program actions, such as the closed date for all properties, the action date and action closing date for acquisition programs, and the demolition date for buyout programs. We conduct geocoding for all properties using the USA Local Composite locator, which is available through the Business Analyst service of ArcGis, to map each participating property to its corresponding longitude and latitude coordinate.

To obtain the damage caused by Hurricane Sandy on these properties, we complement surge measurements from field-verified aerial imagery by FEMA's Modelling Task Force. The inundation map was constructed based on observations from permanent monitoring sites in the USGS network and the NOAA network, calculated as the difference between the observed water level and normal (predicted astronomical) tide level. We also rely on the damage assessment measures provided by FEMA, which complemented aerial imagery with observed inundation depths for each building structure. An important advantage of the damage assessment data is the inclusion of damage estimates for all affected properties beyond those that were surged or applied for assistance. The assessment data contain estimates for all of the 147,702 buildings that were either in the Sandy inundation zone or outside affected properties for which aerial imagery damage determinations were made, including the geo-referenced location, the damage type (wind, surge, or both), the categorical measure of damage broken into four levels (affected, minor damage, major damage, or destroyed), along with the depth of flooding level. To determine the flooding damage of the acquisition and buyout programs, we connect each participating property with the nearest building point within 100 meters for which the damage assessments were determined.

Figure 2.1 displays the geographic distribution of acquisition and buyout programs relative to the inundation zone of the storm. Most of the participating properties are geographically close to or in the inundation zone. The distribution of participating properties display a clustering pattern, with a significant majority of them are concentrated in the coastal areas of Staten Island and Long Island. In particular, more than half of the programs occurred in communities near Oakwood and Midland beach of New York City. Interestingly, a small but nontrivial number of buyout programs was selected into areas that were not affected by the storm surge, including inland of Rockland and Orange counties. Panel A of Table B.1 summarizes the summary statistics of participating properties by program type.

Housing Transaction

We obtain data on the universe of property transactions from Zillow's ZTRAX database (2021 version), which is one of the most comprehensive sets of housing transaction records available. The data were created by combining transaction observations from the buyer's, the seller's, and the county assessor's point of view, along with records from county assessments on an annual basis. This allows us to observe the date and the sale price for each transaction, as well as key characteristics of the property, such as the property type, the year of construction and renovation, the square footage of building area, the number of bedrooms, the number of bathrooms, and other amenity features incorporated in assessments. Each property or parcel point is geographically identified by its street address, and we conduct geocoding using the USA Local Composite locator of ArcGis to obtain the exact geo-referenced location. The complete records of housing transactions are available between 1997 and 2020, allowing us to observe repeated sales over time.

To conduct hedonic valuation, we limit the samples to residential properties of New York

State and eliminate observations that feature non-arm's length transactions (below $10,000) or outlier properties (above $2,000,000). We also eliminate transactions that occurred less than three months from the previous sale, as one transaction might be recorded multiple times by different agents (buyer, seller, and county assessor) at different time points. To determine the flooding exposure to Hurricane Sandy for each property, we assign it with the damage measures of the nearest building point within 500 meters for which the damage assessments were evaluated by FEMA. We restrict the analysis to properties that can potentially receive an effect of Hurricane Sandy or the acquisition and buyout programs, by limiting to properties that are either located in the inundation zone of Sandy, classified as "affected" or above by Sandy's damage according to FEMA's assessments, or within 1000 meter from acquisition and buyout programs. The final full sample data consist of 467,229 transaction observations, with their summary statistics presented for in Panel B of Table B.1 .

Home Mortgage Application

To examine the response of internal migration after the acquisition and buyout programs, we rely on the data of a full sample of home mortgage applications spanning the years of 2000-2020, obtained from the National Archives of Federal Reserve Board of Governors Division of Consumer and Community Affairs. The data contain comprehensive information on every application for a home mortgage received by a lender, as required to report under the Home Mortgage Disclosure Act. This includes key socioeconomic characteristics of the applicant, such as race and ethnicity, gender, and annual income, along with basic information of the loan and securing property, such as loan amount, mortgage application year, census tract of the property, loan purpose, and whether the loan was successfully approved. Thus, the data allow for tracking the intentions and demographic patterns of inter-neighborhood migration flows over time.

We limit the mortgage sample to properties within the 16 counties that were either explicitly exposed to the storm (i.e. having been inundated or having received the damage assessments by FEMA), or received acquisition or buyout programs afterwards. Since some application entries of early years were coded by hand, to best avoid potential mistyping and measurement errors, we exclude mortgages with a loan amount below $5,000, and redefine an annual income below $1,000 or above $10,000,000 as a missing value. This results in 8,072,856 mortgage applications spanning across 3090 census tracts, with 81 tracts having ever received an assignment of acquisition or buyout programs and the remaining 3009 having never been treated. As observations on the exact location of securing property are unavailable, we map each property to its corresponding neighborhood by collapsing the loan-level data into a panel of the census tract by year level, which allows us to best characterize the patterns of inter-neighborhood migration flows over time. The summary statistics of the collapsed panel are presented in Panel C of Table B.2 .

National Establishment Panel

We obtain data on the universe of business performance from the National Establishment Time-Series (NETS) database, which is one of the most comprehensive databases of firm-level information on business establishments in the United States. The data cover all industries and the period from 1976 up to the present, containing detailed information on establishment characteristics, such as geo-referenced location (longitude and latitude), 4-digit industry classification, employment size, and revenue. Additionally, the data are updated annually and provide a host of time-series information on business performance, including births, deaths, and job creation and destruction. To limit our research scope to the damage and recovery of Hurricane Sandy, we restrict our business samples to within 1000 meters of the inundation zone.

One challenge in testing the business effects over the life cycle is the potential bias introduced by selection effects that occur before a firm's birth or after its death. For instance, the screening process may hinder potential entrepreneurs from starting a business, biasing the sample of observed firms towards those with more resources and capabilities and not representative of the population of all potential firms. Moreover, the data are likely to be unbalanced since we cannot observe a firm before its birth or after its death. To analyze the business life cycle without selection bias at a granular geographic level, we collapsed the firm-level data into hexagons by creating a set of hexagonal grids that cover the entire research area„ namely the inundation zone and 1000 meters nearby. We group businesses based on their geographic location and aggregate their data within hexagonal cells. This approach enables us to compute multiple measures of business activity for each hexagon, such as the number of active firms, new births, and deaths, as well as total and average employment for each year. We also construct these measures for each industry categorized by 2-digit SIC code. The hexagon size is selected to have a radius of 100 meters, similar to a large block, resulting in a manageable number of businesses per hexagon while still capturing meaningful spatial variation. The summary statistics of the business performance data on the hexagon level are presented in Panel D of Table B.2 .

2.4 Empirical Strategy

The goal of our analysis is to estimate the impacts of acquisitions and buyouts on local communities. We measure these impacts in three ways: first, by analyzing the capitalization effect of participating properties on neighboring property values using housing transaction data; second, by tracking the sorting outcomes across neighborhoods using data on the demographic distribution of actual and intentional migration flows from mortgage application data; and third, by focusing on the commercial performance, firm survivability, and job creation of local businesses. To isolate the causal relationship between acquisition/buyout programs and these outcomes, we rely on an identification assumption that these programs are plausibly exogenous shocks. However, the assignment of programs may be correlated with other factors that affect local communities, such unobserved effects of Hurricane Sandy. Acknowledging these confounders, we present a set of estimation specifications that help rule out biases resulting from such factors. By adopting these methods, we aim to provide robust estimates of the effects of acquisition and buyout programs on local communities.

Unobservable Effects of Hurricane Sandy

One might consider using a standard difference-in-differences framework that utilizes the temporal and spatial variations driven by acquisition and buyout programs. However, our primary concern is the omitted variable bias resulting from unobserved disaster effects, which could lead to biased estimates if they are also correlated with the selection of acquisitions and buyouts. For example, if the programs are targeted towards communities with less natural ability to recover from flooding, we might underestimate the positive effects or even obtain negative estimates of how acquisitions and buyouts affect local communities after the disaster. Figure 2.3 visualizes this issue and presents the unbiased DiD estimator in an ideal context (Panel A) and how it would be biased if there exists a correlation between the program selection and the storm effect (Panel B). [1]

To test the correlation between the Sandy's damage with the selection of acquisitions and buyouts, we first compare the damage assessments and inundation depth of neighboring areas relative to those farther away from the acquisition and buyout programs, as presented in Tables B.1 and B.2. FEMA assessments suggest that acquisition and buyout programs were spatially selected in areas with more severe property damages. To provide visual evidence that the selection was also contingent on factors other than the property damage caused by Hurricane Sandy, we compute the residuals for measure of housing market as component that cannot be explained by time trends and property damage assessments. By comparing

[1] An ideal solution would be to limit our analysis to a small subset of samples that were affected by Sandy and remained comparable to the participating properties, and only focus on the evolution of these samples in the post-Sandy time periods. However, this strategy would require us to discard a large number of observations that were not affected by the storm as well as exclude the evolution that occurred before Sandy. For the data available only on a yearly basis, such as the mortgage application and the business performance data, the time gap between Sandy and an acquisition or buyout program typically only includes 2 to 4 years. Removing the time periods before Sandy would substantially reduce the sample size and eliminate the temporal variations, potentially resulting in low precision and large measurement errors.

them of different time stage as a function of distance to acquisition and buyout programs, we are able to roughly gauge the correlation between the program selection and the storm effect.

In Figure 2.2, we compute the residuals for property values by regressing the log of prices on interactions of property damage and inundation level with post-Sandy indicator, fixed effects of county-by-year, census tract, and sales month, along with property characteristics included in the main specification. Comparing the residualized prices before Sandy and right afterwards, we find a spatial correlation in the change of property value by how far it is located from acquisition or buyout programs. Contingent on controls for property damage assessments, houses that lie within 300 meter from acquisition or buyout programs have experienced significantly more adverse effects of the storm on their property values, as opposed to those 300 meters away. This provides justification for the selection of acquisitions and buyouts in more disaster-struck areas in terms of detriment on the housing market. [2]

Selection of Acquisition and Buyout Programs

Another major concern in identifying the causal effect of acquisition and buyout programs is the potential for selection bias based on factors unrelated to the disaster. For instance, the under-representation of minority groups among governors and emergency managers has led to a failure to prioritize minority and disadvantaged communities in disaster recovery efforts. On the other hand, specific state and local recovery funds are intended to serve the most vulnerable disaster survivors, who typically involve minority populations and low-income communities. Moreover, factors such as pre-existing disparities in disaster exposure and recovery ability by racial and socioeconomic status, administrative burdens of eligibility requirements and paperwork, and concerns about the loss of income and property tax revenue by local governments, can also contribute to the selection of acquisition and buyout programs

[2] We also tested the effects on the number of active businesses by how far they are located from the acquisition and buyout programs. As Figure B.1 shows, after controlling for property damage assessments and county-specific time trends, we did not find supporting evidence for correlation between the spatial selection of programs and the adverse effect of the storm on local business.

based on pricing and demographic characteristics of targeted communities rather than on property damage and recovery needs.

Here, we examine the extent to which observable factors, such as demographic and economic characteristics of local communities, influence the selection of acquisition and buyout programs. To explicitly test for this dependency, we use a cross-section specification that regresses measures of selection effects on demographic and economic observables while controlling for the damage level caused by Sandy. Specifically, our model takes the following form

$$\text{Selection}_i = \beta_1 D_i + \beta_2 \mathbf{I}(\text{Sandy})_i + \beta_3 \text{Damage}_i + \alpha_c + \epsilon_i$$

Here, the regression unit is a census tract, which represents a unit of community throughout the analysis. We include county fixed effects to control for average selections based on a broader jurisdictional level. D_i represents the demographic and economic factors of interest, including the median household income level, the racial distribution of the total population and those affected by Sandy, and the median housing value. $\mathbf{I}(\text{Sandy})_i$ is an indicator for whether community i is under the inundation zone of Sandy. Damage_i includes various measures of the storm's damage to residential properties, including the number and percentage of households affected by flooding, the number of housing units in each categorical damage level, and the average depth of inundation. Our primary concern with selection is whether a community has been assigned acquisition or buyout programs based on factors other than Sandy's damage. Therefore, we measure the selection effect using an indicator for whether the community has been assigned with acquisition or buyout programs.

The results are presented in Table 2.1. Panel A shows that none of the economic factors of interest, including the median household income level and the median housing value, have a significant effect on the selection of acquisition programs. However, after controlling for the damage level of Hurricane Sandy, we find that the demographic distribution of all populations has a role in acquisition programs. All else being equal, communities with a higher proportion of white residents are significantly more likely to experience housing acquisitions after Hurricane Sandy. In contrast, the demographic distribution of the affected populations does not play a role in the selection of acquisition programs. Finally, as shown in Panel B, we find that neither the economic nor demographic factors of interest serve as significant drivers for the selection of buyout programs. [3]

Estimation Models

Our exploration of identification highlights several concerns regarding the use of a standard DiD approach. Therefore, we base our analysis on the setting of DiD model with multiple treatments, which utilizes both the variations driven by the acquisition and buyout programs, as well as the differences before and after the storm Sandy. While a standard DiD model would only allow us to use the limited subset of sample of the post-disaster period, applying the multiple treatments setting enables us to use all the data we have on hand. [4] This not only significantly improves the precision of our estimates but also enables us to answer a broader set of questions, including the differential effects of Sandy on participating properties and control groups.

Property Value

Thanks to the detailed information on property location and sales date provided by the ZTRAX data, we are able to account for the program selection effect by incorporating neighborhood-specific time trends into the model for property value analysis. Specifically,

[3] To test for robustness, we also examine other economic and demographic factors, such as population density measured by the number of housing units, average rental price, and average income level of different races (see Appendix). We find that the effect of these factors is immaterial for the selection of acquisition and buyout programs. We also explore the selection effect from different dimensions, such as the intensity measured by the number of programs, as well as the urgency captured by the timing of the first program (see Appendix). The results suggest that none of the economic and demographic factors of interest have a role in determining the intensity and the urgency of acquisition and buyout programs. Therefore, conditional on being treated, the intensity and the timing of acquisitions and buyouts are not further contingent on the economic or demographic features.

[4] Our sample periods range from 10-15 years before Sandy to 8 years afterwards, and the acquisition and buyout programs typically occurred 2-3 years after the disaster.

our specification takes the following form

$$
\begin{aligned}
\ln(P_{it}) = & \beta_1 T_i \cdot B_{it}^{\mathrm{P}} + \beta_2 T_i \cdot B_t^{\mathrm{S}} + \beta_3 B_t^{\mathrm{S}} + \beta_4 T_i + [\beta_5 \mathbf{I}(\mathrm{Sandy}_i) + \beta_6 \mathrm{Damage}_i] \cdot B_t^{\mathrm{S}} \\
& + \beta_7 X_i + \alpha_{jy} + \epsilon_{it}
\end{aligned}
$$

Here, each observation corresponds to a transaction for property i that happened on date t, with the outcome variable being the log of sales price P_{it}. T_i is an indicator that denotes whether a property was assigned to the "treated" group, which in the context of housing transactions means whether the property is close to acquisition and buyout programs. B_{it}^{P} is the indicator that denotes whether the property was transacted after the corresponding program had taken place. B_t^{S} is an indicator that denotes whether the transaction happened after Hurricane Sandy. Since the treatment timing differs across properties, it is unclear how to assign a treatment for the untreated group. In the baseline regression, the control group is assumed to never have been treated under any circumstances; hence, a pseudo treatment is not assigned to them. This reduces the primary interaction term of interest, $T_i \cdot B_{it}^{\mathrm{P}}$, to a single indicator B_{it}^{P}. [5] To better control for damage caused by Sandy, the model includes an indicator for whether the property has been inundated, as well as a set of damage measures that are interacted with the post-Sandy indicator. Additionally, we also include a handful of property characteristics X_i, including the year the property was built or renovated, the number of bedrooms and bathrooms, and the lot size acreage.

To control for selection bias in acquisition and buyout programs, we adopt a comprehensive approach by assuming that each community has its own unique time trend after Hurricane Sandy.This approach fully captures any community-specific factors that may have influenced the selection process. Our rich dataset at the location and date level allows us to incorporate these community-specific temporal indicators into our regression analysis. We include fixed effects at the census tract by year level, denoted as α_{jy} for census tract j and year y. This ensures that any factors that correlate with the program selection will be ab-

[5] In further robustness checks, we relax this assumption by assigning a pseudo treatment for the control groups. See section 2.5.

sorbed by these fixed effects, and that the DiD estimator of interest, β_1, is not affected by endogenous selection effects.

As a final note, we define the treatment group as properties within a 1000-meter radius of at least one acquisition or buyout program. To ensure that we compare similar properties that are geographically proximate and consistent and not likely to be affected by the program, we define all other properties affected by Sandy, including those impacted by inundation or included in FEMA's damage assessment, as the control group. If a property is within proximity to multiple acquisition and buyout programs, we use the earliest closing date of all nearby programs to construct the event variable. Additionally, our analysis suggests that the treatment effects decay as we move further away from the programs spatially, as shown in Figure 2.2. We also hypothesize that the effects could vary over time and between acquisition and buyout programs. Therefore, we will use corresponding event study frameworks to test these hypotheses.

Inter-Neighborhood Migration

Because the mortgage application panel is collapsed into the census tract and year level, it is not possible to comprehensively include neighborhood-specific time trends in the model to fully eliminate the selection effect. Instead, we analyze migration using the following specification:

$$\begin{aligned} Y_{jy} =& \beta_1 T_j \cdot B^{\mathrm{P}}_{jy} + \beta_2 \mathrm{T}_j \cdot B^{\mathrm{S}}_y + \beta_3 B^{\mathrm{S}}_y + \beta_4 T_i + \beta_5 \mathrm{Damage}_j \cdot B^{\mathrm{S}}_y \\ &+ \sum_{\tau \geq 2012} \beta_{5\tau} D_i \cdot \mathbf{I}(y = \tau) + \alpha_{1c} y + \alpha_{2c} y^2 + \alpha_j + \alpha_y + \epsilon_{it} \end{aligned}$$

where Y_{jy} is the migration outcome for census tract i and year y. The treatment indicators, B^{P}_{jy} and B^{S}_y, are analogous to the previous specification. T_j also denotes whether the community j was assigned to the "treated" group, while in this context we define the treatment as whether there have ever been any acquisition and buyout programs within the community. Similarly, because the treatment timing is differential across communities, we assume the control communities were never treated under any circumstances, reducing the interaction term $T_j \cdot B^{\mathrm{P}}_{jy}$ down to a single indicator B^{P}_{jy}. To control for Sandy's damage, we include a set of damage measures interacted with the indicator of post-Sandy, $\text{Damage}_i \cdot \mathrm{P}^{\text{Sandy}}_t$, including the indicator for being inundated, the number of residential properties in each damage category of FEMA's assessments, and the average inundation depth.

As the migration data are only available at the census tract by year level, we cannot include a full set of idiosyncratic time trends by neighborhood to control for the program selection effect. Instead, we explicitly control for the confounds that may enter the selection process. As previous sections show, only the racial distribution of all populations enter the selection process of the programs. Thus, we incorporate the 2010 level of the white population share interacted with the year indicators for the post-Sandy periods, denoted as $\sum_{\tau \geq 2012} \beta_{5\tau} D_i \cdot \mathbf{I}(y = \tau)$. Additionally, apart from the census tract fixed effects, we incorporate county-specific linear and quadratic time trends to account for prior trends related to storm damage and program assignment at the county level.

Business Performance

Because the firm-level data are collapsed into hexagons that have a size similar to a block, we can treat each hexagon as a small proportion of a community, instead of an entire community. We use the following specification to analysis the effects on business performance

$$
\begin{aligned}
Y_{iy} = &\beta_1 T_i \cdot B^{\mathrm{P}}_{iy} + \beta_2 \mathrm{T}_i \cdot B^{\mathrm{S}}_y + \beta_3 B^{\mathrm{S}}_y + \beta_4 T_i + [\beta_5 \mathbf{I}(\text{Sandy}_i) + \beta_6 \text{Damage}_i] \cdot B^{\mathrm{S}}_y \\
&+ \sum_{\tau \geq 2012} \beta_{7\tau} D_i \cdot \mathbf{I}(y = \tau) + +\alpha_{1c} y + \alpha_{2c} y^2 + \alpha_i + \alpha_y + +\epsilon_{iy}
\end{aligned}
$$

The dependent variable, Y_{iy}, refers to the performance of a firm located in hexagon i at the end of year y. The treatment indicators B^{P}_{jy} and B^{S}_y, as well as the the damage controls $\mathbf{I}(\text{Sandy}_i)$ and Damage_i, are are analogous to the previous specification. T_i indicates whether the hexagon i was assigned to treatment, with the treatment defined as within a neighborhood range of 1000 meters from acquisition or buyout programs. Similarly, because the treatment timing is differential across programs, we choose to not assign a pseudo treatment for the group, reducing the interaction term $T_i \cdot B^{\mathrm{P}}_{iy}$ down to a single indicator B^{P}_{iy}.

We also incorporate the 2010 level of the white population share interacted with the year indicators for the post-Sandy periods, $\sum_{\tau\geq 2012}\beta_{7\tau}D_i \cdot \mathbf{I}(y=\tau)$, to account for the selection effect of acquisitions and buyouts that relies on neighborhood-specific factors. Finally, the model effectively include a full set of hexagon and year indicators as well as county-specific linear and quadratic trends, to account for time-invariant location-specific differences and common trends across counties.

2.5 Results

Impact on Property Value

To begin, we test how the property value responds to the acquisition and buyout programs using a DiD framework with multiple treatments, and present the baseline regressions in Table 2.2. Our preferred specification in Column (2) indicates that acquisition and buyout programs can significantly increase the property value within a 1000-meter radius by 3.47%. We also identifies a selection effect where these programs were often implemented in places severely impacted by disaster. Contingent on the controls for FEMA damage assessments, we find that places close to these programs remain to have seen a reduction of 4.23% in property value after Hurricane Sandy relative to places farther away. As Column (1) presents, we note that a standard DiD model without an inclusion of this differential response to the storm would underestimate the magnitude and significance of the program effect on property value. Furthermore, we find that the geographical intensity of acquisition and buyout programs matters. Column (3) suggests that places close to more than 20 programs experience an 8.28% increase in property value, compared to an average increase of 3.11% for places exposed to less than 20 programs, after the programs occurred.

We examine the differential impacts of buyout and acquisition on property value, and our results reveal that the effect of acquisition on property value is more significant than that of buyout, as indicated in Column (4). We also observe differential selection effects for buyouts and acquisitions, with acquisitions occurring in places where the property value has been impacted by the storm by 4.96% more than an average inundated property, while buyouts have occurred in places where the property value has reduced by 3.55% less after the storm relative to an average inundated property. Column (5) further suggests that spatial intensity of acquisitions and buyouts also plays a role. Places with more than 10 acquisitions within 1000 meters have experienced an 8.14% growth in their property value, compared to a 4.07% increase in the less intensive acquisition places. Similarly, for buyouts, only places that experienced more than 10 buyouts within 1000 meters have experienced a significant growth, which is on average 3.9%, relative to an insignificant effect for the less intensive buyout places.

We conduct three robustness tests to validate these findings and present their results in Table B.3. Firstly, we test the robustness of the results by limiting the range of the control group to 5 km from acquisition and buyout programs, allowing us to compare treated properties only to their geographically similar counterparts. Secondly, we test the robustness by limiting to repeated sales only, namely sales for which the property have been sold at least once before the storm and afterwards. This strategy reduces the sample size by less than one-third while better controlling for omitted variables on property level. Finally, we relax the assumption made in the baseline regression that the properties of the control group would never be treated. We assign a pseudo-treatment date for the control properties by defining it as the date of the first acquisition or buyout program of its county, if there is any, or the average date of all programs across the state if there were not any participating properties in its county. We find that the significant effect of acquisition and buyout programs on property value, the differential effect by program intensity, and the dominant effect of acquisitions to buyouts remain robust to these tests.

As indicated in Figure 2.2, the impact of acquisition and buyout programs on property value can vary depending on the distance from the program site. To test this relationship, we re-run the baseline specification on the log of sales price, where the indicators of interest were interacted with the indicators of distance bin of a 50-meter range defined by the distance from the nearest acquisition or buyout program. [6] The coefficients by distance bin are presented in the top panel of Figure 2.4, and the results suggest that the average program effects decay as being farther away. Within a close neighborhood range (up to 250 meters), the acquisitions and buyouts can increase the property value by up to 10%. However, after 300 meters away, the effects become imprecisely estimated and negligible. Furthermore, we examine how the effects of acquisitions and buyouts separately respond to distance, as shown in the middle and bottom panels of Figure 2.4. We find that both effects decay as being farther away, with the effect of acquisitions being significant and large up to 15% within a neighborhood range. In contrast, the effects of buyouts are much smaller and become negligible after a block range (100 meters).

One important policy question is whether acquisition and buyout programs are effective in aiding the recovery of disaster-stricken properties. To assess the recovery effect, we use residualized property values, which account for the component that cannot be explained by property characteristics and time trends. By comparing the residuals at different stages, as shown in Figure 2.2, we find that properties located near acquisition and buyout programs were severely affected by the disaster, but also experienced more noticeable recovery effects after the program. Our results suggest that acquisition and buyout programs have played a crucial role in helping disaster-stricken properties to recover back to their pre-disaster level. Therefore, we can infer that these programs are effective in aiding the recovery of disaster-damaged properties.

Lastly, we explore the possibility that the impacts of acquisition and buyout programs could change over time. To test this hypothesis, we expand the baseline specification to an event study framework, defining the event as the first acquisition or buyout program within a close neighborhood of 200 meters. Unlike a standard event study framework, we normalize the response to zero just before Hurricane Sandy, setting the reference year to 3 years before the programs. As shown in the top panel of Figure 2.5, we find that these programs have

[6] We also include the interactions on the post-Sandy indicator, as the specification follows a DiD framework with multiple treatment.

a positive effect on nearby property values immediately afterwards. Importantly, the effects do not attenuate but instead continue to strengthen over the near future. Six years after the program, nearby properties experience an average growth of 20% in property value relative to the pre-disaster level, compared to properties farther away. The middle panel of Figure 2.5 indicates that the persistent effects were primarily driven by acquisition programs. Finally, the bottom panel shows that the effects of buyout programs on property value were negligible, both contemporaneously and over time.

In conclusion, our analysis suggests that acquisition programs have a significant and lasting positive effect on property values, with the greatest impact observed in close neighborhoods that gradually decreases as the distance from the program increases. Furthermore, these effects persist over time and even strengthen. In contrast, the effects of buyout programs on housing markets are much smaller in size, quickly decaying over space, and attenuating over time.

Residential Sorting

In this section, we examine the effects of acquisition and buyout programs on the intentions and patterns of migration across neighborhoods, using mortgage application data and focusing on three key measures: 1) the number of mortgage applications for houses located in communities with participating properties, 2) the income of intentional migrants looking to move in, and 3) the racial distribution of families intending to move in. We control for a comprehensive set of factors, including indicators at the neighborhood and year levels, county-specific linear and quadratic trends, and demographic factors that enter the selection process interacted with the year indicators for the post disaster period, ensuring that any observed effects revealed by the regression results cannot be attributed to differential pre-existing trends among neighborhoods.

Table 2.3 presents the baseline results, with the average effects shown in Panel A. Column (1) tests how these programs attract new families to move in, and we find that the number of mortgage applications for houses inside participating neighborhoods increased by an average of 35.3 per year after the program occurred, equivalent to approximately 28.6% of applications on the pre-disaster level. Columns (2) nd (3) indicate that migration intentions are skewed towards high-income households, with the average income of mortgage applicants increasing significantly by 2.1%. We also compare the income levels of mortgage applicants with the county's median level of 2015 and find that the share of high-income households intending to move in rose noticeably by 1.4 percentage points in places with participating properties after their occurrence. Moreover, acquisition and buyout programs play a role in correcting pre-existing racial inequalities. While places with these programs were more likely to be dominated by white households beforehand, we find that the mortgage applications for the treated communities have seen a 0.4 percentage point increase in the black share of applicants and a 2.1 percentage points reduction in the white share of applicants, after the programs occurred in these communities.

We also analyze the treatment effect by program intensity within communities. We divide the treated communities into high and low intensity based on whether there have been at least 5 programs within the community. As shown in Panel B of Table 2.3, we find that the program effects of attracting wealthy families and correcting racial disparity are more pronounced in places where acquisition and buyout programs have occurred more intensively. Specifically, in places with high program intensity, we observe approximately a half increase in the number of mortgage applications, a 2 percentage point rise in the share of high-income applicants, and a correction of racial inequality driven by a 2.7 percentage points reduction in white applicants and 1.1 percentage points increase in black applicants. In contrast, in places with fewer than 5 programs, these effects are relatively small and statistically insignificant

We further evaluate the differential effects between acquisitions and buyouts, and the results are presented in Table 2.4. Panel A reports the average treatment effects for acquisitions and buyouts separately. Column (1) suggests that while both programs help attract new home buyers to settle down, the effect of acquisitions is more significant. Having acquisition programs has increased the number of mortgage applications by approximately 30%

afterwards, while buyout programs have only increased mortgage applications by roughly 10% for participating communities. Moreover, as shown in Columns (2) and (3), we find that the average program effect of attracting wealthy families is primarily driven by acquisition programs. Additionally, Columns (4) and (5) suggest both acquisitions and buyouts can help attract more racial minority migrations, but their effects operate through different channels. The effect of acquisitions is more centered on attracting families from minority groups, while the effect of buyout programs is more focused on reducing the desirability of families from the dominant group to move in.

Finally, we investigate how the spatial distribution of acquisition and buyout programs affects their treatment effects across communities. Panel B of Table 2.4 presents our findings on differential effects by treatment intensity for acquisition programs. We observe that neighborhoods with high intensity of acquisitions experience a significant increase in mortgage applications afterwards, with migration intentions being skewed towards high-income families. Additionally, the correction effect of racial distribution is only evident for neighborhoods with more than five acquisitions. In contrast, neighborhoods with low acquisition intensity show less significant effects in attracting wealthy homebuyers and reducing racial disparities. Interestingly, we find no significant difference in the intensity of buyouts in determining their effects on migration flows. Neither neighborhoods with high nor low intensity of buyout programs have experienced noticeable changes in mortgage applications after their occurrence.

Business Growth and Job Creation

The aim of this section is to investigate the impact of acquisition and buyout programs on the economic performance of local businesses using the NETS data. We focus on two key aspects of business performance: firm growth and job creation. Firm growth is measured by the growth rate of active businesses, the birth rate (number of new firms as a share of existing firms), and the death rate (number of death firms as a share of all existing firms).

Job creation is measured by the growth rate of employment and the average firm size.

We begin by evaluating the effect of acquisition and buyout programs on businesses across all industries. The results are presented in Panel A of Table 2.5. We find that businesses located in close proximity to acquisition and buyout programs were disproportionately affected by the storm, as indicated by the coefficients on the interactions between the program treatment and the indicator for post-Sandy. However, as shown in Column (1), we also find that these programs helped with business recovery, with treated places experiencing a 0.92% increase in the growth rate of local businesses after the program occurrence. This recovery was primarily driven by a 0.65% reduction in the death rate of local businesses, with a less significant contribution from a 0.33% increase in the birth rate, as suggested in Columns (2)-(3). Regarding employment, our results show that Hurricane Sandy led to a 2.4% greater reduction in total employment in places located close to these programs compared to places farther away, and hence the average employment per firm increased by 2.7% due to the reduced growth rate of local businesses, as indicated in Columns (4)-(5). However, after the acquisitions and buyouts occurred, we find that the treated places experienced a higher recovery of 1.3% in total employment and a 1.5% increase in the average firm size, relative to places located 1km away from acquisition and buyout programs.

In Panel B of Table 2.5, we examine the differential effects between acquisitions and buyouts. The results reveal that businesses located in places soon to be assigned with acquisitions and buyouts were affected differently by Hurricane Sandy. Those located close to acquisition programs experienced a significant reduction in business birth rates, a moderate reduction in total job creation, and a noticeable growth in average firm size, after Hurricane Sandy. In contrast, places close to buyout programs experienced a substantial reduction in the number of active businesses due to the reduced birth rate and increased death rate, and saw a significant reduction in the growth of total employment with no significant change in the average employment per firm after the storm. Moving on to the differential effects between programs, we find that both acquisitions and buyouts have a positive impact on the growth of local businesses but through different channels. Acquisitions result in a significant increase in the birth rate of 5.0%, accompanied by an imprecisely estimated reduction in the death rate of 3.7%. In contrast, buyouts primarily drive a reduction in the death rate by 8.1%. In terms of the impact on employment, the results indicate that only buyout programs have a significant effect on job creation and employment size. The average community treated by buyout programs experienced a growth of 2.0% in total employment and an increase of 2.8% in the average employment per firm. Acquisitions, however, did not play a significant role in affecting the employment of local businesses.

We further investigate the response of firm performance to acquisition and buyout programs by examining the differences across industries. To do so, we rank the industries by the number of businesses in 2010 and report their results sequentially in Tables 2.6 and 2.7. We identify significant differences in the response of local businesses to these programs across industries, which we attribute to three factors: the nature of the acquisition and buyout programs, the effect of land and property values, and the demographic distribution of migration flows, which affects product demand and labor supply and costs. Our analysis yields four key findings.

First, we find that the effects of acquisitions on firm growth and birth are significantly more pronounced in the local businesses of Service and Construction industries. The expansion of the Service sector can be attributed to the increased demand for service products, such as dining and entertainment, due to the influx of high-income populations. In the Construction sector, the growth of local businesses is mainly due to the nature of acquisitions, which require reconstruction and renovation after the auction. On the other hand, the growth rates of local businesses in Retail Trade, Finance, Insurance, and Real Estate industries have declined after the acquisitions. The reduced growth in the Retail sector is driven by the increased land price associated with change in property value, which pushed new stores to locate farther away from the acquisition neighborhoods. The shrinking of the Finance, Insurance, and Real Estate industry can be attributed to the fact that the auction for acquisition programs typically requires all-cash payments, thereby reducing the demand for finance and real estate agents.

Second, we find that while acquisition programs did not have a significant effect on the job creation aggregated across all industries, there are notable compositional effects on specific industries. Our analysis reveals that acquisition neighborhoods experienced significant job creation in the Construction, Transportation and Public Utilities, Wholesale Trade, and Public Administrations sectors, while employment in the Finance, Insurance, and Real Estate sector decreased. The effects on employment in the Construction and Real Estate sectors are due to the nature of acquisitions, while we attribute the job creation in other affected industries to the increased demand and reduced labour cost resulting from attracting migrations of wealthy households. However, we did not observe a response in the number of businesses in these industries, as the average employment size of a representative business in these industries is relatively large, resulting in high fixed costs for new establishments.

Third, we find that the average positive effects of buyouts on business growth are primarily driven by the Service sector, possibly due to a better survival rate resulting from better natural amenities and unresponsive land prices after buyouts. In contrast, some industries, such as Transportation and Public Utilities, Wholesale Trade, and Public Administrations, have experienced reduced growth rates in local businesses after the buyout programs occurred. These reductions are likely related to the decreased demand in aggregate due to the nature of buyout programs, which eliminate residential properties and lead to increased open areas, consequently reducing the number of residents.

Finally, we find that buyouts have a significant positive effect on job creation in aggregate, which is primarily driven by the Service and Retail sectors. This expansion in employment can be attributed to the increased inflow of low-income households following the occurrence of buyouts, which reduces the cost of labor in these labor-intensive industries. Furthermore, we observe an increase in the average employment size of the Retail sector post-buyouts, indicating an general equilibrium consequences resulting from both the increased demand due to new arrivals as well as high fixed cost of starting a new business.

2.6 Conclusion

In conclusion, this paper examines the impact of the NY Rising Program, a post-disaster buyout and acquisition program, on nearby property values, demographic changes, and the business environment. Our findings suggest that these programs can effectively aid in the recovery of disaster-stricken properties, attract new families to settle in disaster-stricken areas, correct pre-existing racial inequalities within communities, and enhance the growth of local businesses. Both types of programs have a positive impact on local business growth and employment, albeit through different channels and industries. Our study also highlights the importance of considering neighborhood-specific time trend parameters and demographic factors when selecting programs across neighborhoods.

Although concerns exist regarding the negative impact of buyout and acquisition programs on the local economy and tax base, our study suggests that the actual economic impacts may be less negative than projected. These programs present a unique opportunity for a community to upgrade and reorganize its housing stock during the recovery process, creating positive general equilibrium effects at the community level.

Overall, our findings suggest that managed retreat strategies, such as buyout and acquisition programs, can effectively address the tension between the need to protect against disasters and the need to maintain a thriving local economy and tax base. Therefore, we recommend that policymakers consider these programs as part of their disaster risk management strategy, particularly in areas prone to natural disasters. We also suggest that future research explore the long-term impacts of these programs and identify additional factors that may influence their effectiveness, as well as how they interact with other policies aimed at disaster risk reduction and climate change adaptation.

Figure 2.1: Acquisition and Buyout Programs

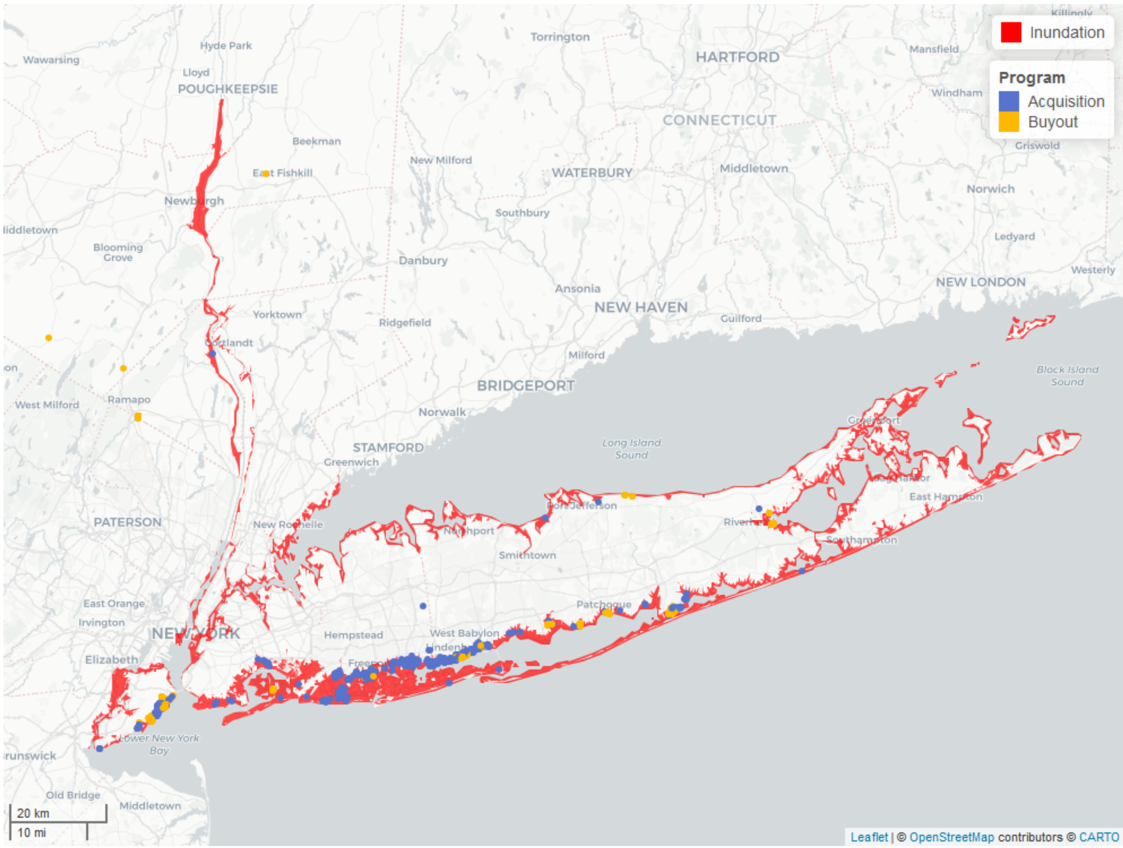

Notes: The red area displays the inundation map of storm Sandy. The colored points show the geographical location of acquisition and buyout programs.
Source: New York State Governor's Office of Storm Recovery and FEMA's Modelling Task Force.

Figure 2.2: Gradient effect of distance from participating properties on property value

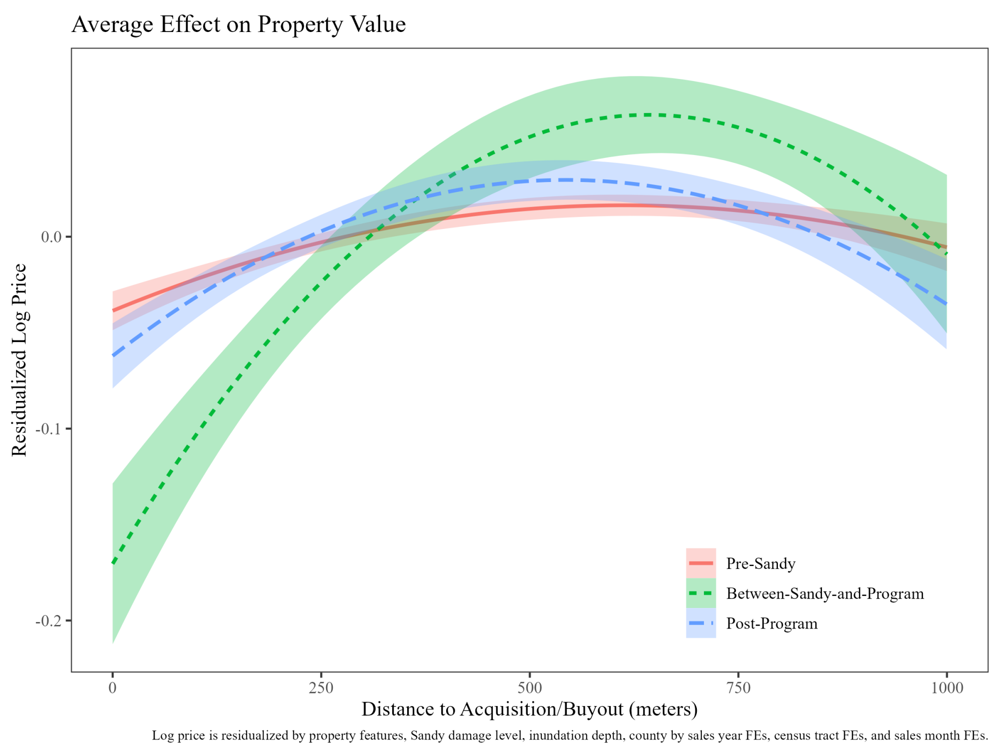

Notes: Log price is residualized by property features, Sandy damage level, inundation depth, county by sales year FEs, census tract FEs, and sales month FEs. Smoothing curves are obtained through a polynomial model fit. Shades show the 95% confidence intervals clustered twoway by census tract and sales year.

Figure 2.3: Omitted Variable Bias from Sandy's Effect

Panel A: No Correlation

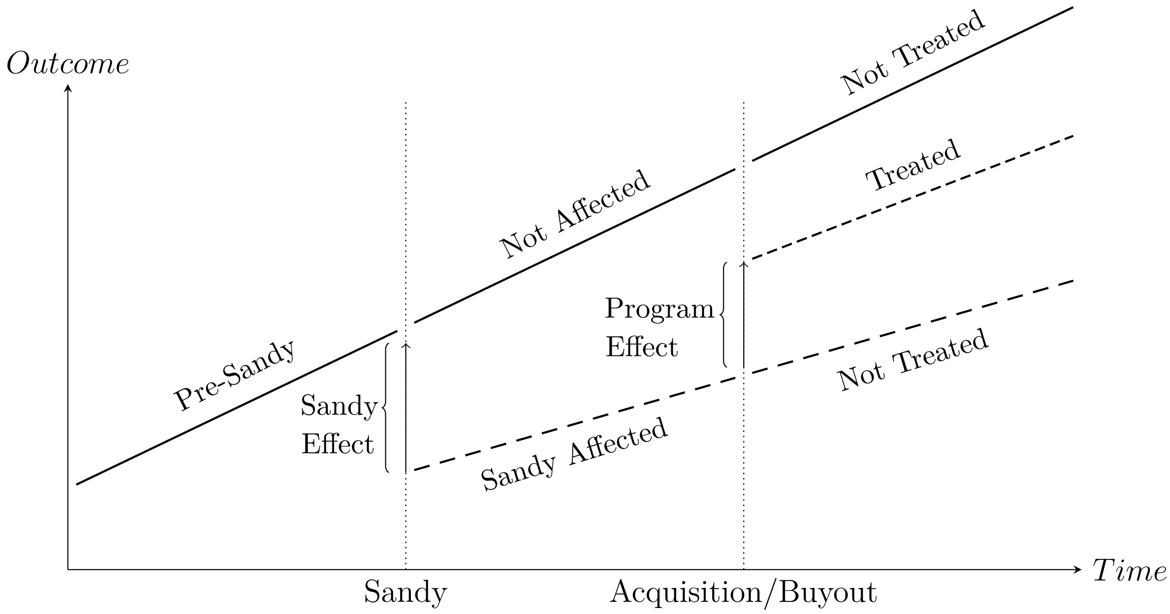

Panel B: Correlation between Sandy Exposure and Program Selection

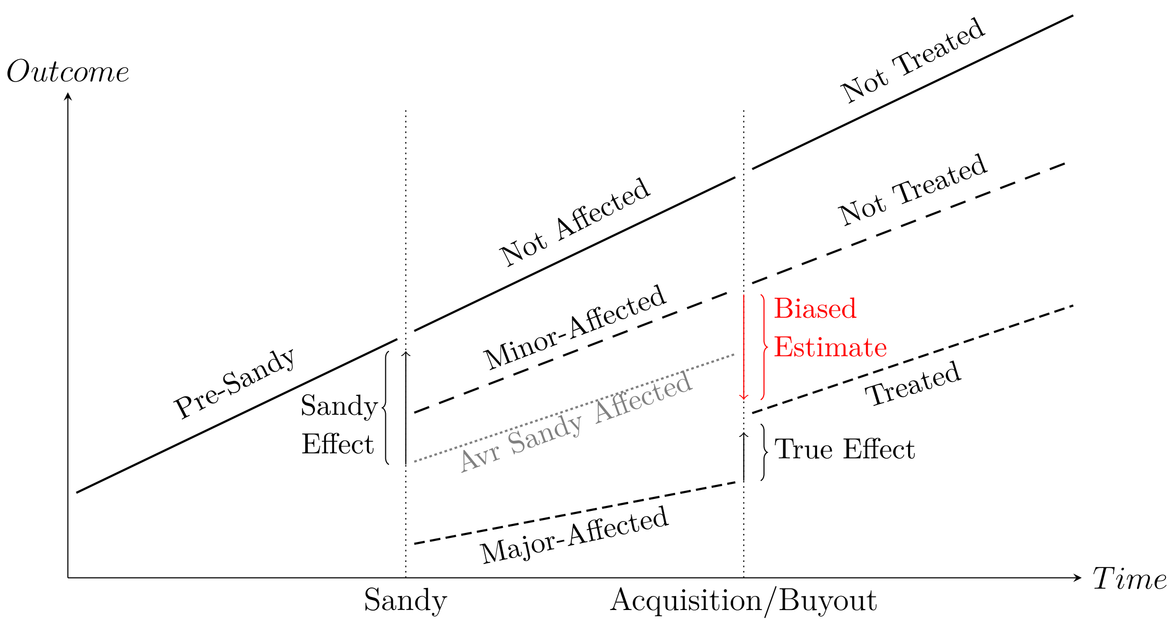

Figure 2.4: Program Treatment Effect on Log(Property Value) by Distance

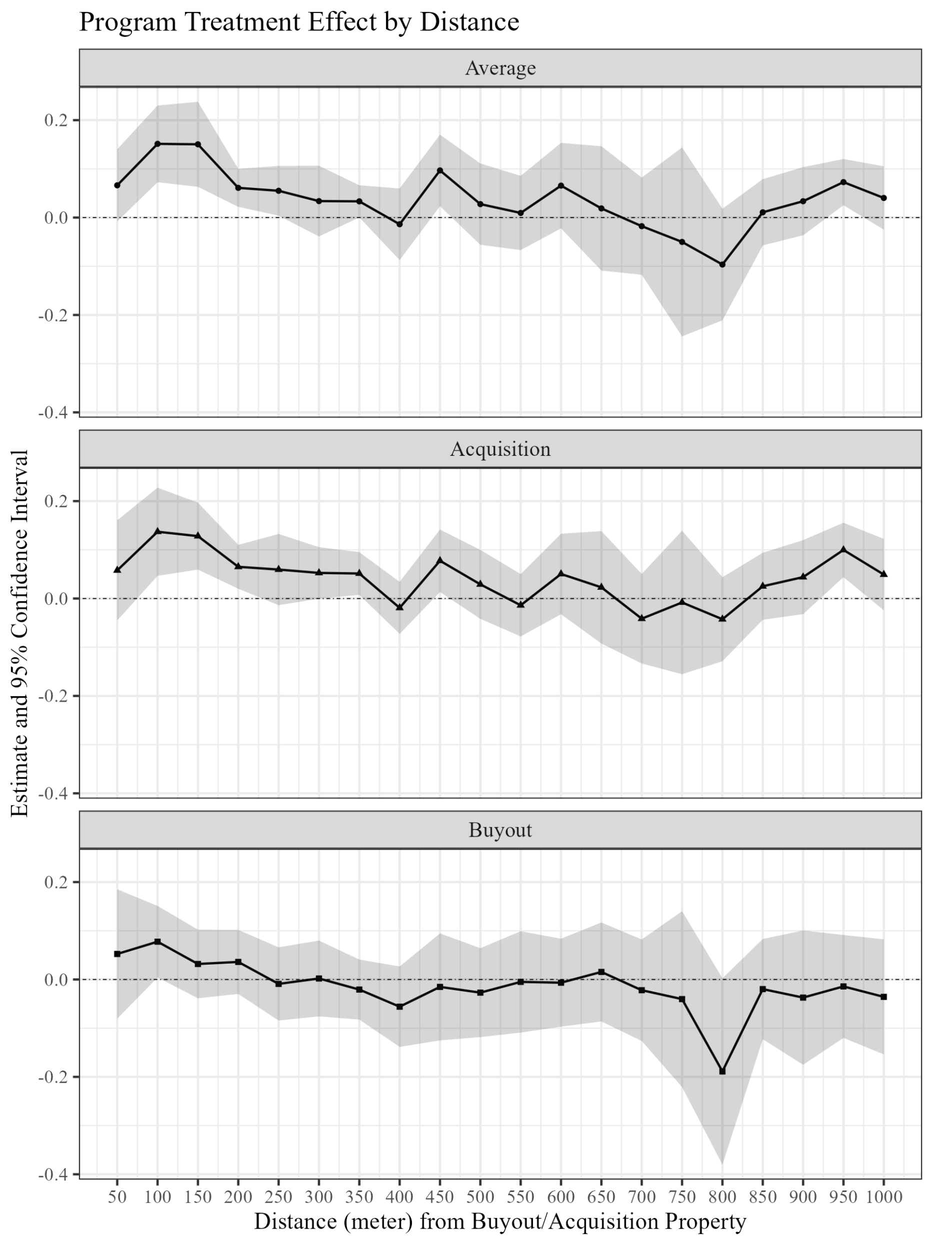

Notes: The three panels display the coefficients from the baseline specification of DiD model with multiple treatment on the log of sales price, where the indicator of interest (post-treatment interacted with being treated) is interacted with the indicators of distance bin of a 50-meter range range defined by the distance from the nearest acquisition or buyout program. The top panel accounts for both acquisition and buyout programs, the middle panel accounts for acquisition programs only, and the bottom panel considers buyout programs only. Shades represent 95% confidence intervals constructed using standard errors clustered twoway at the census tract and year level.

Figure 2.5: Dynamic Program Effect on Log(Property Value) for Close Neighborhood

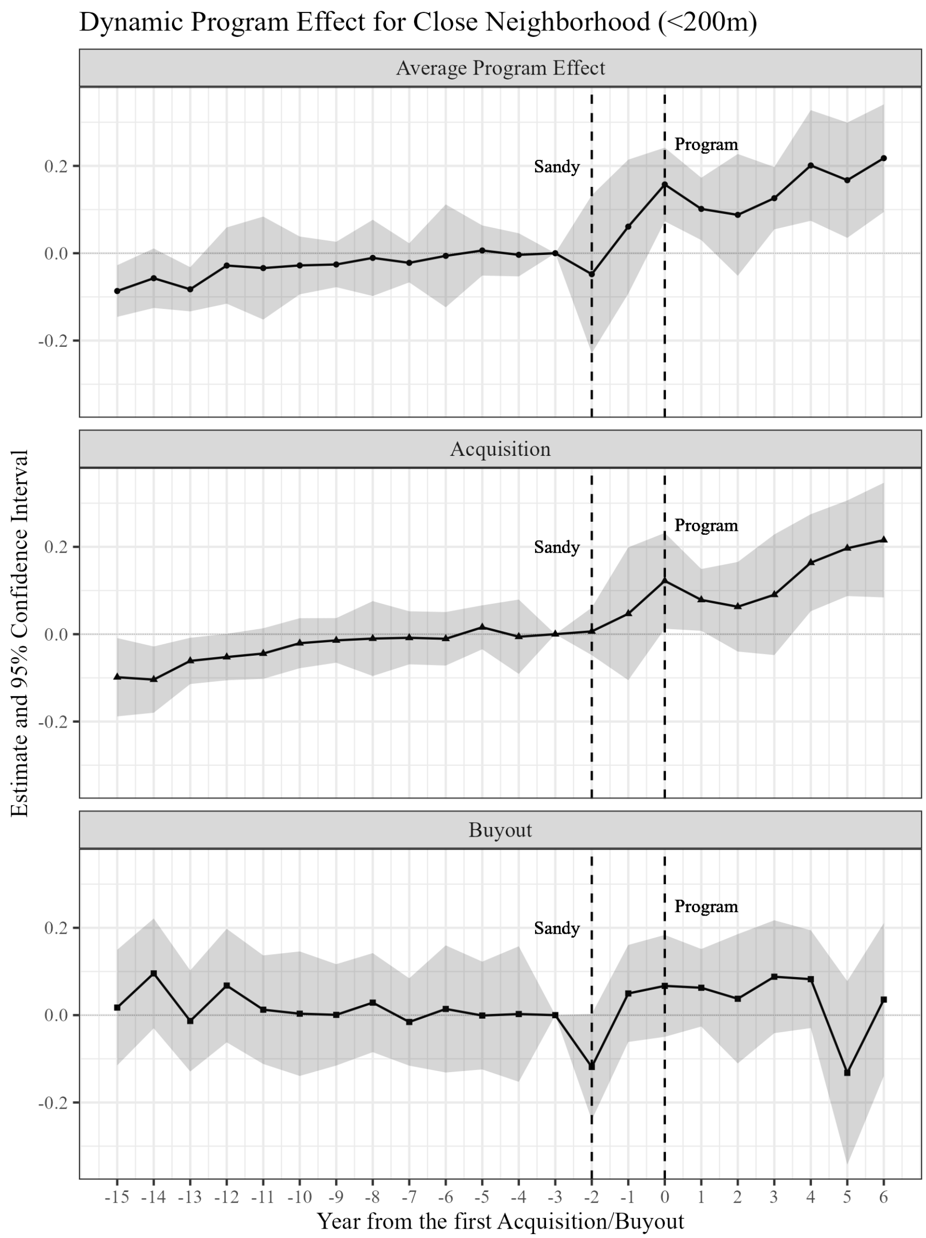

Notes: The three panels displace event study regression coefficients based on the baseline specification of DiD model with multiple treatment on the log of sales price. The treatment group is limited to within 200 meters of the acquisition and buyout programs. The top panel accounts for both acquisition and buyout programs, the middle panel accounts for acquisition programs only, and the bottom panel considers buyout programs only. All panels span 15 years before to 6 years after the treatment, and normalize the coefficient for year -3 (one year before the storm) to zero. Shades represent 95% confidence intervals constructed using standard errors clustered twoway at the census tract and year level.

Table 2.1.
Regression Results for Program Selection by Economic and Demographic Factors

	Economic Factor		Demographic Factor			
	log(HH Income)	log(HU Value)	% Wh	% Wh Sandy	% Bl	% BL Sandy
	(1)	(2)	(3)	(4)	(5)	(6)
Panel A: Indicator for having acquisition or buyout programs						
D_i	0.237	0.109	2.15*	1.88	-2.66	-2.27
	(0.199)	(0.0848)	(1.12)	(1.38)	(1.64)	(1.92)
Pseudo R^2	0.618	0.617	0.623	0.620	0.622	0.620
Panel B: Indicator for having acquisition programs						
D_i	0.222	0.0804	0.917	0.939	-1.39	-1.32
	(0.225)	(0.0527)	(0.674)	(0.996)	(1.3)	(1.59)
Pseudo R^2	0.673	0.672	0.673	0.673	0.674	0.673
Panel C: Indicator for having buyout programs						
D_i	0.0128	0.0484	2.48	1.38	-2.66	-0.78
	(0.136)	(0.18)	(2.24)	(2.32)	(3.22)	(3.09)
Pseudo R^2	0.563	0.563	0.569	0.564	0.567	0.563
Observations	4367	4367	4367	4367	4367	4367
County FE	Y	Y	Y	Y	Y	Y
Clusters	Y	Y	Y	Y	Y	Y

Notes: Estimation results for the dummy for having acquisition programs (Panel A) and the dummy for having buyout programs (Panel B), as a function of the economic and demographic factor indicated in the column title. The sample is a census tract unit, and each regression includes county fixed effects. Standard errors are clustered at the county level. * p<0.1, ** p<0.05, *** p<0.01.

Table 2.2.
Impacts of Acquisition and Buyout Programs on Log(Property Value)

	A. Average Effect			B. Effect by Program			
	(1)	(2)	(3)	(4)		(5)	
				Acquisition	Buyout	Acquisition	Buyout
Treated × Post-Program	0.019	0.0347***		0.0402***	-0.00101		
	(0.0185)	(0.00486)		(0.0111)	(0.0179)		
× low intensity			0.0311***			0.0286**	-0.0129
			(0.00523)			(0.0104)	(0.0225)
× high intensity			0.0828*			0.081***	0.039***
			(0.0463)			(0.0237)	(0.0105)
Treated × Post-Sandy		-0.0423***		-0.0496***	0.0355***		
		(0.00908)		(0.0128)	(0.00996)		
× low intensity			-0.0225			-0.0407**	0.047***
			(0.0163)			(0.0166)	(0.0161)
× high intensity			-0.066			-0.0814***	-0.0179
			(0.0522)			(0.0173)	(0.0251)
Adj R^2	0.599	0.599	0.599	0.599		0.599	
N	467229	467229	467229	467229		467229	

Notes: Estimation results for the property value on the effect of acquisition and buyout programs. Dependent variable is the log of sales price. Columns (1)-(5) represent different specifications of the model. Column (1) applies the standard DiD specification, Column (2) further includes interaction terms between the indicator for being treated and for post-Sandy, Column (3) accounts for the differential effects by program intensity, with treatment intensity classified as "low" or "high" depending on whether there are less or more than 20 programs within a range of 1000 meters. Columns (4) and (5) consider the differential impacts between acquisitions and buyouts. In column (5), the "low" and "high" divisions are made by using the cutoff of 10 acquisitions/buyouts within 1000 meters. Each specification controls for a full set of property characteristics and fixed effects of the census tract by year level. Standard errors are clustered twoway at the census tract and year level. * $p<0.1$, ** $p<0.05$, *** $p<0.01$.

Table 2.3.
Average Program Impacts on Mortgage Applications

	#Loans
	Mean=126
	(1)
		Log(Med Inc)
		Mean=11
		(2)
			%(>Med Inc)
			Mean=63
			(3)
				%(White)
				Mean=65
				(4)
					%(Black)
					Mean=14
					(5)

Panel A: Average Program Effect					
Treated × Post-Program	35.3***	0.0209***	1.36*	-2.07**	0.372***
	(11.8)	(0.00691)	(0.782)	(0.861)	(0.124)
Treated × Post-Sandy	-14.5	-0.013	-1.28	2.85**	-0.143
	(17.5)	(0.00992)	(0.867)	(1.2)	(0.497)
Adj R^2	0.725	0.877	0.739	0.895	0.888
Panel B: Average Program Effect by Treatment Intensity					
Treated × Post-Program:					
× low intensity	19	0.0178**	0.88	-1.29	-0.278
	(13.6)	(0.0068)	(0.786)	(0.914)	(0.345)
×high intensity	57.3***	0.0236*	1.99*	-2.69*	1.13*
	(9.1)	(0.012)	(1.05)	(1.43)	(0.563)
Treated × Post-Sandy					
× low intensity	-6	-0.0153	-1.08	3.6**	-0.421
	(20.4)	(0.0109)	(0.99)	(1.53)	(0.516)
× high intensity	-27.5	-0.00732	-1.57	1.1	0.528
	(25.1)	(0.0133)	(1.26)	(1.29)	(0.836)
Adj R^2	0.725	0.877	0.739	0.895	0.888
N	90867	77925	78202	77826	77826

Notes: Estimation results for the measures of mortgage application on the average effect of acquisition and buyout programs. Each regression utilizes the specification of DiD with multiple treatments, including interaction terms between the indicator for being treated and for post-Sandy. Dependent variable is the number of mortgage applications in column (2), the log of median household annual income of applicants in (2), the share of applicants with household annual income above the county's median level in (3), the share of applicants with household annual income below the county's median level in (4), the number of white applicants as a share of total applicants in (5), and the number of black applicants as a share of total applicants in (6). Panel B further accounts for the differential effects by program intensity, with treatment intensity classified as "low" or "high" depending on whether there are less or more than 5 programs within the census tract. Each specification controls for the fixed effects of the census tract and year level, the linear and quadratic time trends interacted with county dummies, and the share of white populations in 2010 interacted with the year dummies for the post-Sandy period. Standard errors are clustered twoway at the census tract and year level. * p<0.1, ** p<0.05, *** p<0.01.

Table 2.4.
Impacts by Program on Mortgage Applications by Program Type

	#Loans
	Mean=126
	(1)
		Log(Med Inc)
		Mean=11
		(2)
			%(>Med Inc)
			Mean=63
			(3)
				%(White)
				Mean=65
				(4)
					%(Black)
					Mean=14
					(5)

Panel A: Effect by Program Type					
Treated × Post-Acquisition	38.8***	0.0277**	1.8*	-1.09	0.469***
	(9.25)	(0.0113)	(0.91)	(0.74)	(0.146)
Treated × Post-Buyout	12.7*	-0.0146	-1.06	-3.86***	0.3
	(6.65)	(0.0178)	(0.927)	(1.31)	(0.338)
Adj R^2	0.725	0.877	0.739	0.895	0.888
Panel B: Effect by Program Type and Treatment Intensity					
Treated × Post-Acquisition					
× low intensity	26.4**	0.0177	1.23	-0.917	0.201
	(9.43)	(0.0119)	(0.852)	(1.26)	(0.324)
× high intensity	60.6***	0.0485***	2.88**	-1.28	0.771
	(9.12)	(0.0114)	(1.29)	(1.5)	(0.568)
Treated × Post-Buyout					
× low intensity	8.96	0.00212	-0.905	-5.13**	0.401
	(14)	(0.0202)	(0.951)	(2.29)	(0.468)
× high intensity	1.73	-0.0537***	-2.1	-1.87	-0.0686
	(6.3)	(0.0173)	(1.37)	(2.62)	(1.01)
Adj R^2	0.725	0.877	0.739	0.895	0.888
N	90867	77925	78202	77826	77826

Notes: Estimation results for the measures of mortgage application on the separate effect of acquisition and buyout programs. Each regression utilizes the specification of DiD with multiple treatments, including interaction terms between the indicator for being treated and for post-Sandy. Dependent variable is the number of mortgage applications in column (2), the log of median household annual income of applicants in (2), the share of applicants with household annual income above the county's median level in (3), the share of applicants with household annual income below the county's median level in (4), the number of white applicants as a share of total applicants in (5), and the number of black applicants as a share of total applicants in (6). Panel B further accounts for the differential effects by program intensity, with treatment intensity classified as "low" or "high" depending on whether there are less or more than 5 acquisitions or buyouts within the census tract. Each specification controls for the fixed effects of the census tract and year level, the linear and quadratic time trends interacted with county dummies, and the share of white populations in 2010 interacted with the year dummies for the post-Sandy period. Standard errors are clustered twoway at the census tract and year level. * p<0.1, ** p<0.05, *** p<0.01.

Table 2.5.
Impacts of Acquisition and Buyout Programs on Business Performance

	Firm Growth			Job Creation	
	% Dif #Firms	% Birth	% Death	Dif Ln(#Jobs)	Ln(Avr Emp)
	(1)	(2)	(3)	(4)	(5)
Panel A: Average Program Effect					
Treated × Post-Program	0.00918***	0.00331	-0.00647**	0.0134***	0.0146*
	(0.00331)	(0.00248)	(0.00255)	(0.0045)	(0.00812)
Treated × Post-Sandy	-0.0115***	-0.0114***	-0.00108	-0.0235***	0.0269***
	(0.00445)	(0.00266)	(0.00303)	(0.00615)	(0.00969)
R^2	0.153	0.179	0.175	0.079	0.807
Panel B: Effect by Program Type					
Treated × Post-Acquisition	0.00785**	0.00497*	-0.00371	0.00607	0.00441
	(0.00395)	(0.0027)	(0.00291)	(0.00496)	(0.00841)
Treated × Post-Buyout	0.00733	-0.0015	-0.00807*	0.0201***	0.0277**
	(0.0065)	(0.0046)	(0.0042)	(0.00773)	(0.0138)
Acquisition × Post-Sandy	-0.00483	-0.0093***	-0.0041	-0.0148**	0.0269**
	(0.00421)	(0.00286)	(0.00281)	(0.00575)	(0.0109)
Buyout × Post-Sandy	-0.0163*	-0.00689	0.00586	-0.0279***	-0.0013
	(0.00883)	(0.00502)	(0.00536)	(0.00883)	(0.0131)
R^2	0.153	0.179	0.175	0.079	0.807
N	430849	462865	462865	481637	518686

Notes: Estimation results for the measures of business performance on the effect of acquisition and buyout programs. Each regression utilizes the specification of DiD with multiple treatments, including interaction terms between the indicator for being treated and for post-Sandy. Panel A presents the average program effect, and Panel B presents the separate effects of acquisitions and buyouts, Dependent variable is the difference in the number of active businesses as a share of all active business of the previous year in column (1), the number of new firms as a share of all active business of the previous year in (2), the number of terminating firms as a share of all active business of the previous year in (3), the difference in the log of the number of employments of all businesses between the current and previous year in (4), and the log of the average number of employment per enterprise in (5). Each specification controls for the fixed effects of the hexagon level and year level, the linear and quadratic time trends interacted with county dummies, and the share of white populations in 2010 interacted with the year dummies for the post-Sandy period. Standard errors are clustered at the zip code level. * p<0.1, ** p<0.05, *** p<0.01.

Table 2.6.
Impacts on Business Performance by Industry

	Firm Growth			Job Creation	
	% Dif #Firms	% Birth	% Death	Dif Ln(#Jobs)	Ln(Avr Emp)
	(1)	(2)	(3)	(4)	(5)
Panel A: Service (53% of all businesses in 2010)					
Treated × Post-Acquisition	0.0127**	0.00746**	-0.0057	0.0089	-0.00503
	(0.00537)	(0.00346)	(0.0037)	(0.00706)	(0.153)
Treated × Post-Buyout	0.0165**	0.00325	-0.0126***	0.0338***	0.226
	(0.00714)	(0.00528)	(0.00449)	(0.00709)	(0.29)
Panel B: Retail Trade (14% of all businesses in 2010)					
Treated × Post-Acquisition	-0.0148*	-0.0115**	0.00265	-0.000878	-0.0139
	(0.00792)	(0.00486)	(0.00544)	(0.0105)	(0.0139)
Treated × Post-Buyout	0.00826	-0.00831	-0.0177**	0.0232**	0.0477**
	(0.01)	(0.00543)	(0.00837)	(0.0093)	(0.0241)
Panel C: Finance, Insurance, Real Estate (10% of all businesses in 2010)					
Treated × Post-Acquisition	-0.0165*	-0.00906*	0.00707	-0.017*	-0.00656
	(0.00878)	(0.00499)	(0.00661)	(0.00901)	(0.0154)
Treated × Post-Buyout	-0.0126	-0.0016	0.0109	-0.0109	-0.0169
	(0.0162)	(0.00837)	(0.013)	(0.0188)	(0.0296)
Panel D: Construction (8% of all businesses in 2010)					
Treated × Post-Acquisition	0.0191**	0.000901	-0.0183***	0.0255**	0.0206
	(0.00888)	(0.00473)	(0.00691)	(0.00989)	(0.015)
Treated × Post-Buyout	-0.00945	-0.0147***	-0.00444	0.0011	0.0242
	(0.00887)	(0.00398)	(0.00728)	(0.00996)	(0.0172)

Notes: Estimation results for the measures of business performance on the effect of acquisition and buyout programs, by 2-digit SIC industry. Each regression utilizes the specification of DiD with multiple treatments, including interaction terms between the indicator for being treated and for post-Sandy. Each specification controls for the fixed effects of the hexagon level and year level, the linear and quadratic time trends interacted with county dummies, and the share of white populations in 2010 interacted with the year dummies for the post-Sandy period. Standard errors are clustered at the zip code level. * p<0.1, ** p<0.05, *** p<0.01.

Table 2.7.
Impacts on Business Performance by Industry (Continued)

	Firm Growth			Job Creation	
	% Dif #Firms	% Birth	% Death	Dif Ln(#Jobs)	Ln(Avr Emp)
	(1)	(2)	(3)	(4)	(5)
Panel E: Transportation & Public Utilities (6% of all businesses in 2010)					
Treated × Post-Acquisition	-0.00167	-0.00613	-0.00494	0.0315**	0.0344**
	(0.00167)	(0.00676)	(0.00893)	(0.015)	(0.017)
Treated × Post-Buyout	-0.0292**	-0.0246**	0.00421	-0.0177	0.0305
	(0.0136)	(0.0112)	(0.0114)	(0.0199)	(0.0273)
Panel F: Wholesale Trade (5% of all businesses in 2010)					
Treated × Post-Acquisition	0.00983	-0.00172	-0.0106	0.0227*	0.0173
	(0.0125)	(0.0068)	(0.00837)	(0.0121)	(0.0195)
Treated × Post-Buyout	-0.0304**	-0.01	0.0224*	-0.0303*	0.00261
	(0.015)	(0.00696)	(0.0133)	(0.0157)	(0.0286)
Panel G: Manufacturing (3% of all businesses in 2010)					
Treated × Post-Acquisition	0.0123	-0.00637	-0.0165	0.0178	0.0614**
	(0.0122)	(0.00443)	(0.0107)	(0.0167)	(0.0279)
Treated × Post-Buyout	-0.00527	-0.0126**	-0.00444	0.00171	-0.000748
	(0.019)	(0.00591)	(0.0167)	(0.0219)	(0.0305)
Panel H: Public Administration (1% of all businesses in 2010)					
Treated × Post-Acquisition	0.0199	0.00693	-0.0116	0.143**	0.201*
	(0.0162)	(0.0108)	(0.0133)	(0.069)	(0.12)
Treated × Post-Buyout	-0.0532*	0.00626	0.061*	-0.0963	-0.307
	(0.0313)	(0.02)	(0.0321)	(0.17)	(0.235)

Notes: Estimation results for the measures of business performance on the effect of acquisition and buyout programs, by 2-digit SIC industry. Each regression utilizes the specification of DiD with multiple treatments, including interaction terms between the indicator for being treated and for post-Sandy. Each specification controls for the fixed effects of the hexagon level and year level, the linear and quadratic time trends interacted with county dummies, and the share of white populations in 2010 interacted with the year dummies for the post-Sandy period. Standard errors are clustered at the zip code level. * p<0.1, ** p<0.05, *** p<0.01.

Chapter 3

Social Cost of Wind Power: Assessing the Externality of Visual Disamenity on Housing Prices

3.1 Introduction

Renewable power generation has gained significant attention and investment in the United States in recent years, driven by concerns over climate change and the need for more sustainable energy sources (Chu and Majumdar 2012). However, the production of renewable energy may impose external costs on local communities (Westlund and Wilhelmsson 2021; Gowrisankaran et al. 2016). Wind turbines, in particular, have been a topic of controversy due to their potential to create low-frequency noise, cast shadows, create flickering, and visually degrade the landscape (Schmidt and Klokker 2014; Dröes and Koster 2021; Saidur et al. 2011; Krekel and Zerrahn 2017). Visual impacts are particularly concerning because wind turbines are designed to be massive and are often located on high-elevation areas with extensive visibility (Gibbons 2015; Alphan 2021). They are widely perceived as unattractive and disruptive to the landscape, with some polls suggesting that more than 25% of respondents find wind turbines to be "ugly monstrosities" and "horrendous machines" (*YouGov / Renewables UK Survey Results* 2012).

Wind turbines are no longer only erected in rural areas with sparse populations, and their increasing presence in more populated and urbanized areas raises concerns about their impact on urban residents (Hoen and Atkinson-Palombo 2016; Rand and Hoen 2017). Their communities are often concerned about the potential reduction in the appeal and value of local houses due to wind power construction (Heintzelman and Tuttle 2012; Hoen et al. 2015; Carr-Harris and Lang 2019). Furthermore, the public opposition raised by local residents can have a significant impact on the siting decision of wind power infrastructure (Ki et al. 2022; Pepermans and Rousseau 2021). In response to these externalities, local residents may adapt and take precautionary measures to mitigate the potential impact of wind farm developments (Dröes and Koster 2016; Joly and De Jaeger 2021).

This paper presents a national-level analysis of the externality costs of wind power generation in the United States, focusing on the visual disamenity caused by wind power facilities and its impact on the loss of visual landscape amenities. We rely on the value of residential properties retrieved from the universe of housing transactions to reveal local residents' preferences for views of wind turbines, following the theory of hedonic evaluation in public economics, Previous studies have either focused on wind facilities outside of cities in Europe or on selected U.S. metropolitan areas, making their results difficult to generalize to the entire country (Gibbons 2015; Hoen et al. 2011; Vyn and McCullough 2014; Lang et al. 2014; Dröes and Koster 2016). Therefore, our study makes a significant contribution by providing some of the first estimates on the impact of wind facilities across the entire U.S., covering a wide range of land use from rural to urban places.

One of our primary contributions is the creation of a geospatial database on wind turbine visibility throughout the nation. We accomplish this by combining digital elevation models of the landscape with the location and height information of turbines and creating viewshed for each wind facilities, allowing us to precisely characterize whether and when a place is subject to visible impacts from wind facilities, along with information on the visible turbines in view. The computation required to calculate viewsheds for each windmill is substantial, but we utilize advanced geospatial tools from geomorphometry and computer science to address this issue (Zhao et al. 2013; Tabik et al. 2013; Tabik et al. 2014). This database provides a comprehensive and accurate assessment of the visual disamenity created by wind power facilities across the nation, which serves as a crucial component of our analysis on the external costs of wind power generation.

To investigate the causal effect of wind farm development on housing prices, we employ a spatial difference-in-difference design that takes advantage of both temporal variation in turbine installations and spatial variations in proximity and visibility induced by the underlying topography of the landscape. Our analysis estimates the average change in housing prices in areas visible to a wind turbine when it becomes operational, relative to the average change in housing prices in areas not visible to the same facility. The high-resolution housing transaction data, which includes precise property locations, allow us to relax the identification assumption as the exact location and installation of wind turbines being exogenous from nearby housing markets. We also control for other sources of endogeneity, such as location, general economic trends, and housing quality.

Our baseline findings indicate that wind farm developments have a detrimental effect on the property value in locations where the turbines are visible, which is primarily driven by impacts on urban areas. We find a reduction in property values of up to 8% for housing with visibility exposure within a neighborhood range from wind facilities, which decays as the distance from the turbines increases, falling to an average 1% reduction for housing within 10 km of wind turbines. Our analysis also suggests that the price reductions are mainly attributed to visibility, rather than other confounding factors caused by wind facilities, as evidenced by comparisons within a narrow neighborhood where noise and job creation effects are more prominent. We confirm the robustness of the findings through various model specifications and by restricting the study to places with low-height buildings only. Furthermore, we examine the heterogeneity of the effects and find that the visibility impact on property value increases with the number of visible wind turbines on site, but does not vary with the height and size of the wind turbines in view.

The reduction in property value resulting from wind farm developments raises questions about the potential adaptations and precautions that local residents may take and how they might affect siting decisions for future wind farms. To investigate these hypotheses, we examine the differential impacts of wind power developments on housing construction in locations where turbines are visible and not in view. Our findings suggest that urban residents adapt to the visual disamenity of wind turbines by making renovations to improve the elevation of their properties, while rural residents make new constructions with larger sizes in non-visible places. These findings support the notion that reduced desirability of investing in property with damaged views after wind turbine installation leads to significant adaptation behaviors of affected residents to mitigate the negative externalities associated with wind farm developments. Furthermore, our analysis of wind turbine siting indicates that more intensive wind farms as well as larger and taller turbines are less likely to be placed in areas that are highly visible to local residents. This effect is more pronounced in areas with heavily impaired views due to wind power developments. These findings are consistent with public opposition from residents who perceive negative impacts from existing wind turbines and raise concerns and objections to new wind farm developments in their areas, and may inform future decision-making in the wind energy industry.

This paper is highly relevant for wind power developments and offers several significant academic and policy implications. Firstly, this paper sheds light on a fundamental question in environmental economics about the costs and benefits of renewable energy. Besides environmental benefits of reduced carbon emissions and improved air quality as well as economic costs associated with installation and operation, this paper provides insights into the social cost of renewable power generation by examining the implied losses in visual amenity due to wind power developments. Secondly, the findings help inform policymakers about the potential economic impacts of wind power development on local communities. The results suggest that wind turbines have a detrimental effect on property values in urban areas where turbines are visible, indicating that policymakers need to weigh the benefits of wind power against the externalities to determine if the wind farm development is suitable for a given location. Lastly, this paper provides important implications for equity. Our analysis suggests that the social costs associated with renewable power generation are unevenly distributed over space. The wind farm developments have a negative impact on property values through visibility, which can disproportionately affect low-income communities that may not have the resources to relocate or mitigate the negative effects through housing renovation.

The remainder of this paper is structured as follows. Section 3.2 provides background description on wind power developments and associated externalities. Section 3.3 describes the data, followed by the strategy of viewsheds aggregation and the empirical framework discussed in Section 3.4. In Section 3.5 we report the results, and Section 3.6 concludes.

3.2 Background

In recent years, renewable power generation has gained significant attention and investment in the United States, driven by concerns over climate change and the need for more sustainable energy sources. Wind power is one of the fastest-growing sources of renewable energy in the country, accounting for a significant portion of the total renewable energy generation. In 2020, wind power accounted for more than 7% of total electricity generation in the United States, and it has been projected to continue to grow in the coming years (Costoya et al. 2020). In addition, the development of smaller, more efficient wind turbines has made it possible to generate renewable energy in urban areas, where energy demand is high (Watson et al. 2019). Urban wind power can also reduce transmission losses and increase grid resilience by providing a source of renewable energy that is closer to where it is needed (Yang et al. 2016).

However, the development of wind turbines is not without challenges, as some local residents may object to their presence due to the potential negative effects on the local environment and residents. One of the most common concerns raised by local residents is the visual impact of wind turbines, which can be significant due to their size and height.

In some cases, the visual impact can become a major obstacle to the development of wind power projects. For example, a proposed wind farm in the town of Somerset, New York, faced opposition from local residents in 2019 due to concerns about the visual impact of the turbines. The proposed project aimed to install 47 wind turbines, which would have reached heights of up to 680 feet and been visible from many miles away (Town of Somerset 2020). The opposition to the project centered on concerns about the impact on property values and tourism in the area, as well as the potential alteration of the area's character and natural beauty. Ultimately, the project was rejected in 2020 by the town board, citing concerns about the visual impact on the surrounding area.

Public opposition raised by local residents can have a significant impact on the siting decision of wind turbines. Wind turbine developers and local authorities must carefully consider the concerns of the local community when planning and siting wind power projects. If there is significant public opposition to the development of a wind farm, it can lead to delays or even the cancellation of the project. In some cases, local authorities may require developers to take steps to mitigate the negative impacts of wind turbines, such as reducing their height or altering their location to minimize the visual impact on the surrounding landscape.

Furthermore, local residents may adapt and take precautions to mitigate the impacts on their property values and quality of life. For instance, they may opt to make renovations to their homes or properties to reduce the negative visual impact of wind turbines. This could involve planting trees or installing fencing to block the turbines from view. Additionally, some residents may choose to build their homes on higher elevations to avoid the direct visual impact of the turbines. However, these adaptations can be costly and may not always be effective in fully mitigating the negative effects of wind farm development on property values and desirability of the area.

In sum, while wind power generation has numerous benefits, concerns related to the negative impacts of wind turbines on the surrounding environment and communities must be addressed. Quantifying the impact of visual disamenity on property values, and understandings its implications on housing construction and siting decisions of future wind farms, are crucial for the sustainable development of wind power projects.

3.3 Data

The analysis primarily utilizes data from three sources: the wind turbine installation panel, the real estate transaction records, and the digital elevation models.

Wind Turbine Operation

We obtain the full sample of wind turbine installations from the United States Wind Turbine Database (2022 Version) of USGS, which has collected and compiled comprehensive records of wind turbines from various public and private sources on a quarterly basis. The data consist of all utility-scale turbines that have ever generated and fed power into the grid to supply utilities with energy, including both the newly installed as well as the dismantled across the nation. For each facility, the data provide geo-referenced information of longitude and latitude, dates of announcement, construction, and operation, along with technical specifications on turbine make and model such as nameplate capacity, hub height, rotor diameter, and facility size.

To generate a balanced panel, we limit the sample to wind turbines that have started installation or have been in operation anytime since 1997. This includes 68,649 facilities in the continental US, with their summary statistics presented in Table 3.1. These facilities have been predominantly concentrated in rural areas (99.8% of turbines), and have systematic differences between urban and rural locations. Relative to urban wind farms, those located in rural places are significantly greater in terms of the number of turbines on site and their cumulative capacity. Moreover, the average wind facility of rural areas features higher productivity and efficiency, as they are designed with higher capacity, taller height, and larger swept area. While none of urban wind farms have been retrofitted, 9% of wind facilities in rural areas have experienced partially or entirely retrofitting after the initial construction.

Figure 3.1 displays some facts about the wind power generation across the nature. Panel A illustrates the spatial distribution of wind farms as well as their concentrations measured by the number of turbines on site. Geographically, wind power infrastructure spans across 43 states of the continental US, and their facilities have been clustered in a handful of states with abundance of wind resources. The top five states account for more than half of wind power infrastructure across the nation, i.e. Texas (24.7%), California (9.5%), Towa (8.7%), Oklahoma (6.8%), and Kansas (5.4%). In contrast, urban wind farms are concentrated in a different set of places, led by Massachusetts (18.2%), Ohio (12.7%), New York (12.1%), and Rhode Island (10.3%). Panel B plots the historical development of wind power generation from 1980. Over a 40-year period, rural areas have seen a drastic growth in wind power generation, increasing from below 100 mw to more than 100,000 mw of annual generating capacity. This, in principle, amounts to sufficient power for about 60 million homes (or 45.8% of all households across the US) on full capacity. In urban areas, the wind power facilities have also been continually on the rise, from non-existence before 1990 to above 100 MW of generating capacity in 2021.

Housing Transaction

Data on the universe of property transactions are obtained from Zillow's ZTRAX database (2021 version), which is considered one of the most comprehensive databases of housing transaction records. The data are created by combining transaction observations from multiple sources, including records from the buyer's, seller's and county assessor's points of view, along with records from county assessments on an annual basis. This results in a rich dataset that allows us to observe the date and sale price of each transaction, as well as key characteristics of the transacted property, such as the property type, year of construction and renovation, building area, number of bedrooms and bathrooms, and other amenity features included in assessments. Each property or parcel point is geographically identified by its street address, and we conduct geocoding using the USA Local Composite locator of ArcGis to obtain the exact geo-referenced location. The data cover complete records of housing transactions from 1997 to 2020, enabling us to observe repeated sales over time.

To conduct hedonic valuation, we limit our analysis to residential properties within the continental US, and exclude non-arm's-length transactions (below \$10,000) or outlier properties (above \$4,000,000), which account for 3.1% of the total samples. We also exclude transactions that occurred on the same parcel within three months of the previous sale to avoid duplicate observations. To examine the impact of visibility disamenity on property values, we further limit our sample to properties within 10 kilometers of wind turbines, as discussed below. The final data comprise 180,682,544 transaction observations, and their summary statistics are presented in Table 3.2.

Digital Elevation Models

Digital elevation models (DEMs) are an important data source for our study as they provide crucial information on the ground topography of the study area. The DEMs we utilize are based on the Shuttle Radar Topographic Mission produced by NASA, which employs remote sensing technology to gather laser light measurements of the earth's surface. The resulting x, y, z measurements are then used to create a comprehensive and accurate map of elevation for the entire globe. In particular, we use the most recent version of the DEMs, which are from the year 2018, and are available at a high resolution of 90 meters for the entire continental US. The high level of accuracy and resolution of the DEMs is essential to our analysis, as it allows us to capture subtle variations in elevation and terrain that could have a significant impact on the sight of view.

3.4 Empirical Strategy

Viewshed Analysis

One of the key contributions of our analysis is the creation of a comprehensive database that measures the visibility of wind turbines across the United States. This is achieved by generating and aggregating viewsheds from the location point of each wind turbine. Viewshed is a term used in geography and cartography that refers to the area visible from a specific observation point or vantage point, based on the topography of the surrounding terrain and any obstructions that may block the view. Unlike typical viewshed analyses that calculate the viewshed to each property, we compute the viewshed from the site of wind turbines thanks to the duality of vision, which requires less computational effort since the number of wind turbines is much smaller than the number of housing properties. This approach greatly increases computational efficiency.

Our analysis of viewshed generation involves combining the site and height data of each turbine with information on the underlying topography of the landscape and the curvature of the earth. By utilizing the viewshed module in GRASS GIS, we are able to differentiate neighboring residential properties based on their ability to view the facility. The module relies on the direct algorithm based on the line of sight and its geographical intersection with the terrain was used, which offers significant advantages in terms of accuracy, reliability, and efficiency.

The visual significance of an object decreases as its distance from the observer increases, and increases as the observer's location elevates or as their height increases. To account for air quality conditions across the nation, we assume a maximum visible range of 10 kilometers. Given that the horizontal distance of observation and the hub height of wind turbines are significantly greater than the height of a representative person, assuming the observer's height is unlikely to have a significant effect on the visibility analysis. Therefore, we assume a representative observer's height of 1.75 meters.

One concern with visibility analysis is that topographic features that obscure a wind farm from view might also reduce the noise level, and as a consequence, comparisons between the visible and non-visible groups could also capture differences in noise levels. However, this is unlikely to be true for the spatial range of visibility to giant features like wind turbines. The predicted combined noise level from a typical wind farm with a ten turbine array falls to around 40 dBA by 1 km, which is below the background noise level in an average home (Haac et al. 2019). Moreover, much of the nuisance noise from wind farms is low frequency, and low frequency sound, in particular, is not attenuated by large topographic features due to refraction. As the blade movement of a typical wind turbine can be easily visible from 1 km away, comparisons between locations with visible and non-visible turbines are very unlikely to pick up noise-related effects.

To visually illustrate the visibility analysis, we present an example of viewshed generation for a wind turbine in Figure 3.2. This is a wind facility of the Patterson Pass Wind in Altamont, California, which became operational and began providing power in 1985, has the turbine capacity of 65 kilowatts, the hub height of 24 meters, and rotor diameter of 16 meters. This is a fairly typical wind farm development in the sample. Panel A illustrates the topographic features of the neighboring surface to the facility, which is represented by the blue point of center. Located in an approximately 50,000-acre area that extends across the northeastern hills of Alameda County and into a small portion of Contra Costa County to the north, the facility finds the visibility sight to itself largely void by the mountain ridges at high elevations in the north and remains visible from the south side only. This can be seen in Panel B, where the dark shaded areas represent places from which the view to the facility is obscured by geographical elevations, and the light yellow shading indicates lands where the hub of turbine blades are visible. Empirical results presented in the next section will rely on comparisons of outcomes occurring with the start of wind farm operation in the areas where the turbines are visible, and those occurring where they are non-visible.

In Figure 3.3,we present a map that shows the aggregated viewsheds of all wind power facilities in the US, highlighting the spatial distribution of visual impact of wind turbines.

As of the end of 2020, wind power facilities have led to visual disamenity across more than a quarter of the continental US, resulting in exposure for approximately 37.2 million homes, which accounts for 30.6% of all households in the nation. A significant proportion of the affected populations are under the effect of multiple or clustering wind power facilities, with more than 75% of the affected lands exposed to the visibility of more than 10 wind turbines. Notably, while only a small proportion of wind power infrastructure is located in urban areas, many places experiencing visibility disamenity are concentrated in lowland cities of the Midwest, the Southwest, Northeast, and Pacific West states. While only 0.02% of wind turbines are installed in cities, 4.2% of the affected lands are within urban areas, and a vast majority of affected populations are clustered in cities. Approximately 33.6 million urban households, equivalent to 31.1% of all urban populations in the country, are exposed to the visibility disamenity of wind turbines, and 10.1 million of them are subject to an adverse effect of more than 10 facilities.

Estimation Model

Our aim in this analysis is to quantify the visibility disamenity of windmills once they are operational. To accomplish this, we utilize a spatial difference-in-differences (DiD) approach, which compares changes in housing prices in areas where the wind farm is visible after its installation, to the average change in housing prices in non-visible areas. Additionally, we explore the heterogeneity between urban and rural areas, in terms of visibility intensity, as well as how the effect varies by distance from the turbine site. We will also investigate the potential adaptation effect by examining the impact on property construction. Finally, we discuss how wind turbine siting decisions may be influenced by visibility exposure across space.

Property Value Effect

We start by utilizing a standard difference-in-differences (DiD) framework to compare the effects of wind farm development on the property value of homes in visible areas after the wind turbines become operational, relative to places where the turbines are not visible. The specification is as follows

$$\log(P_{it}) = \beta_1 \text{Treat}_i \cdot \text{Post}_{it} + \beta_2 \text{Treat}_i + \beta_3 \text{Post}_{it} + \beta_4 X_{it} + \alpha_{ny} + \alpha_{cm} + \epsilon_{it}$$

Here, each observation corresponds to a transaction for property i that occurred on date t, with the outcome variable being the log of sales price P_{it}. Treat_i is an indicator that denotes whether a property was assigned to the "treated" group, which refers to whether the property is located in areas with any wind turbine in view either currently or in the future. Note that the division between treatment and control group depends only on the location of property i, rather than on the transaction date or wind turbine installation status. Post_{it} is the indicator that denotes whether a property was transacted after the wind turbine in view became operational. Thus, the coefficient β_1 for the interaction term between Treat$i$ and Postit captures the effect of wind turbine installation on visible properties. To account for potential changes in building characteristics that could affect property values, we also include several property characteristics X_{it} that could vary over time, including the most recent year the property was built or renovated, the number of bedrooms and bathrooms, and the lot size in acres.

Crucially, there might exist time-varying location-specific factors that correlate with the visual disamenity created by wind farms. For instance, the spatial distribution of pre-existing windmills may influence the siting decisions for future wind turbines, potentially due to the participation of local communities in policymaking. This correlation might also exist when wind farms are not randomly assigned across space, or if areas close to wind farms where turbines are visible may not be comparable to those further away in terms of other amenities affecting housing prices. To address this, we assume that each community has its own time trends, fully capturing any community-specific factors that impacted the siting of wind turbines. We include these trends in the analysis by incorporating fixed effects on census tract by year level, denoted as α_{ny} for census tract n and year y. Moreover, to control for the seasonal trends in the housing markets that might be specific to each county, we include the fixed effects on the county by month level, denoted as α_{cm} for county c and sales month m. This way, we can ensure the DiD estimator of interest, β_1, is not be contaminated by correlation with the time effects driven by the endogenous selection of wind farm siting and the general trends in property value over time.

We define the treatment group as properties located within a neighborhood range between 1km to 10km and visible from at least one wind turbine, either currently or in the future. The lower bar of 1km is set to remove the confounding effect of noise, which decays quickly and becomes inseparable from home noise beyond 1km from the turbine site. We set the upper limit of visibility distance as 10 km to ensure a sufficient number of properties in the analysis while balancing measurement precision and efficiency. The control properties are defined as those located within a range of 1 km to 10 km from wind turbines but not visible from any of them. We define the post-treatment indicator as transactions that occur after the installation of the first wind turbine visible to the treatment properties. For control properties, the post-treatment indicator is defined based on the installation timing of the first wind turbine within their visibility range (1-10km).

As a final note, the effects of visibility disamenity are likely to decrease as we move further away from the turbine site. Additionally, we hypothesize that the effects could vary between urban and rural places, by the number of turbines in visibility, and by the characteristics of the turbines in view. Therefore, we also utilize corresponding DiD and event study frameworks to test these hypotheses. To evaluate the impact of visibility disamenity in addition to the effect of proximity to wind farms, we will expand the DiD model to a triple and quadruple difference framework, adding dimensions of spatial proximity to windmills as well as the installation of wind turbines nearby. We define proximity as being within a visibility range from wind facilities and accordingly enlarge the sample size to include control properties within 50km from wind farms. Compared with the spatial DiD model in the baseline, the triple and quadruple specifications allow us to estimate the effect of wind farm proximity to property value as well.

Housing Construction Effect

In addition to being capitalized in property value, it is likely that the visibility disamenity of wind turbines may also affect the desirability of constructing new buildings and lead to adaptation of local residents. To test this hypothesis, we employ an analogous spatial difference-in-differences framework:

$$Y_{it} = \beta_1 \text{Treat}_i \cdot \text{Post}_{it} + \beta_2 \text{Treat}_i + \beta_3 \text{Post}_{it} + \beta_4 X_{it} + \alpha_{ny} + \alpha_{cm} + \epsilon_{it}$$

Here, the treatment indicators and control variables are the same as in the previous specification. The outcome variable of interest, denoted by Y_{it}, measures housing construction, and we develop three sets of measures to examine the effects. Firstly, we investigate whether the visual disamenity resulting from wind turbine installation alters the willingness of local residents to make constructions by examining measures on property renovation. Secondly, we explore whether homeowners adapt to the impaired view by elevating their properties. Finally, we investigate whether the unfavoured view from wind turbines affects homeowners' willingness to expand their property into larger sizes.

Windmill Siting Effect

Public opposition from local residents can significantly impact wind farm projects, and it is possible that the visual disamenity created by wind turbines, which is capitalized into the housing market and affects new construction, may also influence the placement of wind power generation. One potential transmission effect is that larger turbines might face more scrutiny and be more difficult to get approved in areas that remain highly visible to local communities. We aim to investigate this siting effect by examining how wind turbine characteristics, such as size and location, impact the siting decision with respect to their visibility to local residents:

$$S_{iy} = \beta_1 \log(C_i) + \alpha_c + \alpha_{sy} + \epsilon_{iy}$$

Here, each observation corresponds to the cross section of a wind turbine i, which was installed in year y, and the outcome variable S_{iy} refers to the visibility measure of the wind turbine i. Our primary variable of interest is C_i, which represents the wind turbine characteristics that may affect the siting decision by correlating with the visibility disamenity. These characteristics might include the intensity of facilities on site, the size of the turbine, as well as the height of the turbine. We also include a set of controls, such as census tract fixed effects and state-specific time trends, to eliminate the time-invariant factors across neighborhoods and the common trends within states that potentially determine the siting decision of wind power development. Ultimately, this specification allows us to examine how wind turbine characteristics affect the siting decision and whether larger turbines are more difficult to site in areas that remain visible to local communities.

3.5 Results

Impact on Property Value

We begin by examining the impact of visual disamenity created by wind farm developments on property values for local communities. We present the baseline results in Table 3.3, which reports estimates for the spatial DiD model with sequentially added controls in Columns (1)-(4). Column (1) suggests no significant difference in average property values between visible and non-visible areas before and after the wind turbine installation, which persists after adding property characteristics to control for changes in housing conditions, as shown in Column (2). However, after accounting for fixed effects on the census tract by year level and seasonal trends specific to each county, as shown in Columns (3) and (4), we find a significant reduction in property values of 1.12% more in the visible areas than in the non-visible areas after the wind turbine installation. This indicates detrimental impact of visual disamenity created by wind farm developments on local communities as reflected in property value. In contrast, properties in non-visible areas do not experience significant changes in their property value after wind farm development.

Additionally, we observe a significant gap of 1.01% in the average property value between visible and non-visible areas, regardless of the wind facility installation status. This gap cannot be explained by differences in observed property characteristics or disparities in neighborhood factors and housing market evolution. Our best explanation for this gap is that wind turbines are sited in areas where their visual disamenity is more likely to affect communities of lower housing values, indicating the potential issue of gentrification resulting from windmill siting. More discussions on the determinants of windmill siting are discussed in the following section.

We investigate how the impact of wind turbine visual disamenity varies with the intensity of visibility using two measures: the number of wind turbines in view and the intensity classified by whether there are more than 20 turbines in sight. The results are presented in Columns (5)-(6) of Table 3.3. We find that the detrimental effect of visual disamenity is largest for the first wind turbine in view. Exposure to the first visible wind turbine significantly reduces the property value by 0.9%, while every additional 10 wind turbines in view further reduces the property value by an additional 0.2%. Furthermore, wind farms with more than 20 turbines reduce the property value in visible areas by an average of 2.48%, while those with less than 20 turbines have a reduction effect of only 1.02% on visible areas. These findings suggest that the intensity of wind facilities in view plays a significant role in the impact magnitude of wind turbine visibility on property value.

It is possible that the capitalization effect of windmill visibility on urban and rural housing markets differs due to pre-existing views of tall constructions in urban areas. To test this hypothesis, we re-run the baseline regressions separately for urban and rural markets, and the results are presented in Table 3.4. Comparing Columns (1) and (4), we find that wind turbines have negligible effects on property values in non-visible areas for both urban and rural properties. However, urban markets experience a significant reduction in property value due to the visual disamenity of wind farm, while the effect on rural properties is insignificant. We also observe a salient gentrification effect of wind turbine visibility on urban areas, with property values in visible areas being 0.8% lower than in non-visible areas regardless of the wind turbine installation status. Furthermore, we investigate the effect by visibility intensity on urban and rural housing markets separately. Columns (2) and (5) show that the first visible wind turbine has a more pronounced effect on urban property values, while treatment intensity in additions after the first turbine plays a more significant role in rural areas. Exposure to an additional 10 wind turbines reduces urban property values by 0.76% and rural property values by 1.67%. The difference in the response to treatment intensity is also highlighted in the comparison of Columns (5) and (6).

Our analysis suggests that the effect of windmill visual disamenity on urban properties exhibits decreasing returns to scale, likely due to the high density of tall constructions that have already compromised their views. Conversely, the initial turbine in rural areas does not have a noticeable effect due to the abundance of available views remaining. However, as the density of visible turbines increases, rural areas experience a more substantial reduction in property values, primarily because of the absence of tall buildings to obstruct sightlines and the larger base of view resources available to be impacted by wind turbine installations.

The impact of visual disamenity created by wind turbines may vary depending on the distance from the nearest visible turbine and the characteristics of the wind facility. To test how the effect varies by distance, we re-run the baseline specification with indicators of interest interacted with distance bin indicators of a 500-meter range. The coefficients by distance, as presented in the top panel of Figure 2.4, suggest the effects of wind turbine visibility decrease as distance increases, with the visual disamenity reducing property values by up to 8% within a neighborhood range of 1.5 km. This impact is more significant in urban areas and diminishes after 8 km, while it is negligible for rural properties after 4 km, as indicated in the middle and bottom panels. Moreover, comparing the results within 1 km and just beyond, we find that the effect of wind turbine visibility is smaller for communities in narrow proximity, where more confounding factors such as noise and job opportunities may be involved. This suggests that positive effects of wind farms on local communities, such as job creation and business attraction, may perform more strongly in visible areas than non-visible areas, potentially offsetting some of the detrimental effects of increased noise and visual disamenity..

We investigate the relationship between wind turbine characteristics and their impact on visual disamenity, by re-running the baseline specification with characteristics of the nearest visible facility interacted with the DiD interaction term of interest. The result, as presented in Table C.1, show that only the installation year of the facility has a statistically significant albeit economically negligible effect on the nearby property value. In contrast, factors such as power generation capacity, height, and rotor size do not have a significant impact on the housing market. This suggests that the characteristics of visible wind turbines do not play a significant role in affecting property values.

To better understand the cross-sectional effects of wind farm developments on housing markets, we modify the baseline DiD specification in various ways to account for different dimensions. The modified specifications, as presented in Table 3.5, only account for the spatial difference by visibility and by proximity (within 10 km) in Columns (1) and (2), incorporate the installation timing of visible wind turbines (baseline DiD model) in Column (3), add another dimension of proximity to expand the model to a triple difference in Column (4), and further allow for effects of proximity to interact with installation in Column (5). The results confirm the detrimental effect of visibility to wind turbines on property value found in the baseline model. Moreover, we find that properties within 10 km from wind turbines are 1.12-1.7% lower in sales price than those 10-50 km away. Within 10 km, properties in visible areas are 1.15-1.62% lower in value relative to non-visible areas, regardless of the installation status of visible turbine. These gaps are not driven by differences in the housing condition of properties located in different communities. Therefore, the cross-sectional difference in property value between visible and non-visible areas as well as between proximate and distant areas, indicates a potential selection effect that leads to the siting of wind turbines in places with lower property values.

Lastly, to validate our primary findings, we conduct two robustness tests. The first test involves using repeated sales only, allowing us to control for unobserved housing quality using indicators for each property. The results, as presented in Table C.2, suggest that the visual disamenity effects are twice as large as those revealed in the baseline regressions. The second test rules out the potential bias of tall buildings blocking the view of wind turbines. We use data on average building height from USGS, as discussed in Appendix C.1, and categorize places into four groups by their average building height and re-run our baseline regression for each group. The results, as presented in Table C.3, confirm the detrimental effect of visual exposure to wind turbines on property value, particularly in properties located in urban areas with average building heights below 3 stories, which becomes insignificant in places with primarily tall buildings. Taken together, these findings validate our primary results and support the conclusion that visual disamenity created by wind turbines significantly reduces property value.

Impact on Housing Construction

The preceding analysis suggests that wind farm developments have a negative impact on nearby communities due to impaired views, resulting in noticeable capitalization effects in housing markets. The reduction in property value could potentially affect the willingness of local residents to invest in property renovation and improvement, as the decreased property values may not provide a good return on investment. Moreover, the visual disamenity may make the area less attractive to live in, leading to a reduction in housing demand and further decreasing the potential return on investment for homeowners. Ultimately, the visual disamenity of wind turbines can have a cascading effect on the housing market and willingness of local residents for investment on property improvement. Therefore, this section aims to investigate the impact of wind turbine installations on housing construction through the visibility channel, which can provide insights into the potential adaptation effects of wind turbine developments on local residents.

We investigate the impact of wind turbine visibility on property construction by creating three sets of measures from the transaction data. First, we assess the desirability of renovation by utilizing an indicator for renovation and the most recent year of renovation. Second, we use the number of stories to measure property elevation. Lastly, we measure property expansion by the number of units on the parcel, number of rooms, and number of bedrooms within the property.

The results, presented in Table 3.6, show the impact of wind turbine visibility on building construction. In Panel A, we find that exposure to wind turbine visibility significantly increases building height, with an average building in visible areas seeing its height increase by 0.055 stories, equivalent to 3% of the building height. This suggests that local residents adapt to the impaired view due to wind farm developments by making elevations to their property. The elevation efforts involve expansions of the building size in terms of the number of rooms, without a significant horizontal effect to set up more construction units within their parcel.

Comparing the cross-sectional differences between properties in visible and non-visible areas to wind farms, we find that properties in visible areas are more likely to experience property renovation and the renovations tend to happen earlier than their counterparts. This is possibly driven by the adaptation and precaution of local residents in making elevations to their properties that have already been affected or are soon to be affected by the visible disamenity created by wind turbines.

Panel B and C present the differential effects on housing construction for urban and rural areas. We find that urban homeowners respond to the visual disamenity of wind turbines with a higher likelihood of renovation following the turbine installation. Specifically, we observe a 0.2% increase in the probability of renovation compared to the pre-installation level of 10%, which primarily involves improving property elevations to adapt to the impaired views and expanding housing size due to higher stories. Additionally, we find that urban residents in non-visible areas respond to the wind turbine installation with lower chances of renovation, which may be due to new constructions without a need for renovation. We also observe that properties in non-visible areas experience lower height and larger size after wind turbine installation, which may be due to the construction of lower buildings with fewer rooms.

These findings suggest differential responses to wind farm developments in the renovation efforts of properties located in visible and non-visible areas.

Lastly, as indicated in Panel C, the installation of new wind turbines in rural areas results in a significant reduction in the likelihood of home renovation for rural homeowners by 0.74%. Rural properties exposed to the visual disamenity experience a reduction in property size in terms of the number of units on the parcel after the turbine installation, with an average reduction of 0.057 units or a decrease of 4.4% compared to those in non-visible areas. The reduced renovation and property size could be due to the decreased desirability of renovation as a result of the worsened visual amenity caused by the wind turbines. Additionally, we find that properties in non-visible areas have a higher renovation rate after the turbine installation, leading to an increase in the average number of units per parcel. The differential responses in adaptation efforts indicates a migration of renovation investment from visible areas to their neighboring areas that are not affected by the visual disamenity after wind farm developments.

Impact on Windmill Siting

The previous analyses have demonstrated that the presence of visible wind turbines can lead to a decrease in property values for homes located in close proximity. This negative effect can result in adaptation and precaution behaviors of local communities, such as making elevations to their affected homes or relocating renovations to non-visible places. As a result, local communities may express opposition to wind farm development in areas that lead to visual disamenity for their residents, especially in cases where the wind farm installation is intensive with a significant number of large and tall turbines.

In this section, we aim to examine how the characteristics of wind turbines can affect the siting decision of wind farms and the creation of visual disamenity to local communities. To accomplish this, we employ two-way-fixed-effect regressions on the cross section of wind turbine location, testing the dependency of windmill siting in terms of visual disamenity created on characteristics of wind facilities. We construct two measures of siting decision: the indicator for whether the wind turbine is located in places that are visible to local communities, and the indicator for whether the location has heavily impaired views due to windmill visibility. The first measure helps test the hypothesis that local opposition will lead wind facilities with giant size to locate in non-visible places to local communities. The second measure will address the question of whether, if a location is already exposed to significant disamenity resulting from wind farm visibility, local opposition will direct large wind facilities to site away from these places with heavily damaged views.

We analyze three sets of windmill characteristics: 1) the intensity of facilities on site, measured by the number of turbines within the farm and their cumulative capacity of power generation; 2) the turbine height, measured by the height from the turbine hub as well as the total height from the tip; and 3) the size of the turbine blade, measured by the rotor diameter and the power generation capacity of the turbine. The results are presented in Table 3.7. As shown in Panel A, we find that all of these turbine characteristics have a both statistically and economically significant negative effect on the likelihood of the turbine being sited in places visible to local residents. Specifically, we observe an 87% reduction in the likelihood of turbine siting in visible locations when the associated wind farm increases its turbine number by 10%, a 37.8% reduction when the cumulative capacity of power generation of the farm increases by 10%, a 40.7% reduction when the total height of the turbine increases by 10%, a 34.6% reduction when the rotor size increases by 10%, and a 26.6% reduction when the turbine capacity increases by 10%.

To ensure that these effects are not driven by selection of wind facilities into neighborhoods of specific factors that accidentally correlate with visibility exposure, we incorporate a full set of indicators at the census tract by year level. Therefore, these findings suggest that wind turbines are sited in places that are less likely to be visible to local residents *within neighborhoods* when the wind farm is intensive in power generation and the turbine is tall and large. This confirms the hypothesis that more intensive wind power developments are more likely to be sited in places from which the view is largely obscured by the large geographical product on the surface, leading to less exposure of visual disamenity to local communities.

Panel B of Table 3.7 provides additional insight into the effect of turbine characteristics on siting decisions of wind farms in areas with heavily impaired views. The dependent variable is an indicator for whether the siting location has been visually affected by at least 50 turbines. Our analysis shows that wind farms with larger size and higher capacity are significantly less likely to be located in these heavily impaired places. Specifically, the likelihood of wind turbines being sited in places exposed to more than 50 turbines decreases by 47% if the number of wind turbines on site increases by 10%, by 30% if the turbine height increases by 10%, by 26.6% if the turbine rotor size increases by 10%, and by 13.7% if the power generation capacity grows by 10%. These findings suggest that the decision to site a wind facility in areas with heavily impaired views relies on the characteristics of the turbine, including wind farm intensity, height, and size. More intensive wind farms and larger turbines are less likely to be sited into places where the views have already been heavily impacted by wind power facilities.

In summary, our analysis indicates that the visual disamenity created by existing windmills can affect the siting decisions of future wind farm development. Our findings suggest that local opposition is likely to direct the location of large and more intensive wind turbines away from places that are visible to local residents and from places with heavily impaired views due to existing wind facilities.

3.6 Conclusion

This paper provides a national-level causal evaluation of the externality costs of wind power generation through the visibility impacts on property value in the United States. We take advantage of the densely populated geographic setting across the nation, with rich geological features such as undulating terrain and prominent elevations on the surface, and numerous wind farms developed within sight of residential properties. To address computational difficulties, we use advanced geospatial tools from geomorphometry and computer science to construct a comprehensive database on the wind turbine visibility throughout the nation. Our analysis relies on the universe of housing transactions spanning over a 20-year period across the country and employs a spatial difference-in-difference design based on a quasi-experimental setting that compares the response to wind power installation in areas visible to the turbines with the change in areas not visible to the same facility.

The findings indicate that wind farm developments have a detrimental effect on property value in locations where the turbines are visible, which is primarily driven by impacts on urban areas. House prices decrease by up to 8% after the construction of a wind turbine in sight of view within close neighborhood range from the property, with the effect decaying as the distance increases. The average effect falls to a 1% reduction for housing within 10 km of visible wind turbines. We also investigate the heterogeneity of the effects and find that the visibility impact on property value increases as the number of visible wind turbines intensifies.

The reduction in property value resulting from wind turbine installations raises questions about the potential adaptations and precautions that local residents may take and how they might affect siting decisions for future wind farms. Our analysis reveals that urban residents adapt to the visual disamenity of wind turbines by making renovations to improve the elevation of their properties, while rural residents make new constructions with larger sizes in non-visible places. Furthermore, our analysis of wind turbine siting indicates that more intensive wind farms as well as larger and taller turbines are less likely to be placed in areas that are highly visible to local residents. In sum, this paper highlights the social cost of wind power developments as they are capitalized in the housing markets, as well as the responses in adaptation behaviors of local residents and their public objections that can alter the siting decisions of future wind power developments.

This paper provides a crucial message on the equity implications of wind power generation. Although wind power provides environmental benefits, the negative externality costs associated with it disproportionately affect local residents who directly experience visual disamenity. While the broader populations benefit from the increased access to renewable energy, this paper emphasizes the need to address the social cost for those impacted by externalities associated with its generation. Additionally, low-income communities may be disproportionately affected by these social costs, as they may lack the resources to mitigate or adapt to the negative effects. Therefore, this paper highlights a need to consider equity in renewable energy development and address potential negative impacts on vulnerable communities.

Figure 3.1: Facts of Wind Farms across the United States

Panel A: Spatial Distribution of Wind Turbines

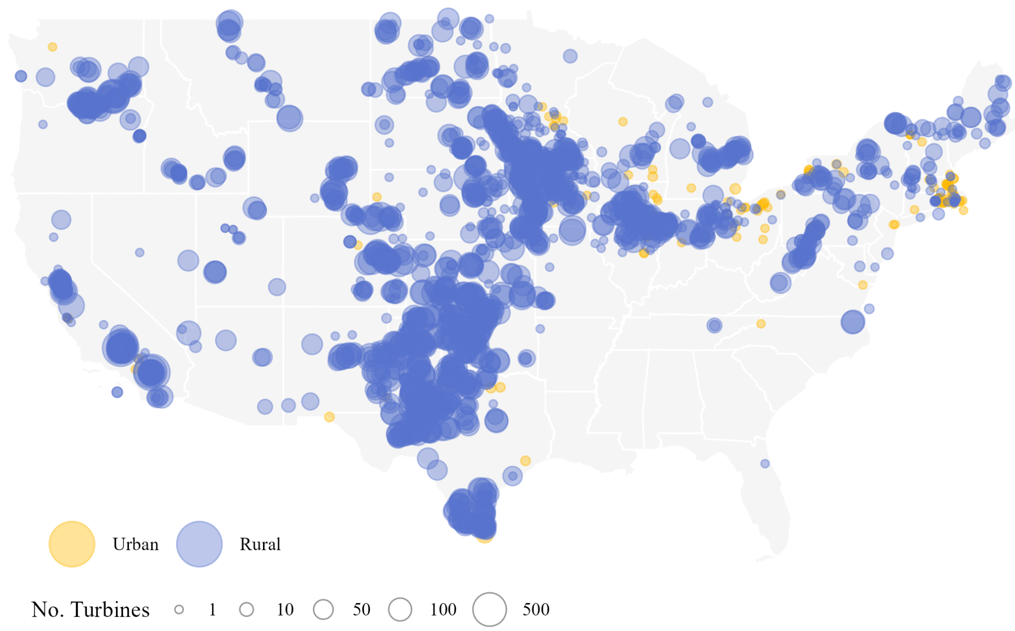

Panel B: Development of Wind Power Generation

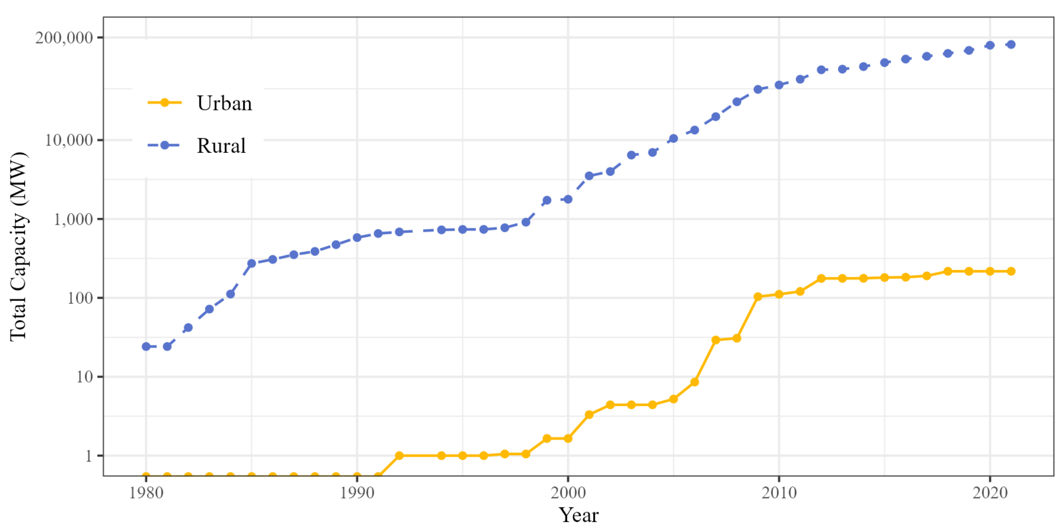

Source: United States Wind Turbine Database (2022 Version) of USGS.

Figure 3.2: Surface and Viewshed of Patterson Pass Wind in Altamont of California

Panel A: Landscape Topology

Panel B: Viewsheds

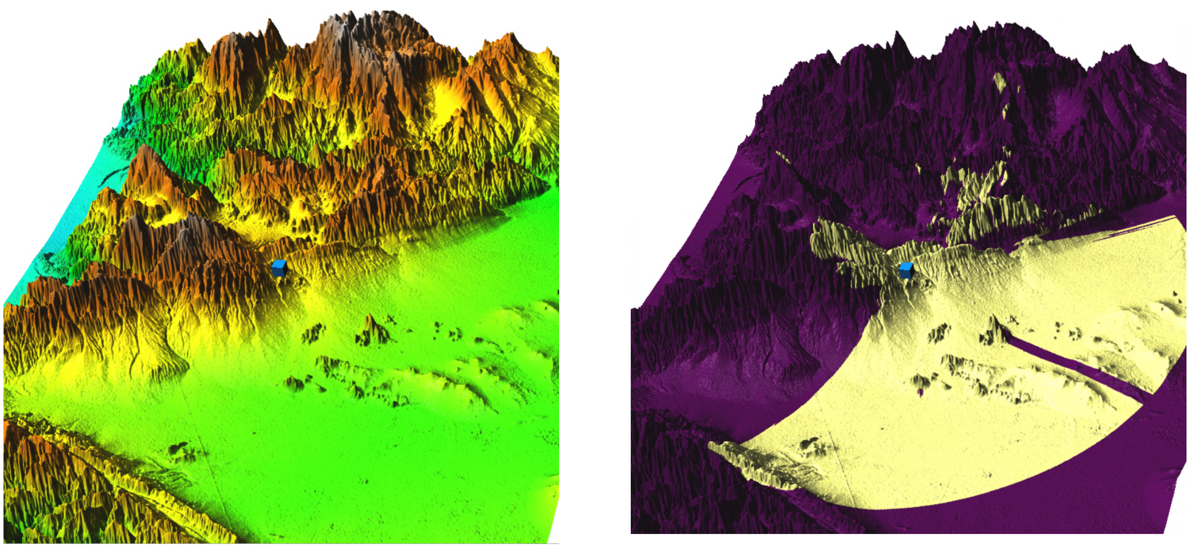

Note: These figures depict the landscape topology and viewshed of a wind turbine located in the Patterson Pass Wind facility in Altamont, California. This wind facility became operational since 1985 and and has the turbine capacity of 65 kilowatts, the hub height of 24 meters, and rotor diameter of 16 meters. The blue point located at the center of both figures represents the wind turbine. In Panel B, light-colored areas indicate locations from which the turbine is visible, while dark-colored areas indicate areas where the turbine is not visible.

Figure 3.3: Number of Wind Turbines in Visibility

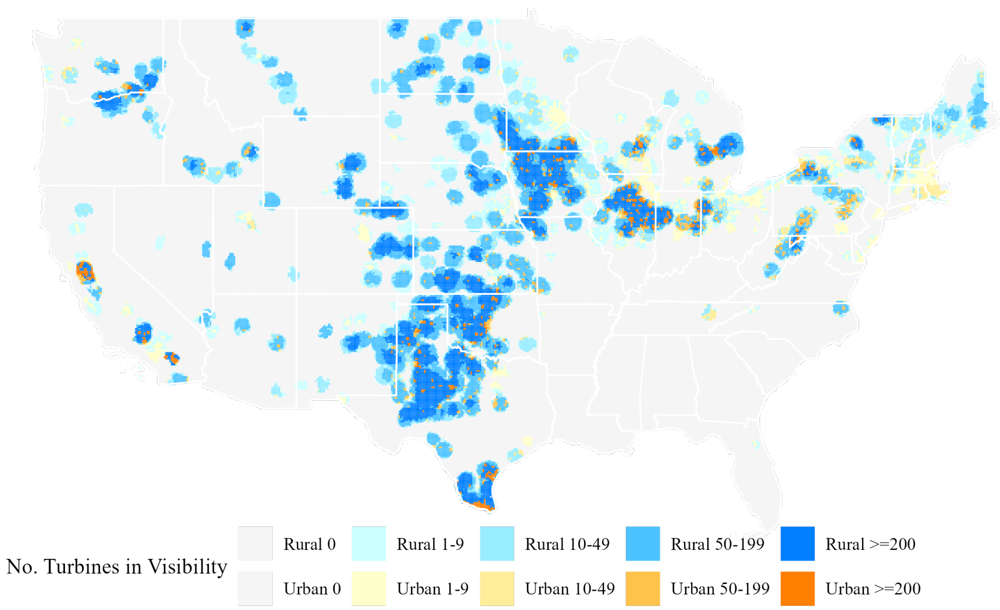

Note: This figure depicts the number of wind turbines in visibility for urban and rural areas across the United States. Each point represents a 10km by 10km grid.

Figure 3.4: Visibility Effect on Log(Property Value) by Distance

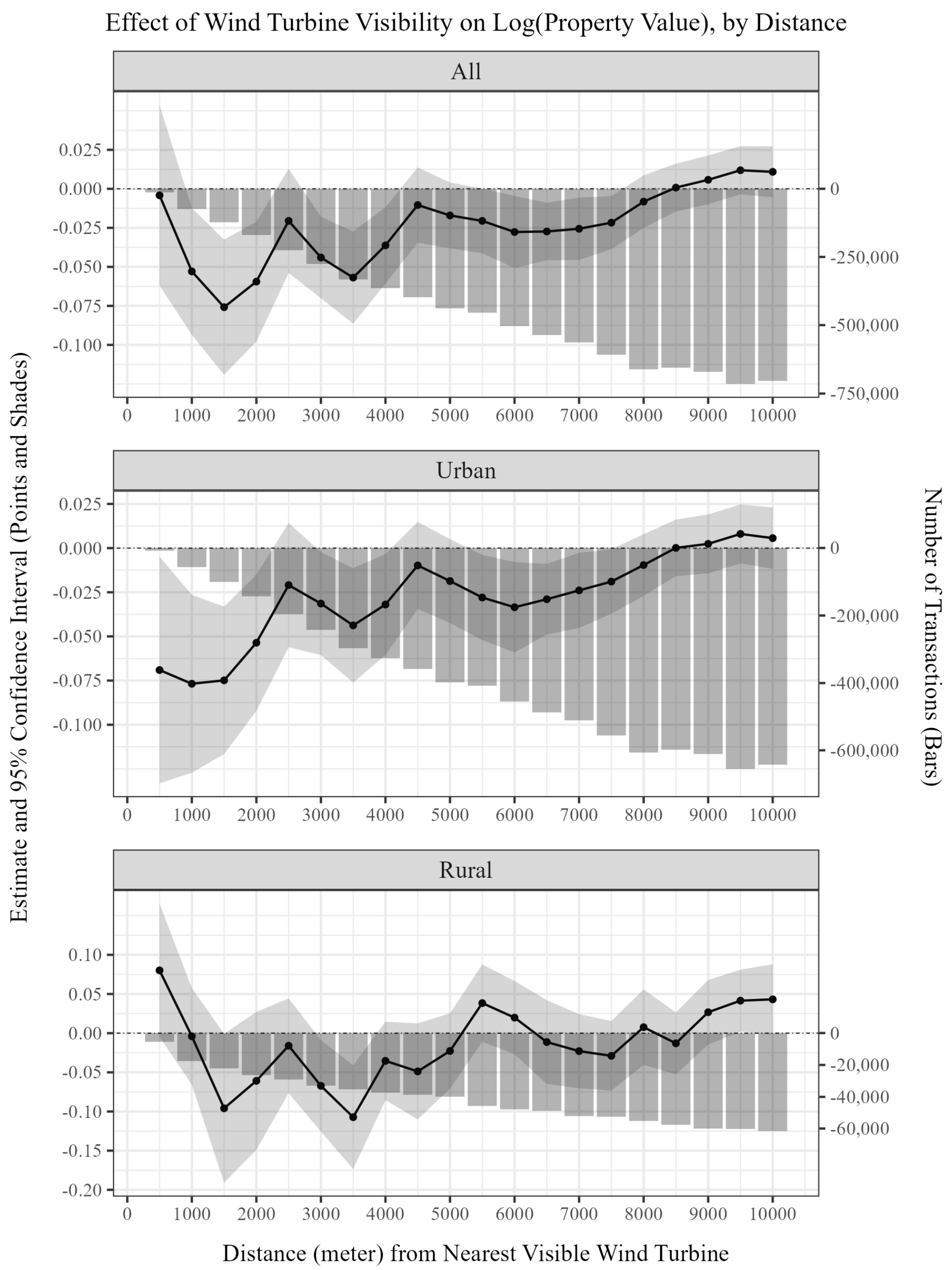

Note: The three panels display the coefficients from the baseline specification of spatial DiD model, where the indicator of interest (post-treatment interacted with being treated) are interacted with the indicators of distance bin of a 500-meter range range defined by the distance from the nearest wind turbine in view. The top panel accounts for all transactions, the middle panel accounts for urban places only, and the bottom panel considers rural transactions only. Shades represent 95% confidence intervals constructed using standard errors clustered twoway at the census tract and year level.

Table 3.1.
Summary Statistics of Wind Turbines.

	All (N = 68649)				Urban (N=165)		Rural (N=68484)	
	Mean	SD	Max	Min	Mean	SD	Mean	SD
Operational Year	2011.15	8.01	2021	1981	2011.12	4.1	2011.15	8.01
# Turbines	105.41	95.41	731	1	3.82	7.62	105.66	95.4
Cum. Capacity (mw)	167.41	103.3	525.02	0.05	6.6	16.8	167.76	103.14
Capacity (kw)	1926.08	711.38	6000	50	1111.09	958.78	1927.86	709.73
Hub Height (m)	80.26	12.47	131	22.8	61.94	22.26	80.3	12.41
Rotor Diameter (m)	94.41	23.86	155	13.4	62.66	32.57	94.47	23.8
Rotor Swept Area (m^2)	7447.13	3289.6	18869.2	141.03	3910.05	3245.54	7454.25	3285.88
Total Height (m)	127.63	22.95	199.6	30.4	93.62	37.98	127.7	22.86
Retrofit = 1	0.09	0.28	1	0	0	0	0.09	0.28

Source: United States Wind Turbine Database (2022 Version) of USGS.

Table 3.2.
Summary Statistics of Housing Transactions.

	All (N=54,415,117)		Visible (N=9,282,588)		Non-Visible (N=45,132,529)	
	Mean	SD	Mean	SD	Mean	SD
Sales Year	2008.2	6.61	2012.11	5.43	2007.4	6.54
Sales Price ($)	234484	256268	235914	249986	234190	257540
Lot Size (sq ft)	37971.13	173684.4	28147.72	140674.5	40122.01	180035
Year Built	1972.57	30.79	1973.57	31.6	1972.36	30.61
Number of Rooms	4.73	3.68	4.96	3.77	4.68	3.65
Number of Bedrooms	2.92	1.33	3	1.27	2.91	1.34
Number of Bathrooms	1.85	1.04	1.86	1.03	1.85	1.05
Number of Visible Turbines	8.61	56.14	50.45	127.93	0	0
Dist Nearest Visible Turbine (m)	16623	9703	16623	9703		
Number of Turbines <50km	66.27	215.68	172.89	371.83	44.34	157.57
Dist to Nearest Turbine (m)	24725	12614	15276	8835	28648	11845

Source: Zillow's ZTRAX database (2021 version).

Table 3.3.
Baseline Regression Results of Windmill Visibility on Property Value

	Average Effect				Effect by Intensity	
	(1)	(2)	(3)	(4)	(5)	(6)
Treated × Post-Treatment	0.00454	-0.0147	-0.0112**	-0.0112**	-0.00901**	
	(0.0338)	(0.0382)	(0.00433)	(0.00431)	(0.00421)	
× # Turbines (×10)					-0.00209***	
					(0.000512)	
× # Turbines <20						-0.0102**
						(0.00422)
× # Turbines ≥ 20						-0.0248**
						(0.00958)
Post-Treatment	0.227***	0.191**	0.00883	0.00896	0.0102*	0.00979*
	(0.0726)	(0.0949)	(0.00595)	(0.00589)	-0.00575	(0.00576)
Treated	-0.23***	-0.206***	-0.0101**	-0.0101**	-0.0101**	-0.0101**
	(0.0303)	(0.0251)	(0.00439)	(0.00439)	(0.00439)	(0.00439)
N	9885084	5705597	5705597	5705597	5705597	5705597
Adj. R^2	0.029	0.089	0.515	0.516	0.516	0.516
Property Char.		X	X	X	X	X
FE: Census Tract × Year			X	X	X	X
FE: County × Sales Month				X	X	X
Std. Errors Clustered at Census Tract and Year Level						

Note Estimation results for the property value on the effect of wind turbine visibility. Dependent variable is the log of sales price. Columns (1)-(6) represent different specifications of the model. Column (1) applies the standard spatial DiD specification without further controls. Column (2) adds controls on property characteristics. Column (3) further includes the fixed effects on census tract by year level. Column (4) adds the fixed effects on county by sales month level on top of (3). Columns (5) and (6) further account for the differential effects by treatment intensity, with treatment intensity measured by the number of turbines in view (divided by 10) in Column (5), treatment intensity classified into two categories by whether there are less or more than 20 turbines in view in Column (6). Standard errors are clustered twoway at the census tract and sales year level. * p<0.1, ** p<0.05, *** p<0.01.

Table 3.4.
Effects of Windmill Visibility on Property Value for Urban and Rural Places

	Urban			Rural		
	(1)	(2)	(3)	(4)	(5)	(6)
Treated × Post-Treatment	-0.00937**	-0.0079*		-0.0202	-0.0159	
	(0.00454)	(0.00443)		(0.0156)	(0.0157)	
× # Turbines (×10)		-0.0076***			-0.0167**	
		(0.000575)			(0.000665)	
× # Turbines <20			-0.00875*			-0.018
			(0.00446)			(0.0157)
× # Turbines ≥ 20			-0.0212*			-0.0274
			(0.0122)			(0.0182)
Post-Treatment	0.00709	0.00795	0.00769	0.00653	0.00801	0.00723
	(0.00572)	(0.0056)	(0.00559)	(0.017)	(0.017)	(0.017)
Treated	-0.00895*	-0.00895*	-0.00895*	-0.0204	-0.0205	-0.0204
	(0.00459)	(0.00459)	(0.00459)	(0.0159)	(0.0159)	(0.0159)
N	5290690	5290690	5290690	414907	414907	414907
Adj. R^2	0.524	0.524	0.524	0.409	0.409	0.409
Property Char.	X	X	X	X	X	X
FE: Census Tract × Year	X	X	X	X	X	X
FE: County × Sales Month	X	X	X	X	X	X
Std. Errors Clustered at Census Tract and Year Level						

Note Estimation results for the property value on the effect of wind turbine visibility, for urban and rural places separately. Dependent variable is the log of sales price. Columns (1)-(3) represent different specifications of the model for urban places. Column (1) applies the standard spatial DiD specification. Columns (2) and (3) further account for the differential effects by treatment intensity, with treatment intensity measured by the number of turbines in view (divided by 10) in Column (2), treatment intensity classified into two categories by whether there are less or more than 20 turbines in view in Column (3). Columns (4)-(6) analogously present different specifications for rural places. Each specification controls for a full set of property characteristics and fixed effects of the census tract by sales year level and the county by sales month level. Standard errors are clustered twoway at the census tract and sales year level. * p<0.1, ** p<0.05, *** p<0.01.

Table 3.5.
Single, Double, Triple and Quadruple Differences Specifications

	Single Diff		DiD	Tri. Diff	Quad. Diff
	(1) 10km	(2) 50km	(3) 10km	(4) 50km	(5) 50km
Post-Treatment (Visibility)			0.00896	2.84e-05	0.00313
			(0.00589)	(0.00568)	(0.00646)
Treated (Visibility)	-0.0162***	-0.0162***	-0.0101**	-0.0124***	-0.0115***
	(0.00397)	(0.00394)	(0.00439)	(0.00411)	(0.00424)
Proximate		-0.0116		-0.0132	-0.017*
		(0.00761)		(0.00807)	(0.00868)
Post-Proximity					0.0016
					(0.0172)
Proximate × Post-Proximity					0.0107
					(0.0111)
× Post-Treatment				0.00207	-0.00353
				(0.00574)	(0.00759)
× Treated × Post-Treatment			-0.0112**	-0.00827*	-0.00899**
			(0.00431)	(0.00428)	(0.00429)
N	5705597	30398120	5705597	30398120	30398120
Adj. R^2	0.516	0.523	0.516	0.523	0.523
FE: Census Tract × Sales Year	X	X	X	X	X
FE: County × Sales Month	X	X	X	X	X
Std. Errors Clustered at Census Tract and Year Level					

Note Estimation results for the property value on the effect of wind turbine visibility, using different specifications. Dependent variable is the log of sales price. Column (1) uses all transactions within 10 km from wind farms and applies a single difference framework that compares between visible and non visible areas. Column (2) uses all transactions within 50 km from wind farms and incorporates another cross-sectional difference by proximity (within 10 km). Column (3) applies our baseline specification of spatial DiD model on all transactions within 10 km from windmills. Column (4) expands the sample size to all transactions within 50 km and adds an interaction term with the indicator for proximity. Column (5) further incorporates another interaction dimension with the indicator for the transaction after the wind turbine installation in proximity. Each specification controls for a full set of property characteristics and fixed effects of the census tract by sales year level and the county by sales month level. Standard errors are clustered twoway at the census tract and year level. * $p<0.1$, ** $p<0.05$, *** $p<0.01$.

Table 3.6.
Regression Results of Windmill Visibility on Housing Construction

	Renovation		Elevation	Expansion		

	Reno = 1
	Mean=0.1
		Reno Year
		Mean=1992
			#Stories
			Mean=1.8
				#Units
				Mean=1.3
					#Rooms
					Mean=4.7
						#Bedrooms
						Mean=2.9

	(1)	(2)	(3)	(4)	(5)	(6)
Panel A: All Transactions (N = 9885084)						
Treated × Post-Treat	0.00118	0.167	0.0553*	-0.091	0.0487**	-0.00864
	(0.00114)	(0.147)	(0.03)	(0.128)	(0.0203)	(0.00829)
Post-Treatment	-0.00203	-0.183	-0.0479*	0.0601	-0.0343	0.00385
	(0.00124)	(0.22)	(0.0263)	(0.124)	(0.0246)	(0.00971)
Treated	0.00371***	-1.1***	-0.0571	-0.0755	-0.0235	0.0087
	(0.0012)	(0.226)	(0.0359)	(0.0982)	(0.0148)	(0.00857)
Adj. R^2	0.670	0.701	0.798	0.342	0.804	0.549
Panel B: Urban Transactions (N = 8930417)						
Treated × Post-Treat	0.00209*	0.126	0.0574*	-0.1	0.0428**	-0.0127
	(0.00122)	(0.148)	(0.0322)	(0.138)	(0.0206)	(0.00872)
Post-Treatment	-0.00312**	-0.164	-0.0506*	0.0668	-0.0441*	0.00387
	(0.00138)	(0.224)	(0.0276)	(0.134)	(0.0257)	(0.0106)
Treated	0.00345***	-1.15***	-0.0618	-0.0829	-0.0184	0.0104
	(0.00128)	(0.233)	(0.0383)	(0.103)	(0.0147)	(0.00883)
Adj. R^2	0.690	0.718	0.799	0.343	0.814	0.555
Panel C: Rural Transactions (N = 954667)						
Treated × Post-Treat	-0.00741***	-0.0511	0.0108	-0.0573***	0.0175	0.0306*
	(0.00252)	(0.6)	(0.00826)	(0.0206)	(0.0428)	(0.0175)
Post-Treatment	0.00713**	0.756	-0.00729	0.0697**	0.0484	-0.0235
	(0.00302)	(0.744)	(0.00885)	(0.0261)	(0.0448)	(0.0197)
Treated	0.00859***	0.135	-0.00817	0.0339**	-0.0387	-0.0128
	(0.00262)	(0.624)	(0.00762)	(0.0141)	(0.0432)	(0.0186)
Adj. R^2	0.387	0.407	0.293	0.579	0.678	0.491

Note Estimation results for the property characteristics on the effect of wind turbine visibility. Columns (1)-(6) represent different dependent variables: (1) on the indicator of being renovated, (2) on the year of most recent renovation, (3) on the number of stories, (4) on the number of units of the parcel, (5) on the number of rooms, and (6) on the number of bedrooms. Each specification applies the standard spatial DiD specification with controls on the fixed effects of the census tract level and the county by sales year level. Standard errors are clustered twoway at the census tract and sales year level. * $p<0.1$, ** $p<0.05$, *** $p<0.01$.

Table 3.7.
Regression Results for Windmill Siting

	Wind Farm Intensity		Turbine Height		Turbine Size	
	# Turbines	Cum.Capacity	Hub Height	Total Height	Rotor Diameter	Capacity
	(1)	(2)	(3)	(4)	(5)	(6)
Panel A: Dependent Variable = I(Visible), Logit Model.						
log(C)	-8.7***	-3.78***	-4.02***	-4.07***	-3.46***	-2.66***
	(0.00499)	(0.00302)	(1.14)	(0.9)	(0.797)	(0.72)
N	69158	65663	63961	63961	64205	64662
Pseudo R^2	0.951	0.947	0.945	0.945	0.945	0.947
Panel B: Dependent Variable = I(# Visible Turbines > 50), Logit Model.						
log(C)	-4.7***	-4.35	-3.09**	-2.98***	-2.66***	-1.37***
	(1.19)	(2.98)	(1.2)	(1.09)	(0.897)	(0.419)
N	69158	65663	63961	63961	64205	64662
Pseudo R^2	0.943	0.946	0.944	0.944	0.944	0.945
FE: Census Tract × Installation Year						
Std. Errors Clustered at Census Tract and Installation Year Level						

Note: Estimation results for the dependency of siting in locations affected by windmill visual disamenity on the characteristics of turbine. Each observation is a wind turbine. In Panel A, the dependent variable is the indicator for whether the turbine is located in places that remain visible to local residents. In panel B, the dependent variable is the indicator for whether the number of windmills in view from the turbine site is above 50. Columns (1)-(6) utilize different turbine characteristics as independent variable: (1) uses the number of turbines in the wind farm, (2) uses the cumulative capacity of all turbines in the farm, (3) uses the height from the hub of the turbine, (4) uses the total height of the turbine, (5) uses the rotor diameter, and (6) uses the capacity of the turbine. The turbine characteristics in each specification are transformed by a log function. Each specification utilizes a logistic linkage and controls for the fixed effects of the census tract by installation year level. Standard errors are clustered twoway at the census tract and installation year level. * p<0.1, ** p<0.05, *** p<0.01.

Bibliography

Aguiar, Luis, and Joel Waldfogel. 2018. *Platforms, promotion, and product discovery: Evidence from Spotify playlists.* Technical report. National Bureau of Economic Research.

Ahrens, Marty, and Ben Evarts. 2021. "Fire Loss in the United States During 2020." *National Fire Protection Association (NFPA).*

Airbnb. 2018. "In the Name of Service: Celebrating Hosts Who Help Those in Need." Accessed August 13, 2018. https://www.12newsnow.com/article/news/air-b-and-b/502-2c879416-9118-46d3-9e37-3ad0069bd74d.

———. 2020. "Celebrating the generous hosts in the Open Homes program." Accessed December 7, 2020. https://www.airbnb.com/resources/hosting-homes/a/celebrating-the-generous-hosts-in-the-open-homes-program-298.

Almagro, Milena, and Tomás Domınguez-Iino. 2019. *Location sorting and endogenous amenities: Evidence from amsterdam.* Technical report. Working Paper.

Alphan, H. 2021. "Modelling potential visibility of wind turbines: A geospatial approach for planning and impact mitigation." *Renewable and Sustainable Energy Reviews* 152:111675.

Atreya, Ajita, Susana Ferreira, and Warren Kriesel. 2013. "Forgetting the flood? An analysis of the flood risk discount over time." *Land Economics* 89 (4): 577–596.

Bakkensen, Laura A, and Lala Ma. 2020. "Sorting over flood risk and implications for policy reform." *Journal of Environmental Economics and Management* 104:102362.

Barron, Kyle, Edward Kung, and Davide Proserpio. 2021. "The effect of home-sharing on house prices and rents: Evidence from Airbnb." *Marketing Science* 40 (1): 23–47.

Bayer, Patrick, Fernando Ferreira, and Robert McMillan. 2007. "A unified framework for measuring preferences for schools and neighborhoods." *Journal of political economy* 115 (4): 588–638.

Baylis, Patrick, and Judson Boomhower. 2019. *Moral hazard, wildfires, and the economic incidence of natural disasters.* Technical report. National Bureau of Economic Research.

Belleflamme, Paul, and Martin Peitz. 2020. "Ratings, reviews and recommendations." In *Handbook of Cultural Economics, Third Edition.* Edward Elgar Publishing.

Bernstein, Asaf, Stephen B Billings, Matthew Gustafson, and Ryan Lewis. 2020. *Partisan Residential Sorting on Climate Change Risk.* Technical report. National Bureau of Economic Research.

Berry, Steven, James Levinsohn, and Ariel Pakes. 1995. "Automobile Prices in Market Equilibrium." *Econometrica* 63 (4): 841–90.

———. 2004. "Differentiated products demand systems from a combination of micro and macro data: The new car market." *Journal of political Economy* 112 (1): 68–105.

Berry, Steven T, and Philip A Haile. 2014. "Identification in differentiated products markets using market level data." *Econometrica* 82 (5): 1749–1797.

Bin, Okmyung, and Craig E Landry. 2013. "Changes in implicit flood risk premiums: Empirical evidence from the housing market." *Journal of Environmental Economics and management* 65 (3): 361–376.

Binder, Sherri Brokopp, Charlene K Baker, and John P Barile. 2015. "Rebuild or relocate? Resilience and postdisaster decision-making after Hurricane Sandy." *American journal of community psychology* 56:180–196.

Boustan, Leah Platt, Matthew E Kahn, and Paul W Rhode. 2012. "Moving to higher ground: Migration response to natural disasters in the early twentieth century." *American Economic Review* 102 (3): 238–44.

Bradt, Jacob T, Carolyn Kousky, and Oliver EJ Wing. 2021. "Voluntary purchases and adverse selection in the market for flood insurance." *Journal of Environmental Economics and Management* 110:102515.

Brown, Zach Y, and Alexander MacKay. 2021. *Competition in pricing algorithms.* Technical report. National Bureau of Economic Research.

Bukvic, Anamaria, Andrew Smith, and Angang Zhang. 2015. "Evaluating drivers of coastal relocation in Hurricane Sandy affected communities." *International Journal of Disaster Risk Reduction* 13:215–228.

Calder-Wang, Sophie. 2021. "The distributional impact of the sharing economy on the housing market." *Available at SSRN 3908062.*

Carr-Harris, Andrew, and Corey Lang. 2019. "Sustainability and tourism: The effect of the United States' first offshore wind farm on the vacation rental market." *Resource and Energy Economics* 57:51–67.

Chu, Steven, and Arun Majumdar. 2012. "Opportunities and challenges for a sustainable energy future." *nature* 488 (7411): 294–303.

Cohen, Peter, Robert Hahn, Jonathan Hall, Steven Levitt, and Robert Metcalfe. 2016. *Using big data to estimate consumer surplus: The case of uber.* Technical report. National Bureau of Economic Research.

Costoya, X, M DeCastro, D Carvalho, and M Gómez-Gesteira. 2020. "On the suitability of offshore wind energy resource in the United States of America for the 21st century." *Applied Energy* 262:114537.

Council, National Research, et al. 2007. *Improving disaster management: the role of IT in mitigation, preparedness, response, and recovery.* National Academies Press.

Dari-Mattiacci, Giuseppe, and Michael G Faure. 2015. "The economics of disaster relief." *Law & Policy* 37 (3): 180–208.

Deryugina, Tatyana. 2017. "The fiscal cost of hurricanes: Disaster aid versus social insurance." *American Economic Journal: Economic Policy* 9 (3): 168–198.

Deryugina, Tatyana, Laura Kawano, and Steven Levitt. 2018. "The economic impact of Hurricane Katrina on its victims: Evidence from individual tax returns." *American Economic Journal: Applied Economics* 10 (2): 202–233.

Dröes, Martijn I, and Hans RA Koster. 2016. "Renewable energy and negative externalities: The effect of wind turbines on house prices." *Journal of Urban Economics* 96:121–141.

———. 2021. "Wind turbines, solar farms, and house prices." *Energy Policy* 155:112327.

Einav, Liran, Chiara Farronato, and Jonathan Levin. 2016. "Peer-to-peer markets." *Annual Review of Economics* 8:615–635.

Elliott, James R, Phylicia Lee Brown, and Kevin Loughran. 2020. "Racial inequities in the federal buyout of flood-prone homes: a nationwide assessment of environmental adaptation." *Socius* 6:2378023120905439.

Farronato, Chiara, and Andrey Fradkin. 2022. "The Welfare Effects of Peer Entry: The Case of Airbnb and the Accommodation Industry." *American Economic Review* 112 (6): 1782–1817.

Frimpong, Eugene, Jamie Kruse, Gregory Howard, Rachel Davidson, Joseph Trainor, and Linda Nozick. 2019. "Measuring heterogeneous price effects for home acquisition programs in at-risk regions." *Southern Economic Journal* 85 (4): 1108–1131.

Garcia-López, Miquel-Àngel, Jordi Jofre-Monseny, Rodrigo Martı nez-Mazza, and Mariona Segú. 2020. "Do short-term rental platforms affect housing markets? Evidence from Airbnb in Barcelona." *Journal of Urban Economics* 119:103278.

Gibbons, Stephen. 2015. "Gone with the wind: Valuing the visual impacts of wind turbines through house prices." *Journal of Environmental Economics and Management* 72:177–196.

Gibson, Raegan. 2019. "Airbnb to offer 'Open Homes' program, free housing to some Louisiana evacuees as Tropical Storm Barry approaches." Accessed July 13, 2019. https://news.airbnb.com/in-the-name-of-service-celebrating-hosts-who-help-those-in-need.

Gowrisankaran, Gautam, Stanley S Reynolds, and Mario Samano. 2016. "Intermittency and the value of renewable energy." *Journal of Political Economy* 124 (4): 1187–1234.

Haac, T Ryan, Kenneth Kaliski, Matthew Landis, Ben Hoen, Joseph Rand, Jeremy Firestone, Debi Elliott, Gundula Huebner, and Johannes Pohl. 2019. "Wind turbine audibility and noise annoyance in a national US survey: Individual perception and influencing factors." *The Journal of the Acoustical Society of America* 146 (2): 1124–1141.

Hallstrom, Daniel G, and V Kerry Smith. 2005. "Market responses to hurricanes." *Journal of Environmental Economics and Management* 50 (3): 541–561.

Hashida, Yukiko, and Steven J Dundas. 2022. "The Effects of Managed Retreat on Coastal Property Markets: Evidence from the NY Rising Buyout and Acquisition Program."

Heintzelman, Martin D, and Carrie M Tuttle. 2012. "Values in the wind: a hedonic analysis of wind power facilities." *Land Economics* 88 (3): 571–588.

Hino, Miyuki, Christopher B Field, and Katharine J Mach. 2017. "Managed retreat as a response to natural hazard risk." *Nature climate change* 7 (5): 364–370.

Hoen, Ben, and Carol Atkinson-Palombo. 2016. "Wind turbines, amenities and disamenitites: astudy of home value impacts in densely populated Massachusetts." *Journal of Real Estate Research* 38 (4): 473–504.

Hoen, Ben, Jason P Brown, Thomas Jackson, Mark A Thayer, Ryan Wiser, and Peter Cappers. 2015. "Spatial hedonic analysis of the effects of US wind energy facilities on surrounding property values." *The Journal of Real Estate Finance and Economics* 51:22–51.

Hoen, Ben, Ryan Wiser, Peter Cappers, Mark Thayer, and Gautam Sethi. 2011. "Wind energy facilities and residential properties: the effect of proximity and view on sales prices." *Journal of Real Estate Research* 33 (3): 279–316.

Horn, Keren, and Mark Merante. 2017. "Is home sharing driving up rents? Evidence from Airbnb in Boston." *Journal of Housing Economics* 38:14–24.

Huang, Yufeng. 2022. "Pricing Frictions and Platform Remedies: The Case of Airbnb." *Available at SSRN 3767103.*

Hui, Xiang, Ginger Zhe Jin, and Meng Liu. 2022. *Designing Quality Certificates: Insights from eBay.* Technical report. National Bureau of Economic Research.

Jia, Jian, Ginger Zhe Jin, and Liad Wagman. 2021. *Platform as a Rule Maker: Evidence from Airbnb's Cancellation Policies.* Technical report. National Bureau of Economic Research.

Joly, Machteld, and Simon De Jaeger. 2021. "Not in my backyard: A hedonic approach to the construction timeline of wind turbines in Flanders, Belgium." *Land Use Policy* 108:105527.

Jowers, Kay, Lala Ma, and Christopher D Timmins. 2022. "Racial Dynamics of Federal Property Buyouts in Flood-Prone Areas."

Karwowski, Nicole. 2022. *Estimating the Effect of Easements on Agricultural Production.* Technical report. National Bureau of Economic Research.

Ki, Jaehong, Sun-Jin Yun, Woo-Chang Kim, Subin Oh, Jihun Ha, Eunyoung Hwangbo, Hyoeun Lee, Sumin Shin, Seulki Yoon, and Hyewon Youn. 2022. "Local residents' attitudes about wind farms and associated noise annoyance in South Korea." *Energy Policy* 163:112847.

Kocornik-Mina, Adriana, Thomas KJ McDermott, Guy Michaels, and Ferdinand Rauch. 2020. "Flooded cities." *American Economic Journal: Applied Economics* 12 (2): 35–66.

Koster, Hans, Jos Van Ommeren, and Nicolas Volkhausen. 2018. "Short-term rentals and the housing market: Quasi-experimental evidence from Airbnb in Los Angeles."

Kraan, Caroline M, Miyuki Hino, Jennifer Niemann, AR Siders, and Katharine J Mach. 2021. "Promoting equity in retreat through voluntary property buyout programs." *Journal of Environmental Studies and Sciences* 11 (3): 481–492.

Krekel, Christian, and Alexander Zerrahn. 2017. "Does the presence of wind turbines have negative externalities for people in their surroundings? Evidence from well-being data." *Journal of Environmental Economics and Management* 82:221–238.

Kroft, Kory, and Devin G Pope. 2014. "Does online search crowd out traditional search and improve matching efficiency? Evidence from Craigslist." *Journal of Labor Economics* 32 (2): 259–303.

Land, Kenneth C, Patricia L McCall, and Daniel S Nagin. 1996. "A comparison of Poisson, negative binomial, and semiparametric mixed Poisson regression models: With empirical applications to criminal careers data." *Sociological Methods & Research* 24 (4): 387–442.

Lang, Corey, James J Opaluch, and George Sfinarolakis. 2014. "The windy city: Property value impacts of wind turbines in an urban setting." *Energy Economics* 44:413–421.

Lee, Donghun, Woochang Hyun, Jeongwoo Ryu, Woo Jung Lee, Wonjong Rhee, and Bongwon Suh. 2015. "An analysis of social features associated with room sales of Airbnb." In *Proceedings of the 18th ACM conference companion on computer supported cooperative work & social computing,* 219–222.

Liao, Yanjun, and Carolyn Kousky. 2022. "The fiscal impacts of wildfires on california municipalities." *Journal of the Association of Environmental and Resource Economists* 9 (3): 455–493.

Lindell, Michael K, Pamela Murray-Tuite, Brian Wolshon, and Earl J Baker. 2018. *Large-scale evacuation: The analysis, modeling, and management of emergency relocation from hazardous areas.* CRC Press.

Lyons, Kim. 2020. "Airbnb asks its hosts to provide 100,000 free rentals to first responders." Accessed March 26, 2020. https://www.theverge.com/2020/3/26/21195307/airbnb-free-first-responders-hosts-coronavirus-rentals.

Mach, Katharine J, Caroline M Kraan, Miyuki Hino, AR Siders, Erica M Johnston, and Christopher B Field. 2019. "Managed retreat through voluntary buyouts of flood-prone properties." *Science Advances* 5 (10): eaax8995.

Mach, Katharine J, and AR Siders. 2021. "Reframing strategic, managed retreat for transformative climate adaptation." *Science* 372 (6548): 1294–1299.

McCaughey, Jamie W, Patrick Daly, Ibnu Mundir, Saiful Mahdi, and Anthony Patt. 2018. "Socio-economic consequences of post-disaster reconstruction in hazard-exposed areas." *Nature Sustainability* 1 (1): 38–43.

McCoy, Shawn J, and Xiaoxi Zhao. 2018. "A city under water: A geospatial analysis of storm damage, changing risk perceptions, and investment in residential housing." *Journal of the Association of Environmental and Resource Economists* 5 (2): 301–330.

McFadden, Daniel. 1978. "Modeling the choice of residential location." *Transportation Research Record,* no. 673.

McIntosh, Molly Fifer. 2008. "Measuring the labor market impacts of Hurricane Katrina migration: Evidence from Houston, Texas." *American Economic Review* 98 (2): 54–57.

Missirian, Anouch, and Wolfram Schlenker. 2017. "Asylum applications respond to temperature fluctuations." *Science* 358 (6370): 1610–1614.

Mulder, Philip. 2021. *Mismeasuring Risk: The Welfare Effects of Flood Risk Information.* Technical report. Working Paper.

Ortega, Francesc, and Süleyman Taṣpınar. 2018. "Rising sea levels and sinking property values: Hurricane Sandy and New York's housing market." *Journal of Urban Economics* 106:81–100.

Pan, Qi, and Wen Wang. 2021. "Costly price adjustment and automated pricing: The case of Airbnb." *Available at SSRN 4077985.*

Papastamoulis, Panagiotis, Marie-Laure Martin-Magniette, and Cathy Maugis-Rabusseau. 2016. "On the estimation of mixtures of Poisson regression models with large number of components." *Computational Statistics & Data Analysis* 93:97–106.

Pepermans, Guido, and Sandra Rousseau. 2021. "Consumers and citizens: Identity salience in choice settings focusing on local wind turbines." *Journal of Environmental Management* 281:111857.

Rand, Joseph, and Ben Hoen. 2017. "Thirty years of North American wind energy acceptance research: What have we learned?" *Energy research & social science* 29:135–148.

Rolph, Glenn D, Roland R Draxler, Ariel F Stein, Albion Taylor, Mark G Ruminski, Shobha Kondragunta, Jian Zeng, Ho-Chun Huang, Geoffrey Manikin, Jeffery T McQueen, et al. 2009. "Description and verification of the NOAA smoke forecasting system: the 2007 fire season." *Weather and Forecasting* 24 (2): 361–378.

Ronchi, Enrico, Stephen Wong, Sayaka Suzuki, Maria Theodori, Rahul Wadhwani, Sandra Vaiciulyte, Steve Gwynne, et al. 2021. *Case studies of large outdoor fires involving evacuations.* https://doi.org/10.5281/zenodo.4504853.

Ruminski, Mark, Shobha Kondragunta, Roland Draxler, and Jian Zeng. 2006. "Recent changes to the hazard mapping system." In *Proceedings of the 15th International Emission Inventory Conference,* 15:18.

Saidur, Rahman, Nasrudin A Rahim, Monirul Rafiqu Islam, and Khalid H Solangi. 2011. "Environmental impact of wind energy." *Renewable and sustainable energy reviews* 15 (5): 2423–2430.

Schmidt, Jesper Hvass, and Mads Klokker. 2014. "Health effects related to wind turbine noise exposure: a systematic review." *PloS one* 9 (12): e114183.

Schultz, Clark. 2022. "Airbnb increases market share in latest read from M Science." Accessed June 6, 2022. https://seekingalpha.com/news/3846023-airbnb-increases-market-share-in-latest-read-from-m-science.

Seamans, Robert, and Feng Zhu. 2014. "Responses to entry in multi-sided markets: The impact of Craigslist on local newspapers." *Management Science* 60 (2): 476–493.

Shi, Linda, Anjali Fisher, Rebecca M Brenner, Amelia Greiner-Safi, Christine Shepard, and Jamie Vanucchi. 2022. "Equitable buyouts? Learning from state, county, and local floodplain management programs." *Climatic Change* 174 (3-4): 29.

Swapan, Mohammad Shahidul Hasan, and Saalem Sadeque. 2021. "Place attachment in natural hazard-prone areas and decision to relocate: Research review and agenda for developing countries." *International Journal of Disaster Risk Reduction* 52:101937.

Tabik, Siham, Antonio R Cervilla, Emilio Zapata, and Luis F Romero. 2014. "Efficient data structure and highly scalable algorithm for total-viewshed computation." *IEEE Journal of Selected Topics in Applied Earth Observations and Remote Sensing* 8 (1): 304–310.

Tabik, Siham, Emilio L Zapata, and Luis F Romero. 2013. "Simultaneous computation of total viewshed on large high resolution grids." *International Journal of Geographical Information Science* 27 (4): 804–814.

Taylor, Charles A, and Hannah Druckenmiller. 2022. "Wetlands, Flooding, and the Clean Water Act." *American Economic Review* 112 (4): 1334–63.

The United Nations High Commissioner for Refugees. 2022. "Global Trends: Forced Displacement in 2021."

Town of Somerset. 2020. "Wind Energy Project Survey Comments." https://www.somersetny.org/home/pages/wind-energy-project-survey-comments.

Valentin, Maxence. 2021. “Regulating short-term rental housing: Evidence from New Orleans.” *Real Estate Economics* 49 (1): 152–186.

Vyn, Richard J, and Ryan M McCullough. 2014. “The effects of wind turbines on property values in Ontario: does public perception match empirical evidence?” *Canadian Journal of Agricultural Economics/Revue canadienne d’agroeconomie* 62 (3): 365–392.

Wagner, Katherine RH. 2022. “Adaptation and adverse selection in markets for natural disaster insurance.” *American Economic Journal: Economic Policy* 14 (3): 380–421.

Wang, Kui, Kelvin KW Yau, Andy H Lee, and Geoffrey J McLachlan. 2007. “Two-component Poisson mixture regression modelling of count data with bivariate random effects.” *Mathematical and Computer Modelling* 46 (11-12): 1468–1476.

Watson, Simon, Alberto Moro, Vera Reis, Charalampos Baniotopoulos, Stephan Barth, Gianni Bartoli, Florian Bauer, Elisa Boelman, Dennis Bosse, Antonello Cherubini, et al. 2019. “Future emerging technologies in the wind power sector: A European perspective.” *Renewable and sustainable energy reviews* 113:109270.

Westlund, Hans, and Mats Wilhelmsson. 2021. “The socio-economic cost of wind turbines: A Swedish case study.” *Sustainability* 13 (12): 6892.

Wong, Stephen D, Jacquelyn C Broader, and Susan A Shaheen. 2020. “Review of California wildfire evacuations from 2017 to 2019.”

Wong, Stephen D, Jacquelyn C Broader, Joan L Walker, and Susan A Shaheen. 2022. “Understanding California wildfire evacuee behavior and joint choice making.” *Transportation,* 1–47.

Yang, An-Shik, Ying-Ming Su, Chih-Yung Wen, Yu-Hsuan Juan, Wei-Siang Wang, and Chiang-Ho Cheng. 2016. “Estimation of wind power generation in dense urban area.” *Applied Energy* 171:213–230.

YouGov / Renewables UK Survey Results. 2012. Technical report. Scottish Renewables.

Zervas, Georgios, Davide Proserpio, and John W Byers. 2017. “The rise of the sharing economy: Estimating the impact of Airbnb on the hotel industry.” *Journal of marketing research* 54 (5): 687–705.

Zhang, Lei. 2016. “Flood hazards impact on neighborhood house prices: A spatial quantile regression analysis.” *Regional Science and Urban Economics* 60:12–19.

Zhao, Yanli, Anand Padmanabhan, and Shaowen Wang. 2013. “A parallel computing approach to viewshed analysis of large terrain data using graphics processing units.” *International Journal of Geographical Information Science* 27 (2): 363–384.

Appendix A

Appendix for Chapter 1

A.1 Mixed Poisson Model Estimation and Fit

The BLUP log-likelihood function is $l = l_1 + l_2$,

$$l_1 = \sum_t \left[-(\lambda_t^1 + \lambda_t^2) + M_t \log(\lambda_t^1 + \lambda_t^2) - \log(M_t!\,) \right]$$
$$l_2 = -\frac{1}{2} \left[T \log(2\pi\sigma_1^2) + \frac{\sum_t u_t^{1\prime} u_t^1}{\sigma_1^2} + T \log(2\pi\sigma_2^2) + \frac{\sum_t u_t^{2\prime} u_t^2}{\sigma_2^2} \right]$$

where σ_1 and σ_2 are the standard errors of random terms for travelers and evacuees respectively.

The EM algorithm is based on maximizing the expectation of the log-likelihood conditionally on a parameter vector, and updating the parameter space iteratively, so a Newton–Raphson approach is considered. The EM algorithm consists of an expectation step (E-step) and a maximization step (M-step). The E-step involves evaluating the expected complete log-likelihood, that is equivalent to compute the conditional probability given the current parameter vector. In the M-step, given a model parameterization and conditional probability, the expected complete log-likelihood is maximized with respect to the parameter space.

In this context, log-likelihood function l is parameterized by $\Phi = (\gamma_1, \gamma_2, \sigma_1^2, \sigma_2^2)$. Given an initialization of $\Phi^{(r)} = \Phi_0$ at iteration r, the iterative equation is

$$\Phi^{(r+1)} = \Phi^{(r)} + \mathcal{H}^{-1}(\Phi^{(r)}) \cdot \nabla(\Phi^{(r)})$$

where $\nabla(\cdot)$ and $\mathcal{H}(\cdot)$ respectively denote the gradient vector and Hessian matrix of the log-likelihood function l with respect to Φ. The EM iterations are repeated until convergence. In practice, the iteration is considered as converged if the increase of the log-likelihood between two successive iterations is less than a small tolerance level.

Figure A.1 plots the model fit relative to the data. I find the model predictions can fairly match with the observed aggregate customer arrival in the research period, and can reflect the seasonality and the trend of demand variations over time.

A.2 Counterfactual Analysis and Welfare Calculation

No Altruism

Under this scenario, I recompute the rental price $\hat{p}_{jnt}$ and supply decision $\hat{j}_{jnt}$ for all residents and all evacuation days when $\beta_i^S(j \cdot I_{\{E_t=1\}}) = 0$, by maximizing the expected utility of home-sharing:

$$\max_{j,p_{jnt}} \hat{u}^S_{jnt}(p_{jnt}) = u^S_{jnt}(p_{jnt}) \cdot \mathbf{E}\left(\frac{D_{jnt}}{S(p_{jnt})}\right), \text{ s.t. } D_{jnt} = D^T(p_{jnt}) + D^E(p_{jnt})$$

where $D^T(p_{jnt})$ and $D^E(p_{jnt})$ respectively denote the Airbnb demand of travelers and evacuees if the prevailing market price is p_{jnt}. Note that there could exist excessive supply, so instead of setting the supply equals demand I compute the *expected* utility by multiplying the utility of home-sharing with the occupancy rate, measured by the share of demand to supply.

As the counterfactual price would increase if there were no altruism, both altruistic and non-altruistic hosts lose from altruistic sharing due to price suppression. I define the loss of generosity as the welfare difference between the status quo and the No Altruism world.

With logit errors, the compensating variation for host i is

$$\text{CV}_{int}^{S} = \frac{1}{\alpha_i^S}\left[\ln(1 + u_{intj}^{S}(p_{jnt})) - \ln(1 + \hat{u}_{intj}^{S}(\hat{p}_{jnt}))\right]$$

where α_i^S is the price coefficient of the utility estimate in the supply model.

It is apparent that evacuees can gain from altruistic sharing. As hosts cannot differentiate by customer types, regular travelers are also able to enjoy the discounted price offered by altruistic hosts. Such free-riding creates a welfare gains for travelers as well, following

$$\text{CV}_{int}^{D} = \frac{1}{\alpha_i^D}\left(\ln \sum_{j,n \in S_{nj}} \exp(u_{ntj}^{D}(p_{ijnt})) - \ln \sum_{j,n \in \hat{S}_{nj}} \exp(u_{injt}^{D}(\hat{p}_{injt}))\right)$$

where α_i^D is the price coefficient of the utility estimate in the demand model.

No Airbnb

With logit errors, the welfare gain from Airbnb hosting for resident i simply follows:

$$\text{CV}_{int}^{S} = \frac{1}{\alpha_i^S}\ln(1 + u_{intj}^{S}(p_{jnt}))$$

where α_i^S is the price coefficient of the utility estimate in the supply model.

If the option to reside on Airbnb were no longer available, travelers could only choose between hotels and the outside choice of not traveling. Because a typical hotel room offers a private space with one bedroom, I assume the utility of hotel staying is the same as the Airbnb staying of a compact room in the same location at the hotel price, $u_{int}^{D}(\text{Hotel}) = u_{int}^{D}(j = \text{Compact},\ p_{nt}^{Hotel})$. Similarly, evacuees could only choose between hotels and public shelters (outside option). Therefore, the welfare gains from Airbnb option for travelers and evacuees follow:

$$\text{CV}_{int}^{D} = \frac{1}{\alpha_i^T}\left[\ln \sum_{j,n \in S_{nj}} \exp(u_{intj}^{D}(p_{jnt})) - \ln\left(1 + \sum_{n \in N} \exp(u_{int}^{D}(\text{Hotel}))\right)\right]$$

where α_i^D is the price coefficient of the utility estimate in the demand model.

No Free-Riding

The separate pricing levels for evacuees and travelers follow

$$i \in \text{Non-Alt: } \max_{j, p_{jnt}} \hat{u}^S_{NA,tntj}(p_{jnt}) = \int_i u^S_{intj}(p_{jnt}) dF(i \in \text{Non-Alt}) \cdot \mathbf{E}\left(\frac{D^T_{jnt}(p_{jnt})}{S(NA, p_{jnt})}\right)$$

$$i \in \text{Alt: } \max_{j, p_{jnt}} \hat{u}^S_{A,tntj}(p_{jnt}) = \int_i u^S_{intj}(p_{jnt}) dF(i \in \text{Alt}) \cdot \mathbf{E}\left(\frac{D^E_{jnt}(p_{jnt})}{S(A, p_{jnt})}\right)$$

where $F(\cdot)$ denotes the demographic distribution a subset of hosts, $S(NA, p_{jnt})$ and $S(A, p_{jnt})$ denote the home-sharing supply of altruistic hosts and non-altruistic hosts respectively. I define a host as altruistic if she experiences additional utility gains for making home-sharing on disaster moments, $\beta^S_i(j \cdot I_{\{E_t=1\}}) < 0$. Moreover, for non-altruistic hosts, I assume $\beta^S_{Non-Alt}(j \cdot I_{\{E_t=1\}}) = 0$. As non-altruistic hosts serve the same set of customers with and without disaster, their pricing problem should also keep consistent over time.

As a direct result, regular travelers would not gain or loss from altruistic sharing, as they are not allowed to enjoy the discounted price offered by generous families. Similarly, non-altruistic hosts would not suffer from the loss of generosity, as their pricing decision is independent from the generous hosts'. For altruistic hosts, their welfare loss from generosity is measured by the utility difference between this world and the scenario without altruistic sharing:

$$\text{CV}^{S,Alt}_{int} = \frac{1}{\alpha^S_i}\left[\ln(1 + u^S_{intj}(p_{jnt})) - \ln(1 + \hat{u}^S_{intj}(\hat{p}_{Alt,jnt}))\right]$$

It is worth-noting that the model tends to underestimate the true welfare loss from generosity under perfect matching. Knowing that regular travelers are not able to free ride, altruistic hosts might become more willing to perform generously by setting a even lower price or making even more supplies to disaster refugees. Hosts who used to perform non-altruistically under the status quo may want to switch to altruistic sharing as well. Therefore, the model estimates suggest a lower bar for the true loss from generosity for both altruistic and non-altruistic families. Similarly, evacuees would benefit from the altruistic sharing in presence of perfect matching, and the model tends to underestimate their true gains.

Welfare Calculation of the Displacement Costs

The absolute value of the welfare loss from displacements for evacuee i follows

$$\frac{1}{\alpha_i^E}\left[\ln \sum_{j,n \in S_{nj}} \exp(u_{intj}^E(p_{jnt})) + \alpha_i^E p_{j_i nt} - \ln\left(1 + \sum_{n \in N} \exp(u_{int}^E(\text{Hotel}_n))\right)\right]$$

where $u_{int}^E()$ represents the utility for evacuee i on Airbnb choice j, $p_{j_i nt}$ represents the price charged by her actual choice j_i, $u_{int}^E(\text{Hotel}_n)$ represents the utility of hotel choice in neighborhood n, and α_i^E represents the price coefficients in the demand model for evacuee i.

A.3 Supplementary Results

Figure A.1: Customer Arrival: Model Prediction and Data Fit

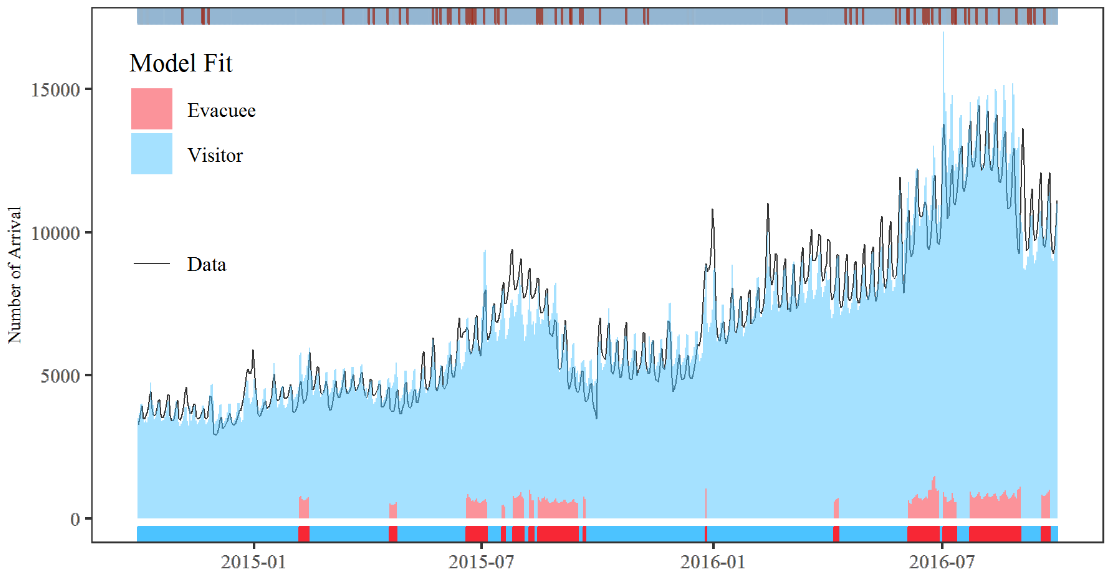

Notes: The line shows the number of aggregate number of Airbnb customers at the daily level. The blue and red bars respectively show the model predictions for the arrival of regular travelers and evacuees. In the bottom bar, red color suggests the days with evacuation order, and blue color suggests the days without evacuation order. In the top bar, orange color suggests the days with smoke exposure, while blue color suggests the days without.
Source: AirDNA and model estimates.

Figure A.2: Airbnb Listings in Los Angeles

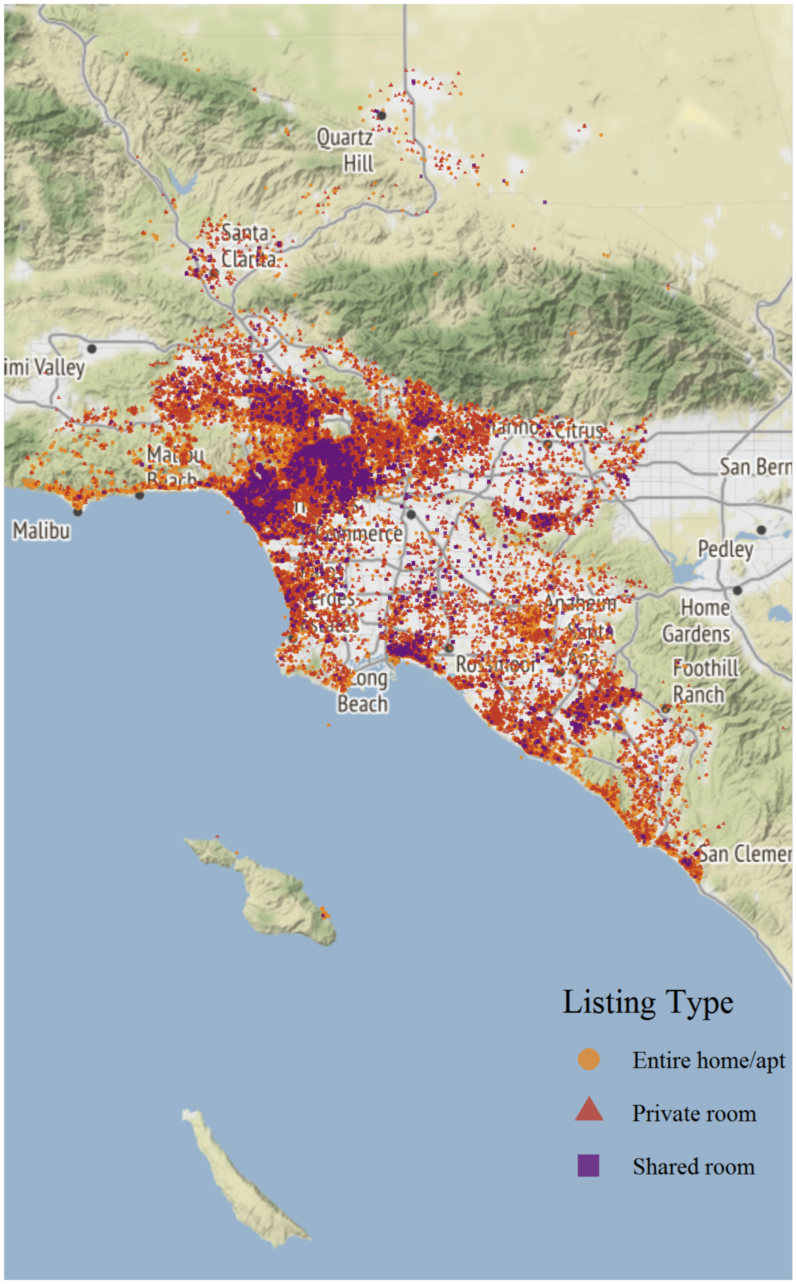

Notes: The figure plots the location of each listing that has ever been active on Airbnb in Los Angeles, during 2014/8-2016/10.

Figure A.3: Dynamic Patterns of Airbnb Market

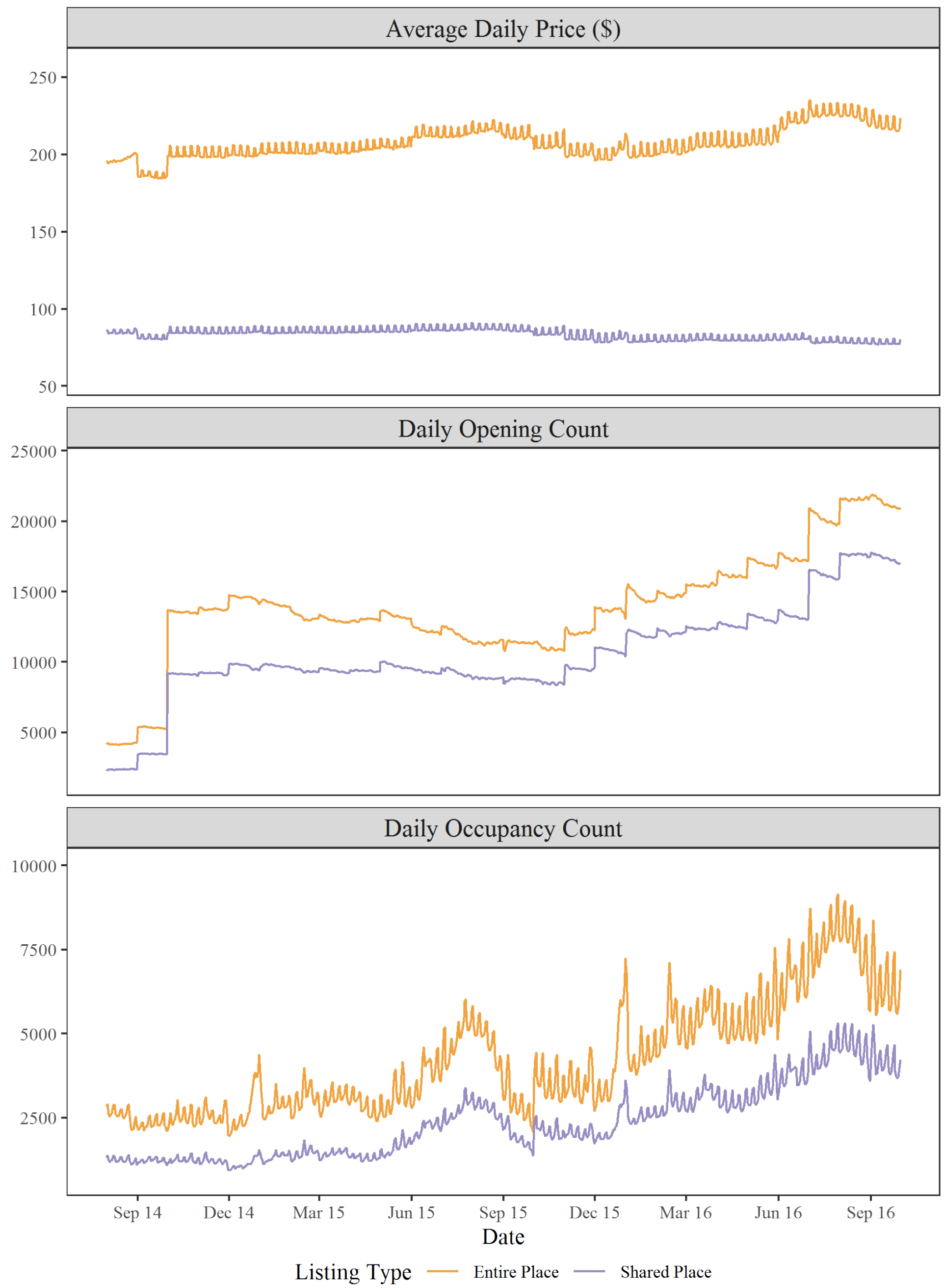

Notes: The figure plots the dynamics of the daily average price (top), the daily number of openings (middle), and the daily number of reservations (bottom) of all listings in the Los Angeles Airbnb market over the research period. The type is reclassified as to combine "private room" and "single room" as a single category "shared place".
Source: AirDNA.

Figure A.4: Variations across Airbnb Listings

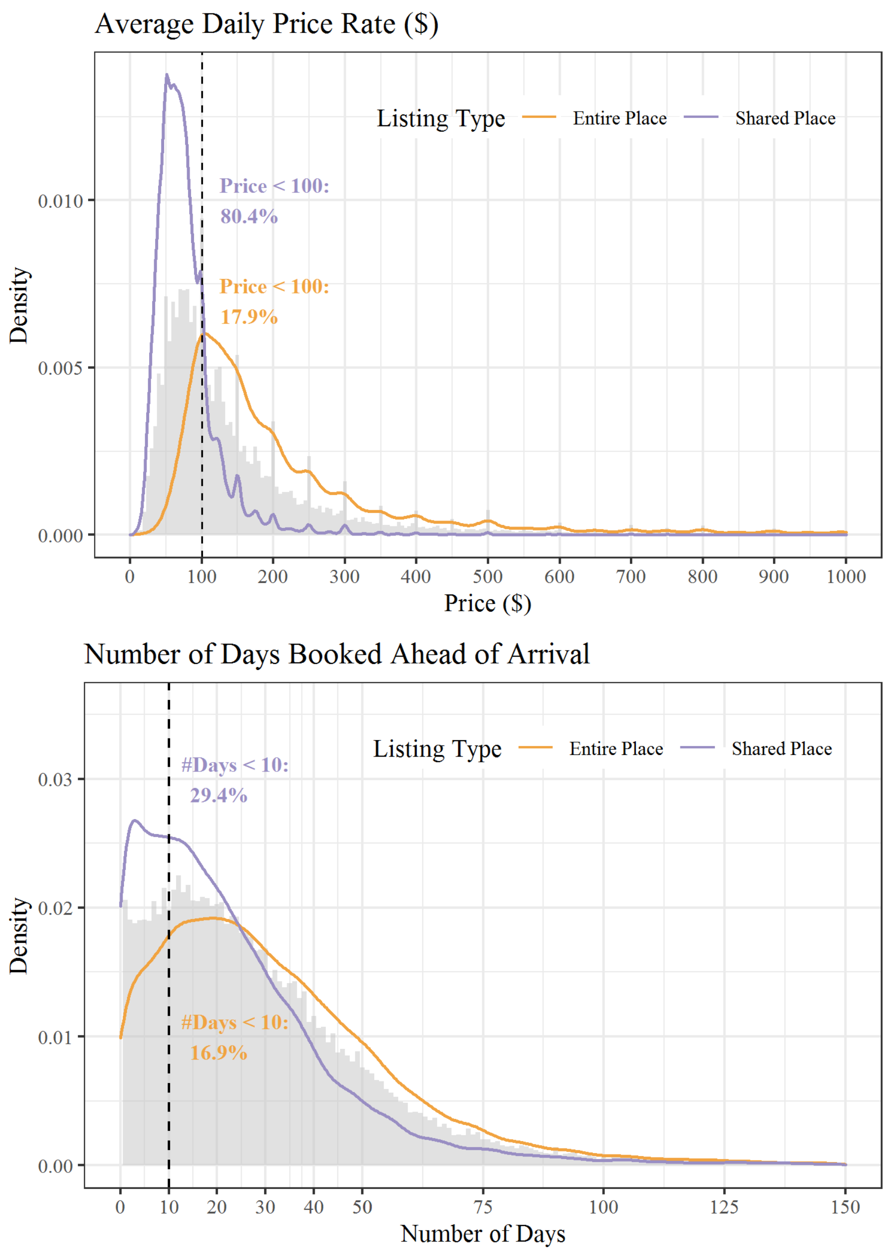

Notes: The figure plots the distribution in the number of days of booking ahead of checking-in (top panel), and of the daily price rate (bottom panel), of all listings in the Los Angeles Airbnb market.
Source: AirDNA.

Figure A.5: Wildfire and Induced Smoke

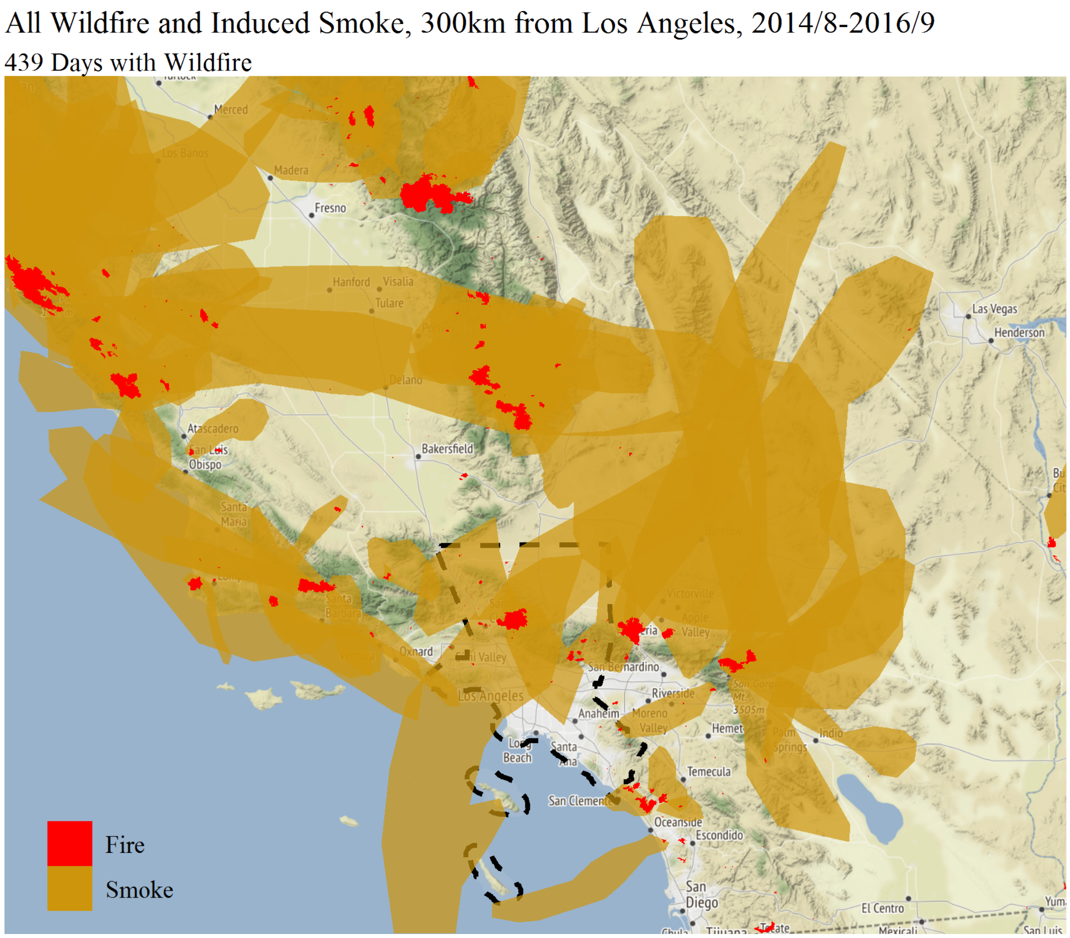

Notes: The graph shows all fires and their associated smoke plumes within 300km from Los Angeles in the research period. Red polygons represent fire extent, brown polygons represent smoke plumes.

Figure A.6: Evacuation Warnings for the Soberanes Fire, 2016-07-31

CAL FIRE NEWS RELEASE

California Department of Forestry and Fire Protection

CONTACT: Soberanes Information Line (831) 204-0446

RELEASE DATE: July 31, 2016
TIME: 9:00 A.M.

PORTIONS OF CACHAGUA AND TASSAJAR UNDER EVACUATION WARNING FOR SOBERANES FIRE

Effective immediately, the Monterey County Sheriff's Department has placed portions of the community of CACHAGUA and TASSAJARA under EVACUATION WARNING, which includes:

- All residences South of the intersection of E. Carmel Valley Rd. at San Clemente Dr. and extending to the intersection of E. Carmel Valley Rd. at Tassajara Rd. All residences along Tassajara Rd. from the intersection of Tassajara Rd. at E. Carmel Valley Rd. and extending approximately 17 miles to the end of Tassajara Rd. at the Tassajara Hot Springs Zen Center.
- This includes all roads that lead from the above described roads. This does not include residences on San Clemente Dr.

Residents should ***prepare*** to leave these areas listed above and be sure to take any medications, pets, family valuables, etc. with you. Close all windows and leave all doors closed.

All residents are asked to be READY: Create and maintain defensible space and harden your home against flying embers. Get SET: Prepare your family and home ahead of time for the possibility of having to evacuate. Be Ready to GO! Take the evacuation steps necessary to give your family and home the best chance of surviving a wildfire.

For more information on "Ready, Set, Go", go to www.readyforwildfire.org.

For additional information on the Soberanes Fire, Monterey County residents should contact Soberanes Fire Information Line at (831) 204-0446. Or visit CAL FIRE online @ www.fire.ca.gov

###

Notes: This figure shows the evacuation warnings for the Soberanes fire (Monterey county) for the portions of Cachagua & Tassajar, published by Cal Fire on July 31, 2016.

Figure A.7: Placebo Tests: Event Study Based on Public Holiday

Panel A: Extensive Margin of Supply - Log of the Number of Hosts

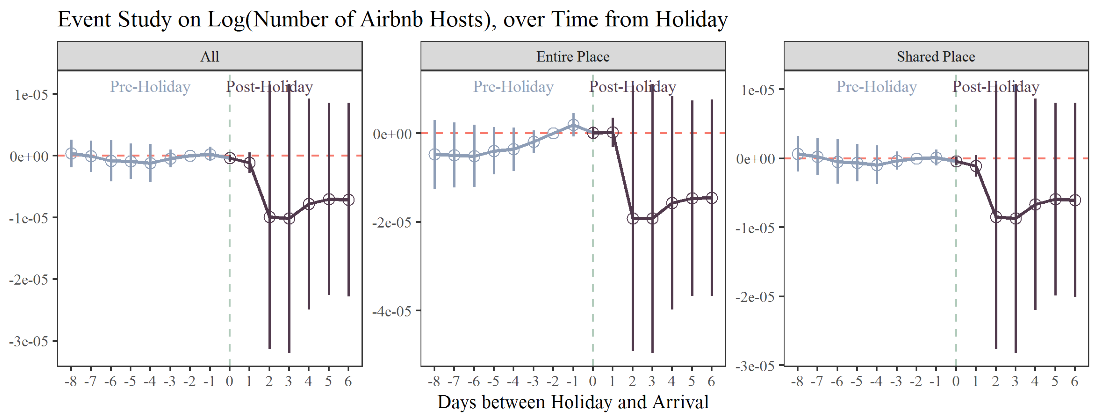

Panel B: Extensive Margin of Supply - Probability for Opening

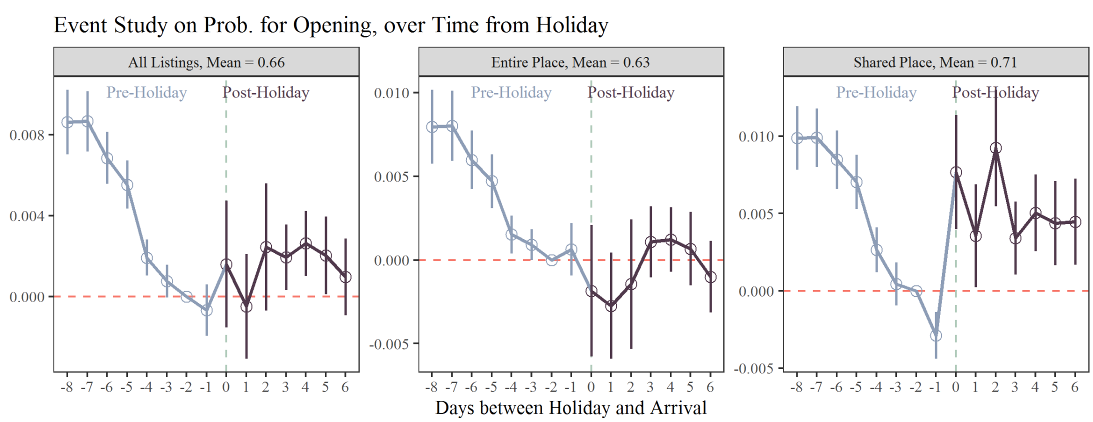

Notes: Top panels show event study regression coefficient on the log of the number of hosts at the PUMA level, controlling for PUMA fixed effects, year-month fixed effects, day-of-week fixed effects and holiday fixed effects. Bottom panels run a event study logit regression on the opening dummy at the property level, controlling for listing type fixed effects, zip code fixed effects, year-month fixed effects, day-of-week fixed effects and holiday fixed effects, and the coefficients reported are the marginal effects at the mean (MEM). Both panels use a 14-days window around the public holiday (day 0). Bars show 95% confidence intervals constructed using standard errors clustered at the zip code level.

Figure A.8: Patterns of Airbnb Pricing

Panel A: Price Dynamics of 20 Randomly Drawn Listings

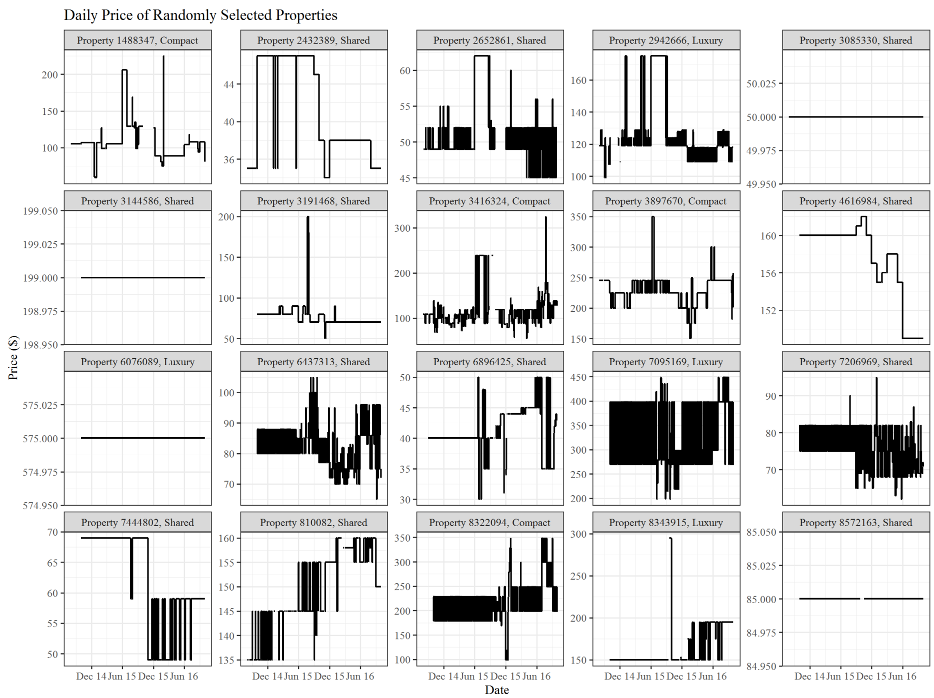

Panel B: Frequency of Price Adjustment

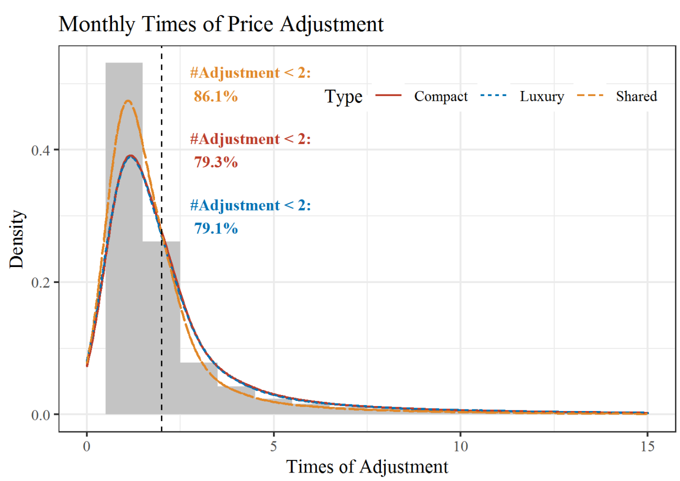

Notes: The top panel displays the price dynamics of 20 randomly drawn listings from the sample over the research period. The bottom panel presents the distribution of the number of price adjustments within a month for all listings.
Source: AirDNA.

Figure A.9: Average Daily Rate of Airbnb Listings on Evacuation Days

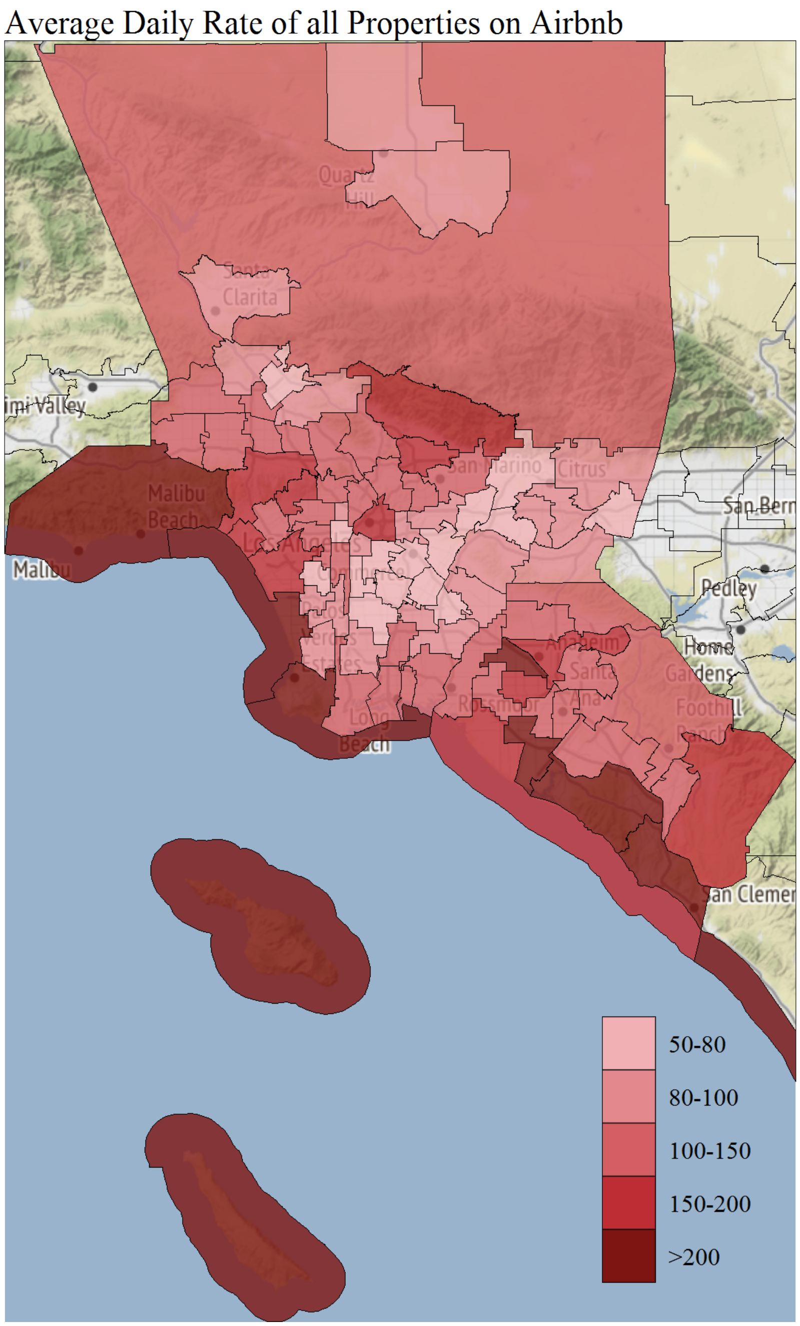

Notes: The average price of staying one night on Airbnb of days under evacuation, at the level of Public Use Microdata Area. Samples are all properties that are made available for occupancy at a price below $1000 per day.
Source: AirDNA.

Figure A.10: Evacuees' Destination by Housing Type

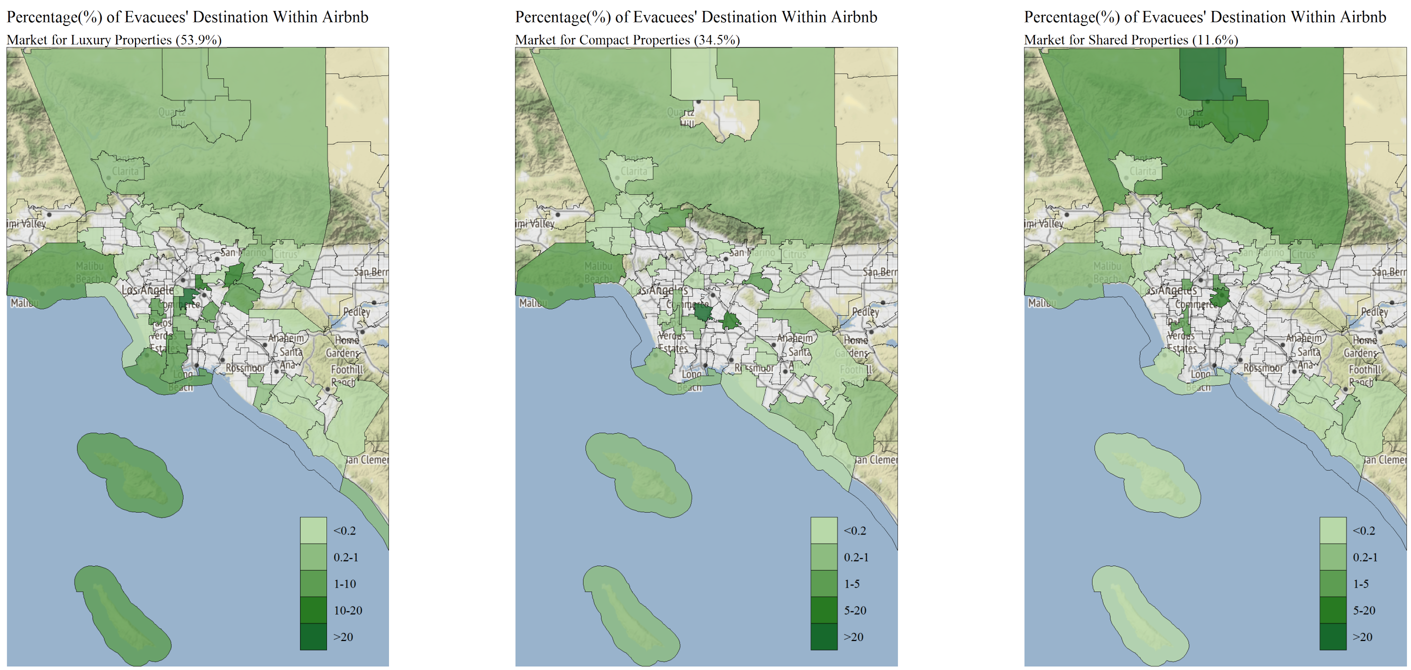

Notes: The share of the number of housing units taken by evacuees relative to the number of evacuees, at the level of Public Use Microdata Area. The count of evacuee arrivals is estimated from the mixture poisson regression model in section 1.4.
Source: model predictions.

Figure A.11: Percentage Change in Airbnb Supply without Altruistic Sharing

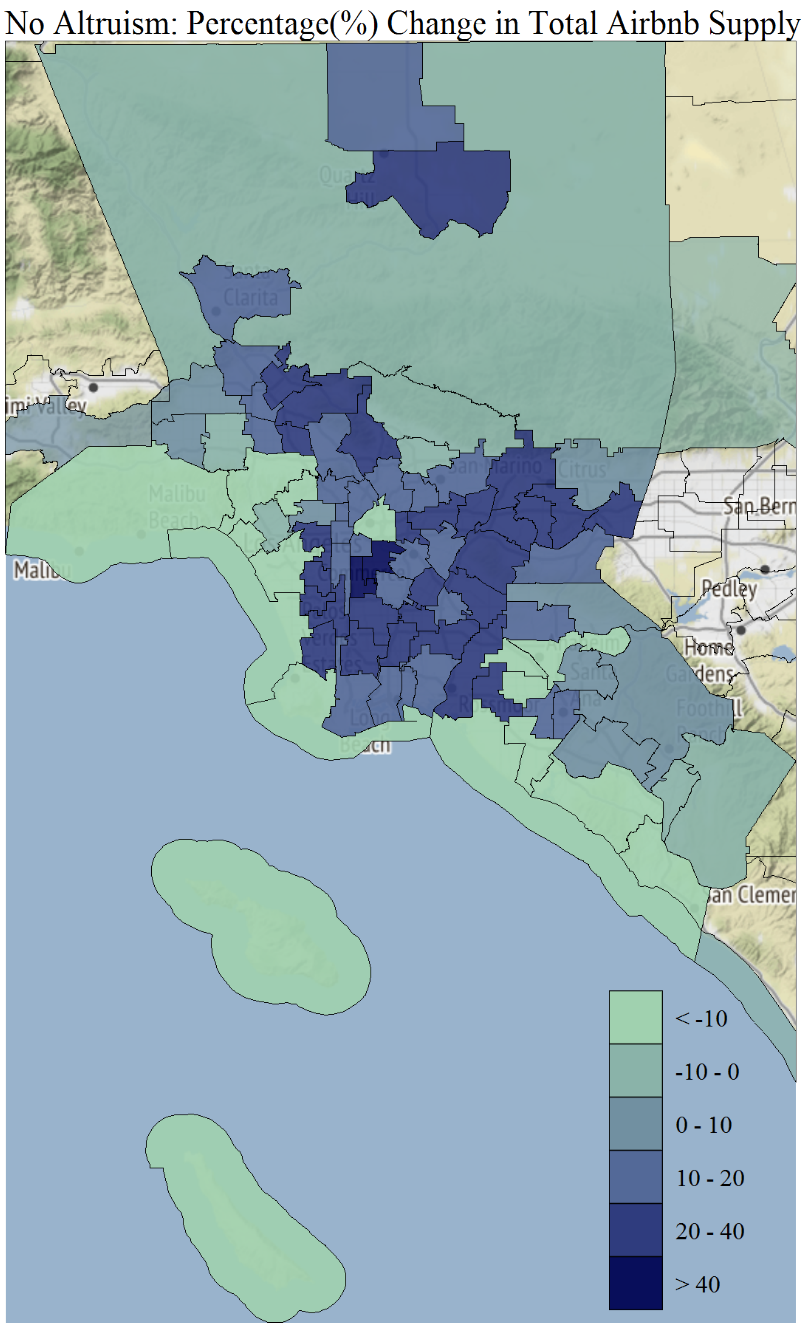

Notes: The percentage change in the number of Airbnb openings if the utility gains from altruistic sharing are removed, at the level of Public Use Microdata Area. Samples are limited to the days with an evacuation order in place.
Source: model estimate.

Figure A.12: Counterfactual Price and Supply by Housing Type

Panel A: Percentage Change in Counterfactual Price

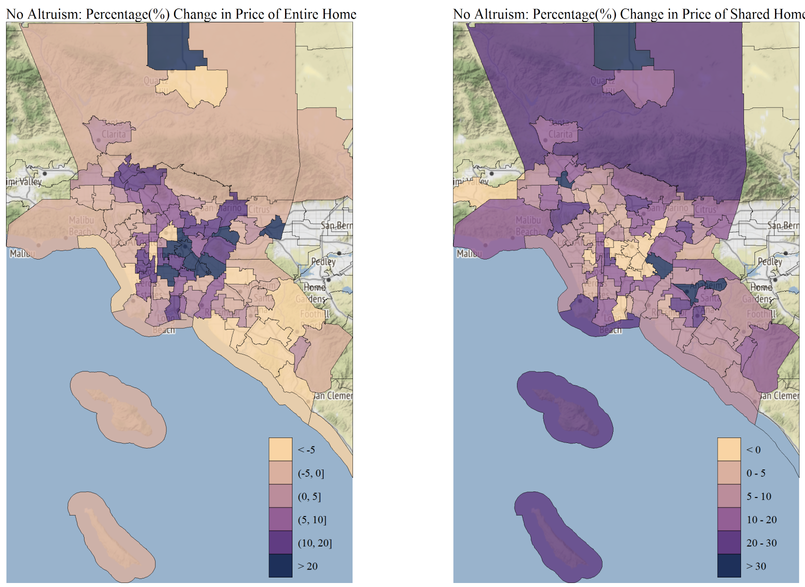

Panel B: Percentage Change in Counterfactual Supply

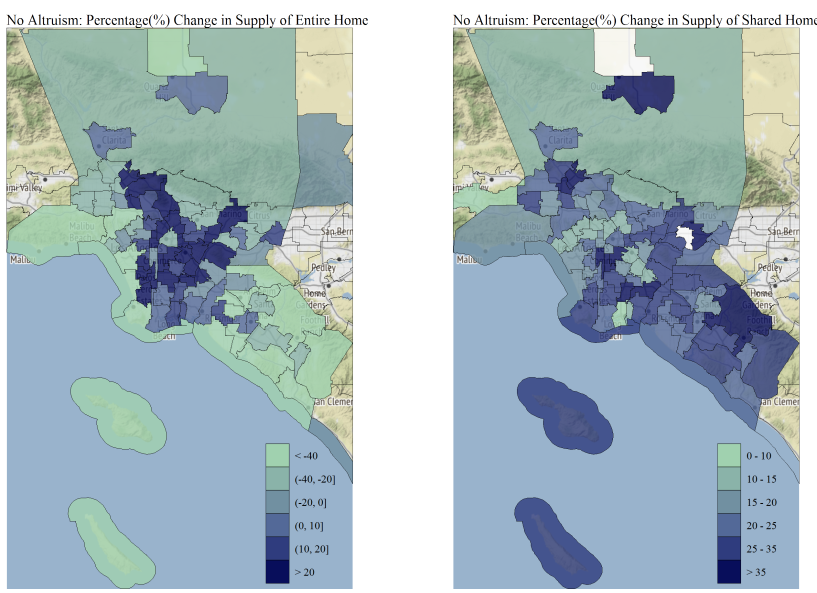

Notes: The figures present the counterfactual change in market outcomes if the altruistic sharing is removed. Panel A presents the percentage change in the price of entire sharing and partial sharing. Panel B presents the percentage change in the Airbnb supply of entire sharing and partial sharing.
Source: model predictions.

Figure A.13: Distribution of Displacement Loss

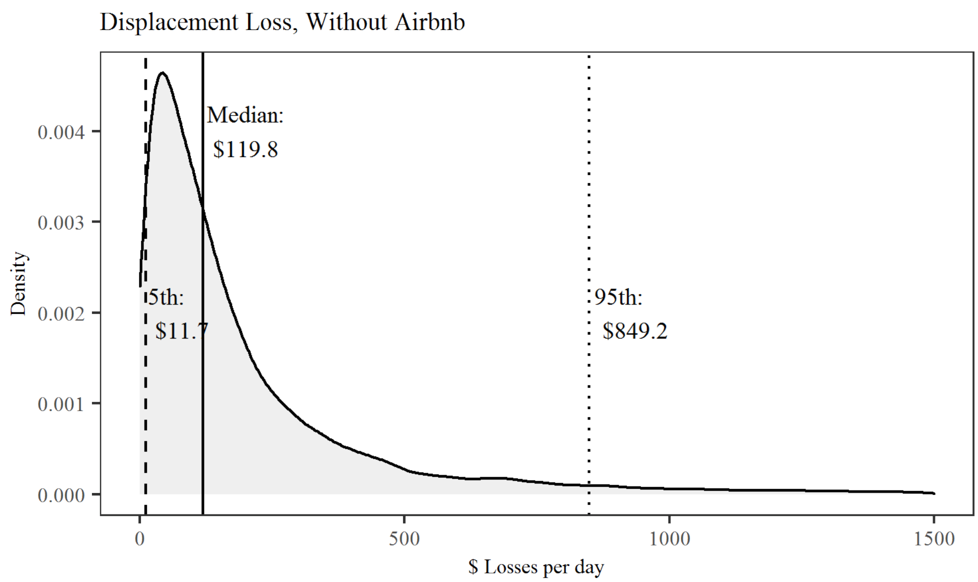

Notes: The figure displays the distribution of the displacement loss across evacuees, truncated at $1500 per day.
Source: model estimate.

Figure A.14: Welfare Gains of Evacuees from Altruistic Sharing

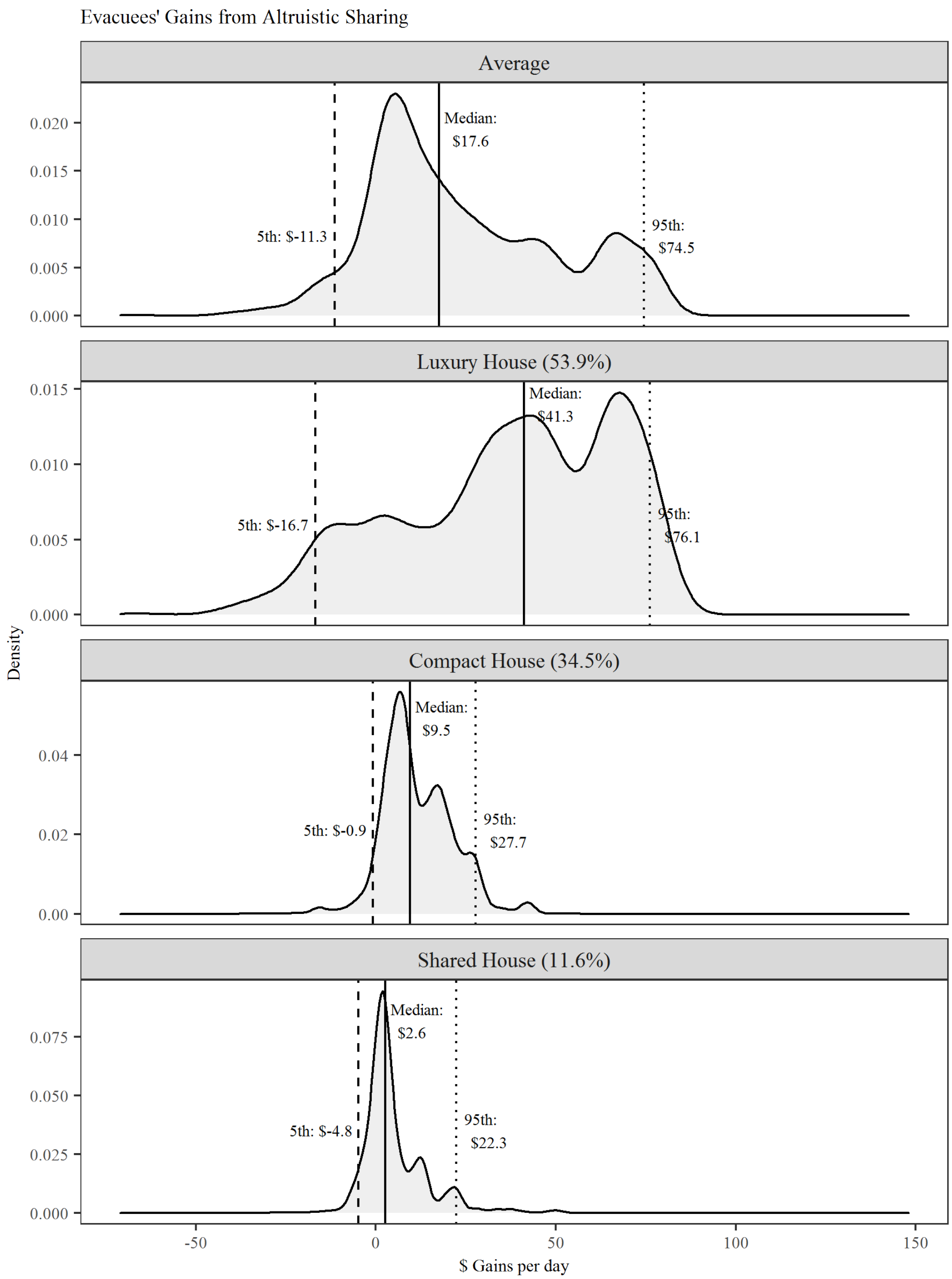

Notes: The figure presents the distribution of evacuees' welfare gains from altruistic sharing. Top panel displays the average distribution for all evacuees. The next three panels respective display the distribution for evacuees who have chosen Upscale house, Midscale house, and shared house, respectively.
Source: model predictions.

Figure A.15: Welfare Gains of Travelers from Altruistic Sharing

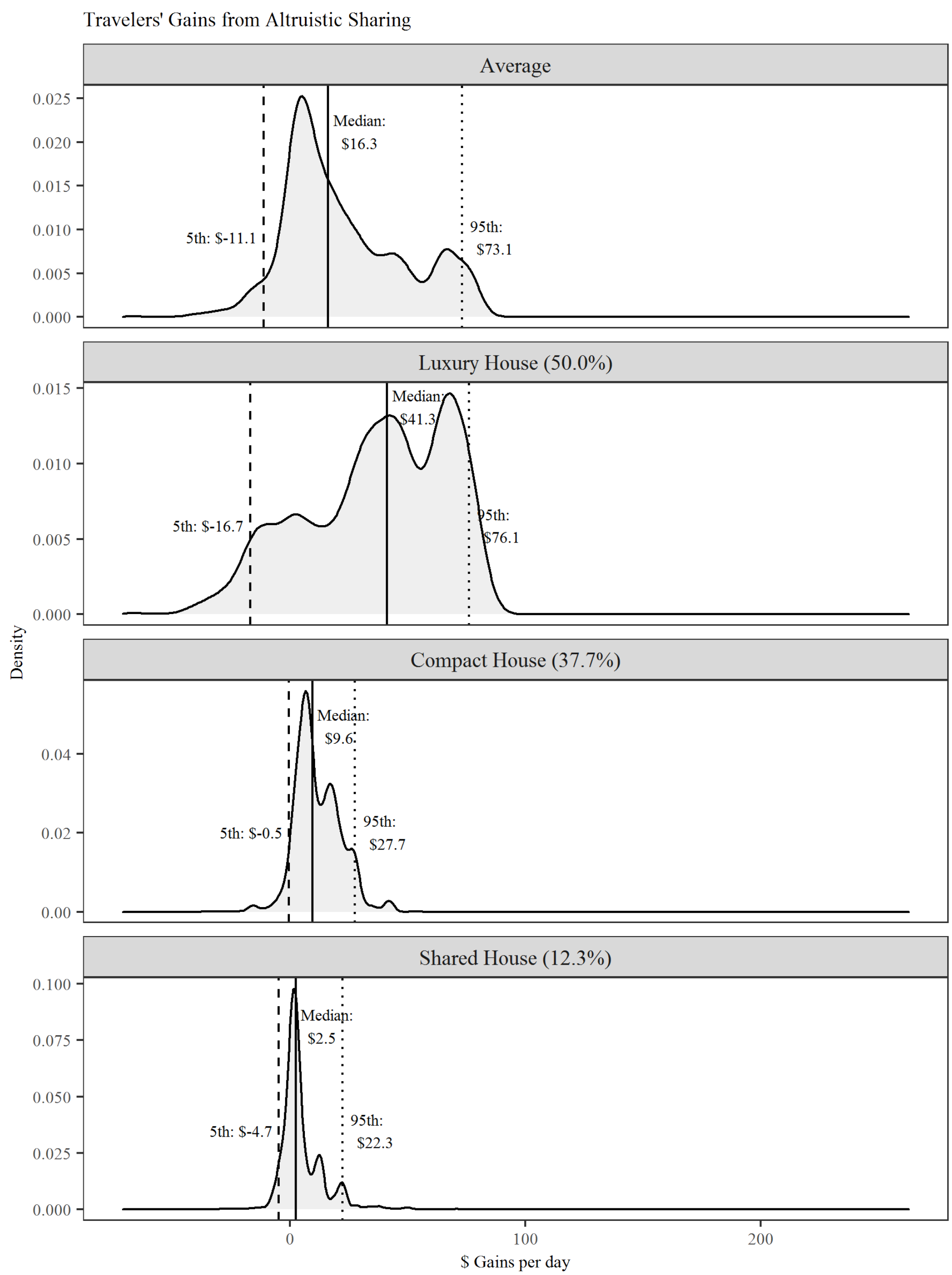

Notes: The figure presents the distribution of travelers' welfare gains from altruistic sharing. Top panel displays the average distribution for all travelers. The next three panels respective display the distribution for travelers who have chosen Upscale house, Midscale house, and shared house, respectively.
Source: model predictions.

Table A.1.
Summary Statistics for Airbnb Listings in Los Angeles, 2014/08-2016/09

	All						Entire Place			Shared Place		
	N	Mean	SD	P25	P50	P75	N	Mean	SD	N	Mean	SD
Price ($)	75254	154.67	142.46	71.00	108.63	180.12	43228	210.80	160.92	32026	78.91	52.37
Opening Rate	77353	0.71	0.29	0.53	0.82	0.97	45032	0.68	0.31	32321	0.76	0.27
Occupancy Rate	75254	0.26	0.27	0.01	0.15	0.45	43228	0.29	0.28	32026	0.22	0.26
Days Booked Ahead	51542	29.52	26.06	11.5	23.69	40.18	31117	33.0	26.63	20425	24.2	24.21
Superhost=1	77353	0.34	0.47	0.00	0.00	1.00	45032	0.33	0.47	32321	0.35	0.48
Days in Operation	77353	345.10	259.28	122.0	243.00	609.00	45032	353.8	260.94	32321	333.0	256.46
Bedrooms	77353	1.39	1.02	1.00	1.00	2.00	45032	1.67	1.27	32321	1.00	0.01
Bathrooms	77353	1.41	0.88	1.00	1.00	2.00	45032	1.60	1.02	32321	1.15	0.52
Minimum Stay Days	77353	1.98	1.51	1.00	1.00	2.00	45032	2.27	1.63	32321	1.58	1.22
Overall Rating	43646	4.65	0.49	4.50	4.80	5.00	26490	4.65	0.46	17156	4.65	0.53
Security Deposit ($)	77353	244.96	592.55	0.00	95.00	250.00	45032	359.03	730.93	32321	86.03	229.27
Cleaning Fee ($)	77353	55.90	78.52	0.00	30.00	79.00	45032	81.51	90.20	32321	20.21	35.06

Notes: This table shows descriptive statistics for Airbnb listings in Los Angeles over the research period. For each listing, I compute the mean, median, standard deviation, 25% quantile, median, 75% quantile of daily metrics for all Airbnb listings and by listing type. The metrics are daily price rate. opening rate, occupancy rate, superhost dummy, the number of days between booking and arrival, the number of days in operation, the number of bedrooms, the number of bathrooms, overall rating score (over 5), security deposit, and cleaning fee.
Source: AirDNA.

Table A.2.
Summary Statistics for Evacuation Orders surrounding Los Angeles, 2014/08-2016/09

	N	Mean	Median	SD	Min	Max
Evacuation Issuance Date	16	2016-02	2016-06	223.76	2014-08	2016-09
Evacuation Days	16	7.25	4.00	7.39	2.00	29.00
Evacuation Zone Acres (1000)	16	4960.11	1092.13	7751.32	87.73	28794.47
Fire Acres (1000)	16	53.55	10.18	84.44	1.68	232.58
Population Ordered to Evacuate (1000)	16	12.20	2.32	26.06	0.01	98.43
Household Ordered to Evacuate (1000)	16	5.39	1.04	11.81	0.01	45.56
Housing Units in Evacuation (1000)	16	7.85	1.75	16.09	0.01	59.51
Population Exposed to Fire	16	265.12	54.00	516.21	1.00	1969.00
Distance from Los Angeles (km)	16	133.26	103.09	97.00	4.02	297.60

Notes: This table shows descriptive statistics for wildfire evacuation of wildfire that have been sourced within 300km from Los Angeles, over the research period. I merge evacuation events that happened on the same days or within 3 days. Eventually there are 16 evacuation events.
Source: USGS, HMS, and Cal Fire documents.

Table A.3.
Parameter Estimates for the Airbnb Supply

Utility Estimate from the Random Utility Model (Instrumented, F-Stat = 185)					
	Linear Coef.	Interaction Coef.			
	(1)	(2) ×Log(Income)	(3) ×College= 1	(4) ×Having Child	(5) ×Tenant= 1
Price ($)	0.15***	−0.06***	−0.03***	−0.02***	0.02***
	(0.00)	(0.00)	(0.01)	(0.00)	(0.00)
Entire Sharing	−25.03***	0.36	1.64***	−2.19***	2.06***
	(0.68)	(1.01)	(0.37)	(0.35)	(0.22)
Partial Sharing	−9.24***	0.18	0.81	−1.59***	1.55***
	(0.54)	(0.31)	(0.71)	(0.47)	(0.45)
Entire × Evacuation	−3.16***	1.61***	2.18***	1.81***	0.86***
	(0.39)	(0.41)	(0.30)	(0.22)	(0.23)
Partial × Evacuation	−3.24***	1.27***	3.86***	0.63	0.74***
	(0.67)	(0.11)	(0.07)	(0.55)	(0.18)
Fire= 1	−0.58				
	(0.59)				
Smoke= 1	0.21***				
	(0.10)				
Holiday= 1	−0.15***				
	(0.07)				
Neighborhood FEs	Y	Y	Y	Y	Y
DOW FEs	Y	Y	Y	Y	Y
Month FEs	Y	Y	Y	Y	Y
Quadratic Time	Y	Y	Y	Y	Y
N	$132,302$	$132,302$	$132,302$	$132,302$	$132,302$
GMM Objective	12560.60	12560.60	12560.60	12560.60	12560.60

Notes: Estimation results for supply coefficients on the utility of home sharing. Column (1) reports the linear coefficient, with column (2)-(5) reporting the interacted terms with the log of income, the indicator for college degree, the indicator for having kids, the indicator for not holding homeownership, respectively. Standard errors are clustered at the PUMA level. * p<0.1, ** p<0.05, *** p<0.01.

Appendix B

Appendix for Chapter 2

B.1 Additional Results

Figure B.1: Gradient of distance from Programs on business performance

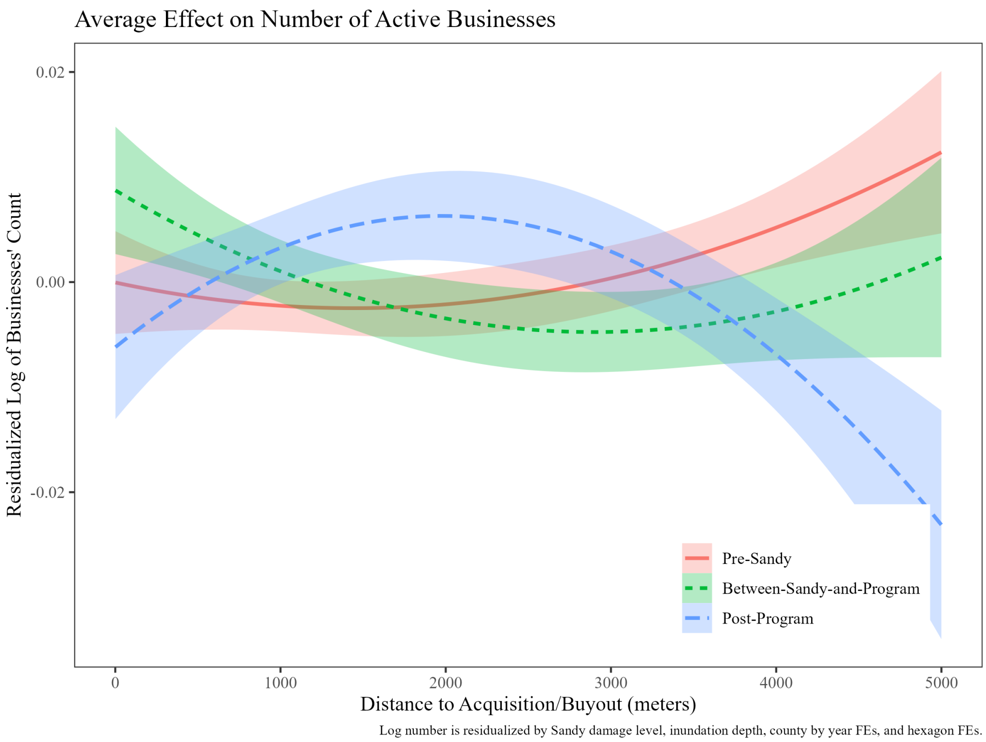

Notes: Log number of active businesses is residualized by Sandy damage level, inundation depth, county by year FEs, and hexagon FEs. Smoothing curves are obtained through a polynomial model fit. Shades show the 95% confidence intervals clustered twoway by census tract and sales year.

Table B.1.
Summary Statistics

Panel A: Acquisitions and Buyouts

	All Programs (N=1289)				Acquisition (N=566)		Buyout (N=723)	
	Mean	SD	Min	Max	Mean	SD	Mean	SD
Purchase Price ($)	377050	159986	4536	893199	373068	142298	380168	172607
Closed Date	2015-06	429	2013-07	2019-05	2015-08	318	2015-05	494
Demolition Date							2017-01	545
Auction Date					2016-04	335		

Panel B: Housing Transaction

	All Transactions (N=467229)				Treated (N=90163)		Control (N=377066)	
	Mean	SD	Min	Max	Mean	SD	Mean	SD
Sales Price (1000$)	423.64	353.49	10.00	4000.00	373.10	237.38	435.73	374.97
Sales Year	2006.02	7.34	1995.00	2020.00	2006.14	7.42	2005.99	7.32
post-Sandy = 1	0.25	0.44	0.00	1.00	0.26	0.44	0.25	0.43
Inundated = 1	0.51	0.50	0.00	1.00	0.84	0.37	0.43	0.50
Inundated Depth	0.61	1.57	0.00	28.00	2.06	2.41	0.27	1.02
# Programs	3.61	20.66	0.00	328.00	18.70	43.94	0.00	0.00
# Buyouts	1.82	17.15	0.00	294.00	9.41	38.10	0.00	0.00
# Acquisitions	1.79	6.39	0.00	65.00	9.29	11.90	0.00	0.00
Distance (m)	6853.00	7054.66	0.00	33877.38	441.52	288.97	8386.09	7033.42
# Rooms	2.01	3.38	0.00	55.00	3.62	3.64	1.62	3.20
# Bedrooms	0.30	1.07	0.00	17.00	0.29	1.03	0.30	1.08
# Bathrooms	0.62	1.13	0.00	17.50	1.11	1.19	0.51	1.08
Year Built	1950.67	32.43	1728.00	2018.00	1957.69	29.80	1949.00	32.81
Building Area (sqft)	1984.29	2186.98	100.00	895015.00	1804.84	832.94	2027.20	2398.17
Lot Size (acre)	0.22	0.84	0.00	52.62	0.18	0.55	0.23	0.90

Source: New York State Governor's Office of Storm Recovery, FEMA's Modelling Task Force, Zillow's ZTRAX database (2021 version).

Table B.2.
Summary Statistics (Continued)

Panel C: Mortgage Applications

	All Census Tracts (N=64890)				Treated (N=1701)		Control (N=63189)	
	Mean	SD	Min	Max	Mean	SD	Mean	SD
# Loans	124.41	148.10	0.00	1784.00	214.29	191.75	121.99	145.99
Avr Loan (1000$)	460.10	1968.86	6.00	190655.00	280.11	94.12	464.66	1993.36
Annual Income (1000$)	126.34	64.54	4.00	944.50	124.97	38.22	126.37	65.07
% > Median Income	67.39	16.53	0.00	100.00	60.79	13.55	67.56	16.56
% White Applicant	0.55	0.33	0.00	1.00	0.83	0.19	0.54	0.33
% Black Applicant	0.17	0.26	0.00	1.00	0.05	0.10	0.18	0.26
# Damaged Properties	16.90	104.00	0.00	1677.00	328.12	404.79	8.53	63.42
% White Population	0.56	0.33	0.00	1.00	0.87	0.15	0.55	0.33
% White Affected	0.63	0.28	0.00	0.98	0.85	0.15	0.61	0.28
% Black Population	0.21	0.28	0.00	1.00	0.05	0.10	0.21	0.29
% Black Affected	0.18	0.23	0.00	0.92	0.06	0.11	0.19	0.24

Panel D: Business Performance

	All (N=518868)				Treated (N=83412)		Control (N=435456)	
	Mean	SD	Min	Max	Mean	SD	Mean	SD
# Active Firms	12.65	41.43	0	1732	7.22	11.06	13.69	44.88
# Birth	1.22	4.61	0	313	0.68	1.6	1.32	4.98
# Death	1.11	4.69	0	925	0.61	1.42	1.2	5.08
Growth Rate of # Firms	0.02	0.29	-1	7	0.03	0.3	0.02	0.28
Total Employment	89.07	623.66	0	100771	32.16	119.61	99.97	678.21
Employment per Firm	4.88	26.75	0	8765	4	18.03	5.05	28.11
Inundated = 1	0.34	0.47	0	1	0.71	0.46	0.27	0.44
# Damaged Properties	1.5	6.97	0	124	5.97	12.94	0.64	4.6
# Programs < 1km	11.22	81.51	0	2625	69.8	192.97	0	0
# Buyouts < 1km	5.07	68.39	0	2543	31.51	168.12	0	0
# Acquisitions < 1km	6.16	27.53	0	391	38.29	59.03	0	0

Source: New York State Governor's Office of Storm Recovery, FEMA's Modelling Task Force, National Archives of Federal Reserve Board of Governors Division of Consumer and Community Affairs, National Establishment Time-Series (NETS) database, .

Table B.3.
Robustness Checks: Impacts of Acquisition and Buyout Programs on Log(Property Value)

	Average Effect		Effect by Program			
	(1)	(2)	(3)		(4)	
			Acquisition	Buyout	Acquisition	Buyout
Panel A: 5km from the acquisition and buyout programs ($N = 268143$)						
Treated × Post-Program	0.0352***		0.0407***	-0.0017		
	(0.00514)		(0.0105)	(0.0171)		
× low intensity		0.0318***			0.029***	-0.0136
		(0.00464)			(0.00952)	(0.0217)
× high intensity		0.0831*			0.0822***	0.0364***
		(0.0447)			(0.0239)	(0.00834)
Adj R^2	0.553	0.553	0.553		0.553	
Panel B: Repeated sales only ($N = 306141$)						
Treated × Post-Program	0.0552***		0.0461**	0.026		
	(0.0141)		(0.0172)	(0.0281)		
× low intensity		0.0572***			0.0444**	0.02
		(0.0182)			(0.0202)	(0.0305)
× high intensity		0.0527			0.0509*	0.088***
		(0.0503)			(0.0259)	(0.0131)
Adj R^2	0.580	0.580	0.580		0.580	
Panel C: Pseudo treatment assigned to control properties ($N = 467229$)						
Treated × Post-Program	0.046***		0.0449***	0.0381***		
	(0.00912)		(0.00529)	(0.00646)		
× low intensity		0.0441***			0.0388***	-0.00118
		(0.008)			(0.0133)	(0.0215)
× high intensity		0.0903*			0.0814***	0.0548***
		(0.0442)			(0.018)	(0.00979)
Adj R^2	0.599	0.599	0.599		0.599	

Notes: Robustness tests for the effect of acquisition and buyout programs on the property value. Panel A limits the group group to 5 kilometers from acquisition and buyout programs. Panel B uses the repeated sales only. Panel C assigns a pseudo treatment timing to the control properties. The specifications and the definition for low and high intensity are analogous to the baseline model. Standard errors are clustered twoway at the census tract and year level. * p<0.1, ** p<0.05, *** p<0.01.

Appendix C

Appendix for Chapter 3

C.1 Average Building Height Data

Data on the average building height are obtained from the U.S. national categorical mapping of building heights from Shuttle Radar Topography Mission (SRTM). The data are a categorical mapping of estimated mean building heights, by census block group, for the conterminous United States.

The data were derived from the NASA Shuttle Radar Topography Mission, which collected "first return" (top of canopy and buildings) radar data at 30-m resolution in February, 2000 aboard the Space Shuttle Endeavor. These data were processed to estimate building heights nationally, and then aggregated to block group boundaries. Aggregation was done by calculating a zonal sum by census block group of elevations from the SRTM urban area grid, then dividing the sum by the land area of the block group in hectares . This resulted in a sum of the elevations in meters per hectare (SEPH). This dataset was assessed in three ways: (1) by comparing it by block group to the actual buildings heights of a detailed dataset from the city of San Francisco, (2) by identifying the class for 858 random points over low-density residential areas, and (3) by qualitatively checking the dataset against known tall landmarks in major cities.

Block groups were then categorized into six groups using the statistical distribution of this average elevation, namely using multiples of standard deviation from the mean as breakpoints. The categories were named “Low”, “Low-Medium”, “Medium”, “Medium-High”, “High”, and “Very High”. The classifications were assigned as follows: the “Low” category was assigned values where SEPH was in the range 0 to 0.5851; “Low-Medium” category: SEPH = 0.5851 to 6.9151; “Medium” category: SEPH = 6.9151 to 19.5776; “Medium-High” category: SEPH = 19.5776 to 32.24; “High” category: SEPH = 32.24 to 57.5651; and “Very High” category: SEPH greater than 57.5651. Of the 216,291 block groups, 33.5% are Low, 36.7% are Low-Medium, 20.0% are Medium, 6.5% are Medium-High, 2.5% are High, and 0.8% (1,722) are Very High. Block groups categorized as “Very High” tend to be focused in a small number of the very densest cities, such as Manhattan and Los Angeles. From these means and standard deviations we also roughly make an estimate of how tall and how many stories buildings typically would have in each category. Exact number of meters per story varies widely, so an estimate of 3.5 was used, based on a height per story of 10-12 feet. Low category of building heights has primarily 1-2 story buildings; Low-Medium category has primarily 2-3 story buildings; Medium category has primarily 3-4 story buildings; Medium-High category has primarily 3-6 story buildings; High category has primarily 4-9 story buildings; Very High category of building heights has buildings average 10 stories or higher. Figure C.1 presents the spatial distribution of the average building height categories. The majority of places fall in the group of “Low” and “Low-Medium” groups.

In the regression analysis, we combine the groups of Medium and Medium-High into the category of “Medium”, which represents places with primary buildings of 3-6 stories. We also combine the groups of “High” and “Very High” into a single category denoted as “High”, which typically represents places with primary buildings above 5 stories.

C.2 Additional Results

Figure C.1: Average Building Height by Census Block

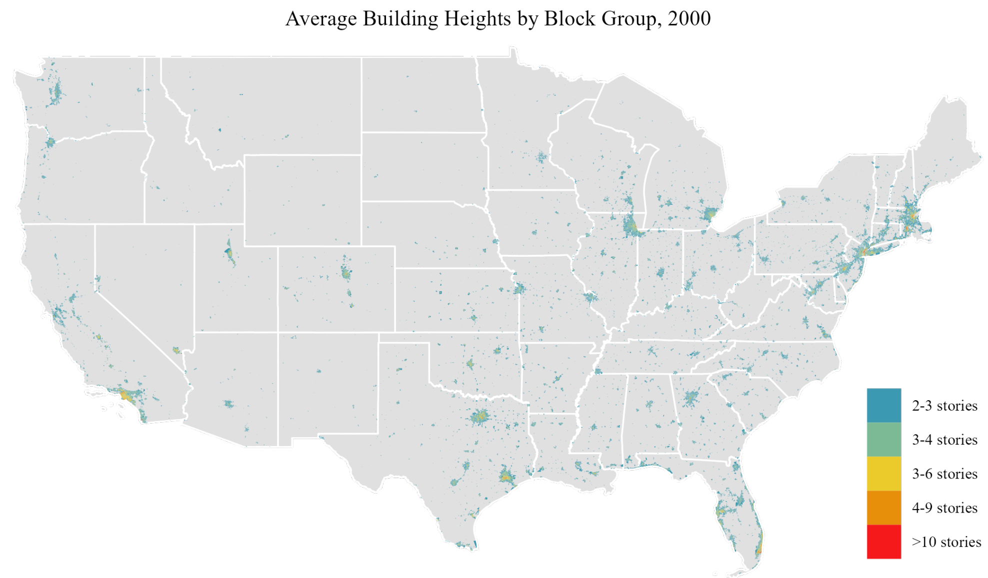

Source: U.S. national categorical mapping of building heights from Shuttle Radar Topography Mission

Table C.1.
Effect of Windmill Visibility on Property Value by Turbine Characteristics

Dependent Variable: Log(Property Value)					
	Instal.Year	Cum.Capacity	Capacity	Height	Rotor Diam.
	(1)	(2)	(3)	(4)	(5)
Treated × Post-Treatment	-0.0105**	-0.0112**	-0.0112**	-0.0111**	-0.0112**
	(0.00433)	(0.00431)	(0.00431)	(0.00431)	(0.00431)
× IHS(Turbine Char.)	-0.00798*	-0.0017	0.00031	0.000686	0.000106
	(0.00406)	(0.00164)	(0.000955)	(0.00141)	(0.00134)
Post-Treatment	0.0073	0.00827	0.00905	0.00915	0.00899
	(0.00595)	(0.00587)	(0.00583)	(0.0058)	(0.00581)
Treated	-0.0101**	-0.0098**	-0.0103**	-0.0104**	-0.0101**
	(0.00439)	(0.00444)	(0.00463)	(0.0046)	(0.0046)
N	5705597	5705597	5705597	5705597	5705597
Adj. R^2	0.516	0.516	0.516	0.516	0.516
FE: Census Tract × Year	X	X	X	X	X
FE: County × Sales Month	X	X	X	X	X
Std. Errors Clustered at Census Tract and Year Level					

Note Estimation results for the property value on the effect of wind turbine visibility, by wind turbine characteristics. Dependent variable is the log of sales price. Each regression utilizes the baseline specification of DiD with an inclusion of wind turbine characteristic interacted with the primary interaction term of interest. Columns (1)-(5) utilize different turbine characteristics, with (1) using the installation year, (2) the cumulative capacity, (3) the individual capacity, (4) the turbine height from the hub, and (5) the rotor diameter. The turbine characteristic in each specification is transformed using an inverse hyperbolic sine function. Each specification controls for a full set of property characteristics and fixed effects of the census tract by sales year level and the county by sales month level. Standard errors are clustered twoway at the census tract and sales year level. * p<0.1, ** p<0.05, *** p<0.01.

Table C.2.
Robustness Test: Repeated Sales Only

	All (1)	Urban (2)	Rural (3)
Treated × Post-Treatment	-0.028***	-0.028***	-0.00659
	(0.00813)	(0.00817)	(0.0206)
Post-Treatment	0.071**	0.0736**	0.00951
	(0.0307)	(0.0321)	(0.0277)
Treated	0.0711	0.0811	-0.0329
	(0.0751)	(0.0806)	(0.0883)
N	1803579	1718191	85388
Adj. R^2	0.489	0.490	0.433
FE: County × Sales Month	X	X	X
FE: County × Sales Year	X	X	X
FE: Parcel ID	X	X	X
Std. Errors Clustered at Census Tract and Year Level			

Note Robustness tests for the property value on the effect of wind turbine visibility, using repeated sales only. Repeated sales are defined as transactions on parcels that have been transacted for at least once both before and after the installation of turbine within the visibility range. Each specification controls for the fixed effects of the parcel level, the county by sales year level and the county by sales month level. Standard errors are clustered twoway at the census tract and year level. * p<0.1, ** p<0.05, *** p<0.01.

Table C.3.
Robustness Test: Average Building Height

Panel A: Low Building	Low (≤ 1 Stories)			Low-Medium (1-2 Stories)		
	All	Urban	Rural	All	Urban	Rural
	(1)	(2)	(3)	(4)	(5)	(6)
Treated × Post-Treatment	-0.0141**	-0.0118*	-0.0229	-0.015**	-0.0159**	0.0753
	(0.00583)	(0.00656)	(0.0162)	(0.00732)	(0.00691)	(0.0606)
Post-Treatment	0.00676	0.00305	0.00673	0.0252***	0.0254***	0.0131
	(0.00861)	(0.00856)	(0.0179)	(0.00951)	(0.00937)	(0.0548)
Treated	-0.0151**	-0.0125*	-0.0189	0.00864	0.0101	-0.0628
	(0.00634)	(0.00698)	(0.0166)	(0.00803)	(0.00794)	(0.0513)
N	2417916	2021891	396025	1515155	1496666	18489
Adj. R^2	0.467	0.476	0.404	0.536	0.537	0.513

Panel B: High Building	Medium (3-6 Stories)			High (≥ 5 Stories)		
	All	Urban	Rural	All	Urban	Rural
	(1)	(2)	(3)	(4)	(5)	(6)
Treated × Post-Treatment	0.00306	0.00314		0.0295	0.0296	
	(0.00783)	(0.00782)		(0.032)	(0.032)	
Post-Treatment	-0.00565	-0.00564		-0.0473	-0.0475	
	(0.0112)	(0.0112)		(0.0565)	(0.0567)	
Treated	-0.00595	-0.00598		-0.0519	-0.052	
	(0.00576)	(0.00576)		(0.0509)	(0.0509)	
N	1606426	1606129	297	166100	166004	96
Adj. R^2	0.544	0.544		0.394	0.394	

Note Robustness tests for the property value on the effect of wind turbine visibility, by average building height within the census block. Block groups are categorized into four groups using the statistical distribution of the sum-elevations per hectare and comparing it with the average height of buildings by the number of stories. Each specification controls for a full set of property characteristics and fixed effects of the census tract by sales year level and the county by sales month level. Standard errors are clustered twoway at the census tract and year level. * p<0.1, ** p<0.05, *** p<0.01.